

1987

A Study Of Deep Fluid Circulation In The Troodos Ophiolite, Cyprus

Ndoba Joseph Vibetti

Follow this and additional works at: <https://ir.lib.uwo.ca/digitizedtheses>

Recommended Citation

Vibetti, Ndoba Joseph, "A Study Of Deep Fluid Circulation In The Troodos Ophiolite, Cyprus" (1987). *Digitized Theses*. 1617.
<https://ir.lib.uwo.ca/digitizedtheses/1617>

This Dissertation is brought to you for free and open access by the Digitized Special Collections at Scholarship@Western. It has been accepted for inclusion in Digitized Theses by an authorized administrator of Scholarship@Western. For more information, please contact tadam@uwo.ca, wlsadmin@uwo.ca.



National Library
of Canada

Bibliothèque nationale
du Canada

Canadian Theses Service

Services des thèses canadiennes

Ottawa, Canada
K1A 0N4

CANADIAN THESES

THÈSES CANADIENNES

NOTICE

The quality of this microfiche is heavily dependent upon the quality of the original thesis submitted for microfilming. Every effort has been made to ensure the highest quality of reproduction possible.

If pages are missing, contact the university which granted the degree.

Some pages may have indistinct print especially if the original pages were typed with a poor typewriter ribbon or if the university sent us an inferior photocopy.

Previously copyrighted materials (journal articles, published tests, etc.) are not filmed.

Reproduction in full or in part of this film is governed by the Canadian Copyright Act, R.S.C. 1970, c. C-30.

**THIS DISSERTATION
HAS BEEN MICROFILMED
EXACTLY AS RECEIVED**

AVIS

La qualité de cette microfiche dépend grandement de la qualité de la thèse soumise au microfilmage. Nous avons tout fait pour assurer une qualité supérieure de reproduction.

S'il manque des pages, veuillez communiquer avec l'université qui a conféré le grade.

La qualité d'impression de certaines pages peut laisser à désirer, surtout si les pages originales ont été dactylographiées à l'aide d'un ruban usé ou si l'université nous a fait parvenir une photocopie de qualité inférieure.

Les documents qui font déjà l'objet d'un droit d'auteur (articles de revue, examens publiés, etc.) ne sont pas microfilmés.

La reproduction, même partielle, de ce microfilm est soumise à la Loi canadienne sur le droit d'auteur, SRC 1970, c. C-30.

**LA THÈSE A ÉTÉ
MICROFILMÉE TELLE QUE
NOUS L'AVONS REÇUE**

A STUDY OF DEEP FLUID CIRCULATION
IN THE TROODOS OPHIOLITE, CYPRUS

by

Ndoba Joseph Vibetti

Department of Geology

Submitted in partial fulfillment
of the requirements for the degree of
Doctor of Philosophy

Faculty of Graduate Studies
The University of Western Ontario
London, Ontario
October 1986

© Ndoba Joseph Vibetti 1986

Permission has been granted to the National Library of Canada to microfilm this thesis and to lend or sell copies of the film.

The author (copyright owner) has reserved other publication rights, and neither the thesis nor extensive extracts from it may be printed or otherwise reproduced without his/her written permission.

L'autorisation a été accordée à la Bibliothèque nationale du Canada de microfilmer cette thèse et de prêter ou de vendre des exemplaires du film.

L'auteur (titulaire du droit d'auteur) se réserve les autres droits de publication; ni la thèse ni de longs extraits de celle-ci ne doivent être imprimés ou autrement reproduits sans son autorisation écrite.

ISBN 0-315-36056-9



ABSTRACT

Submarine upwelling of magma at a constructive tectonic plate margin took place at Troodos 85 Ma B.P. forming oceanic lithosphere which proceeded to cool both by conductive heat transfer as well as by convective mass transfer of seawater. The convection of seawater through the newly formed crust initiated complex and highly variable hydrothermal alteration which in places culminated in the complete recrystallization of parts of the oceanic crust. The circulation of seawater through the uppermost layers of the newly formed crust caused major changes in the chemistry of the oceanic lithosphere and ultimately led to the formation of the base and precious metal deposits of Cyprus, originally in excess of forty million tonnes of ore.

Drawing on samples collected from sites far removed from mineralized areas, the current study, utilizing petrological and geochemical methods, reports extensive hydrothermal alteration attributable to sub-oceanic processes throughout the ophiolite sequence. It also indicates that the overall plititic composition of the ophiolite is the result of prolonged seawater-basalt interaction at continuously variable water/rock ratios at low pressures and low to high temperatures, up to 600°C. Metamorphic mineral assemblages and microthermometric data from fluid inclusions point to the local evolution of seawater into a hot hypersaline brine which appears to have been an ideal agent for the leaching of a host of major elements, transition metals, and trace elements from oceanic lithosphere.

Observations on fracture distribution and alteration indicates that fluids infiltrated to great depth, apparently beyond the oceanic moho. Oxygen and strontium isotope analyses positively identify the alteration fluids as being seawater derived, with the oxygen isotope pattern indicating that the fluid/rock

Interaction was complex and depth related. The metamorphic mineral assemblages present reflect an evolving cycle from high to low temperatures, and water/rock ratios involving fluids of continuously evolving composition.

Current models of oceanic lithosphere cooling that involve the dissipation of heat by mass transfer in the sub-seafloor environment adequately explain the nature and pattern of observed postmagmatic alteration with the additional observations that locally, the process of seawater infiltration appears to extend to depths in the oceanic crust beyond the Moho and that it also appears to be responsible for the development of at least two chemically distinct types of hydrothermal fluid.

ACKNOWLEDGEMENTS

My thanks go to Professor W.S.Fyfe who suggested the thesis topic and provided the rare opportunity and the resources that enabled me to participate in a fundamental scientific research project. He is also thanked for his unique brand of supervision which he provided throughout the duration of the study. Dr. J.Malpas of Memorial University is thanked for introducing me to ophiolite geology as well as getting me started in cyprus. Drs. C. Xenophonos, A. Panayiotou and the men and women of the Geological Survey in Nicosia, Cyprus are thanked for logistical assistance in the field.

At Western my thanks go to the faculty, students and staff of the geology department for making the years I spent in the department memorable ones. Particular mention go to J. Forth, Tsal-Way Wu, R. Barnett, W. Harley, R. Sharma, C. Haameja Muyovwe, A. Noon, I. Craig, P. Thomson, Dr. B. Kronberg and Professor R. Kerrich for invaluable assistance at various stages in the preparation of this thesis.

Support from the University of Zambia Faculty Development Program is acknowledged.

Special thanks go to my parents, brothers and sisters who provided support, encouragement, guidance and mail without limit, and to whom I apologise for being absent for such a long time.

Last but not least I thank Sindisiwe Phumlile for her friendship, love, support and patience. This time I promise to be sweeter.

TABLE OF CONTENTS

	Page
CERTIFICATE OF EXAMINATION	ii
ABSTRACT	iii
ACKNOWLEDGMENTS	iv
TABLE OF CONTENTS	vi
LIST OF PHOTOGRAPHIC PLATES	vii
LIST OF TABLES	x
LIST OF FIGURES	lxi
CHAPTER 1 - STATEMENT OF PROBLEM	1
CHAPTER 2 - PREVIOUS WORK ON OPHIOLITES	5
2.1 OPHIOLITES	5
2.2 PETROGENESIS OF OPHIOLITES	6
2.3 COOLING OF OCEANIC LITHOSPHERE	6
2.4 CONVECTIVE HYDROTHERMAL CIRCULATION AS AN OCEAN LITHOSPHERE COOLING MECHANISM	8
2.5 CHEMICAL AND MASS ASPECTS OF SEAWATER-OCEAN CRUST INTERACTION	13
2.6 EXPERIMENTAL WORK	14
CHAPTER 3 - THE GEOLOGY OF CYPRUS	17
3.1 INTRODUCTION	17
3.2 THE TROODOS OPHIOLITE COMPLEX	19
3.3 CYPRUS-TYPE MASSIVE SULPHIDES	24
3.4 SUMMARY	26
CHAPTER 4 - TROODOS PETROLOGY	27
4.1 INTRODUCTION	27
4.2 IGNEOUS PETROGRAPHY	27
4.3 METAMORPHIC PETROGRAPHY	35
4.4 MINERAL CHEMISTRY	49
4.5 METAMORPHISM	65
4.6 METAMORPHISM AT AYIOS IOANNIS PITSILIA	75
4.7 PHYSICAL CONDITIONS OF HYDROTHERMAL METAMORPHISM	79
CHAPTER 5 - GEOCHEMISTRY	84
5.1 WHOLE ROCK GEOCHEMISTRY	84
5.2 MAJOR ELEMENTS	84
5.3 TRACE ELEMENTS	91
5.4 STRONTIUM ISOTOPE GEOCHEMISTRY	98

5.5 OXYGEN ISOTOPE GEOCHEMISTRY	101
5.6 CARBON ISOTOPE SYSTEMATICS	108
5.7 SUMMARY	111
CHAPTER 6 - FLUID INCLUSION ANALYSIS	113
6.1 INTRODUCTION	113
6.2 EXPERIMENTAL TECHNIQUE	115
6.3 RESULTS	115
6.4 DISCUSSION	124
6.5 SUMMARY	127
CHAPTER 7 - SUMMARY AND CONCLUSIONS	128
* * *	
APPENDIX A - SAMPLING AND ANALYTICAL METHODS	132
A.1 MAJOR AND TRACE ELEMENT ANALYSIS	132
A.2 MINERAL CHEMISTRY	133
A.3 RARE EARTH ELEMENTS	134
A.4 OXYGEN AND CARBON ISOTOPE ANALYSIS	134
A.5 MAJOR AND TRACE ELEMENT ANALYSES	136
A.6 FERRIC/FERROUS IRON RATIOS	152
A.7 RARE EARTH ELEMENT DATA	156
A.8 SELECT TRACE ELEMENT DATA	158
A.9 BORON ANALYSIS DATA	159
A.10 TROODOS PLAGIOCLASE ANALYSES	161
A.11 TROODOS HYDROTHERMAL PLAGIOCLASE ANALYSES	164
A.12 TROODOS CLINOPYROXENE ANALYSES	171
A.13 TROODOS ORTHOPYROXENE ANALYSES	184
A.14 TROODOS AMPHIBOLE ANALYSES	186
A.15 TROODOS CHLORITE ANALYSES	192
A.16 TROODOS EPIDOTE/CLINOZOISITE ANALYSES	195
A.17 TROODOS PREHNITE ANALYSES	197
A.18 TROODOS GARNET ANALYSES	202
A.19 TROODOS SPHENE ANALYSES	202
A.20 TROODOS ZEOLITE ANALYSES	204
REFERENCES	205
VITA	238

LIST OF PHOTOGRAPHIC PLATES

Plate	Description	Page
1.A.	Microporphyritic texture in diabase.	29
B.	Diabase/diabase contact.	
C.	Formation of amphibole.	
D.	Formation of serpentine.	
E.	Chlorite vein in diabase.	
2.A.	Rodingitized gabbro.	31
B.	Same as 2A.	
C.	Andradite bearing rodingitized gabbro.	
D.	Metasomatized diabase.	
3.A.	Zoned epidote.	34
B.	Alteration of Ca-plagioclase.	
C.	Spilitized diabase dyke.	
D.	Metaplagioclase.	
E.	Same as 2D.	
F.	Green and brown ^h amphibole.	
4.A.	Amphibolite facies assemblage.	37
B.	Metadiabase mineralogy.	
C.	Development of Prehnite.	
D.	Diabase alteration zone.	
E.	Graphic texture in microgranite.	
F.	Quartz - albite vein in diabase.	
5.A.	Relict Ca-plagioclase.	40
B.	Metadiabase mineralogy.	
C.	Relict plagioclase in gabbro.	
D.	Incipient alteration in gabbro.	
E.	Metasomatized gabbro.	
F.	Spilitized diabase.	
6.A.	Prehnite displaying "bow-tie" form.	43
B.	Prehnite of reniform globular form.	
C.	Serpentinized olivine.	
D.	Hydrothermal hornblende.	
E.	Anhydrite in metadiabase.	
F.	Spilitized diabase.	
7.A.	Fibrous prehnite.	45
B.	Interstitial prehnite.	
C.	Kelyphitic amphibole.	
D.	Same as 7C.	
E.	Spilite vein mineralogy.	
F.	Metagabbro mineralogy.	

8.A. Hydrothermal anorthite in gabbro.	48
B. Relict orthopyroxene.	
C. Metagabbro mineralogy.	
D. Development of amphibole in metagabbro.	
E. Diopside in metagabbro.	
F. Mineralogy of metagabbro.	
9.A. Mineralogy of metagabbro.	50
B. Alteration in websterites.	
C. Relict orthopyroxenes in metagabbro.	
D. Mineralogy and texture of metagabbro.	
E. Roddingitized gabbro mineralogy.	
F. Same as 9E.	
10.A. Alteration zone in websterites.	52
B. Same as 10A.	
C. Same as 10A.	
D. Same as 10A.	
E. Mineralogy of metagabbro.	
F. Same as 10E.	
11.N. Two and three phase fluid inclusions.	118
O. Same as 11A.	
P. Primary two and three phase fluid inclusions.	
Q. Primary three-phase fluid inclusions.	
12.W. Three phase fluid inclusions in vein	
X. quartz.	121
Cluster of three phase primary fluid inclusions.	
Y. Primary fluid inclusions with three phases.	
Z. Same as 12Y.	
13.U. Halite daughter crystals in primary fluid inclusions.	123
V. Primary fluid inclusions in quartz.	
W. Enhanced reproduction of U.	
X. Enhanced reproduction of V.	
Y. Primary fluid inclusions in quartz.	
Z. Enhanced reproduction of Y.	

LIST OF TABLES

Table	Description	Page
2.1.	Composition of seawater and vent fluids from 21°N EPR.	15
4.3.	Amphibole analyses from Ayios Ioannis.	77
4.4.	Plagioclase analyses from Ayios Ioannis.	78
5.2.	Boron analyses for diabase dykes and gabbros.	94
5.3.	Present day $^{86}\text{Sr}/^{87}\text{Sr}$ ratios for Troodos rocks.	97
5.4.	Present day and initial $^{86}\text{Sr}/^{87}\text{Sr}$ values for Troodos rocks.	99
5.6.	$^{86}\text{Sr}/^{87}\text{Sr}$ values for crust and seawater.	99
5.7.	Whole rock $^{18}\text{O}/^{16}\text{O}$ profile for CY-4.	104
5.8.	$^{18}\text{O}/^{16}\text{O}$ data for Troodos mineral separates.	105
5.9.	Isotopic composition of CY-4 calcites.	108
6.1.	Fluid inclusion data for two phase primary inclusions.	116
6.2.	Data for three phase fluid inclusions.	117
6.3.	Data for secondary inclusions.	119
6.4.	Salinities of two phase inclusions.	120

LIST OF FIGURES

Figure	Description	Page
1.1.	Location map showing CY-4 site.	2
2.1.	Schematic model of ocean crust formation.	7
2.2.	Generalized schematic model of the mechanism of allochthonous ophiolite formation.	9
2.3.	Schematic model for cooling of oceanic crust by convective mass transfer.	11
3.1.	Geologic map of the Troodos ophiolite complex.	18
3.2.	Location of the main Cu-Fe massive sulphide orebodies of the Troodos ophiolite.	25
4.1.	Plot of Troodos plagioclase analyses.	53
4.2.	Plot of Troodos pyroxene analyses.	55
4.3.	Plot of Troodos amphibole analyses.	57
4.4.	Plot of Troodos chlorite analyses.	59
4.5.	Plot of proportions of octahedrally coordinated Al and Fe(III) in epidote/clinozoisite from Troodos.	61
4.6.	Plot of proportions of octahedrally coordinated Al and Fe(III) in prehnite from Troodos.	63
4.7.	Plot of Troodos sphenes in Al-Ti-Fe space.	64
5.1A.	Plot of $\text{Na}_2\text{O} + \text{K}_2\text{O}$ vs. SiO_2 in wt.% for fresh diabase.	86
B., C., D.	Trends of the major elements MgO, CaO and Na_2O against LOI.	
E.	Plots of SiO_2 vs. MgO and Al_2O_3 vs. MgO for Troodos diabase and gabbros.	
5.2A., B., C.	Trends of the major elements Na_2O , CaO, and TiO_2 against MgO in wt.% for Troodos diabase and gabbro.	88
D.	TiO_2 vs. SiO_2 wt. % for Troodos diabase and gabbros.	
5.3.	FeO wt. % vs. $\text{Fe}^{2+}/\text{Total FeO}$ for Troodos diabase and gabbros.	90
5.4.	Histograms for the abundances in ppm of Sr,	

Rb, Zn and Cu in samples from Troodos diabase dykes.	92
5.5. Plot of Zr/Y vs. Zr for Troodos diabase.	95
5.6. $\delta^{18}\text{O}$ whole rock profile for Troodos ophiolite as intersected by CY-4.	100
5.7. Plot of $\delta^{18}\text{O}_{\text{SMOW}}$ vs. $\delta^{13}\text{C}_{\text{PDB}}$ for Troodos calcites occurring in veins and fractures of CY-4.	110

The author of this thesis has granted The University of Western Ontario a non-exclusive license to reproduce and distribute copies of this thesis to users of Western Libraries. Copyright remains with the author.

Electronic theses and dissertations available in The University of Western Ontario's institutional repository (Scholarship@Western) are solely for the purpose of private study and research. They may not be copied or reproduced, except as permitted by copyright laws, without written authority of the copyright owner. Any commercial use or publication is strictly prohibited.

The original copyright license attesting to these terms and signed by the author of this thesis may be found in the original print version of the thesis, held by Western Libraries.

The thesis approval page signed by the examining committee may also be found in the original print version of the thesis held in Western Libraries.

Please contact Western Libraries for further information:

E-mail: libadmin@uwo.ca

Telephone: (519) 661-2111 Ext. 84796

Web site: <http://www.lib.uwo.ca/>

Chapter One

STATEMENT OF PROBLEM.

The current study developed out of the participation by this writer in the Cyprus Crustal Study Project, (CCSP), a joint venture of the International Crustal Research Drilling Group (ICRDG) and the Government of Cyprus through the Cyprus Geological Survey over the period 1983 till the present.

The aim of the CCSP has been to investigate the Troodos Ophiolite Complex of Cyprus as it is generally recognised as one of the best preserved examples of ancient ocean crust available for detailed study.

The project, a coordinated interdisciplinary study, has applied the experience gained over a decade by the ICRDG in studying insitu oceanic crust using shallow (to 1 km) samples to study the Troodos ophiolite mainly using research drilling with continuous coring as well as field studies to test current models of oceanic crust and to obtain a three dimensional record of the structure of Troodos.

Participation by the present writer in the project centred mainly on a study of rock core obtained from drillhole CY-4 located at coordinates $34^{\circ} 54'06''$ N latitude and $33^{\circ}05'38''$ E longitude on the outskirts of Palekhorl village, central Cyprus (fig.1.1).

CY-4 was drilled by ICRDG with the stated intention of recovery of a complete section of the plutonic rocks of the ophiolite. Commencing in the lower part of the Sheeted Complex the drillhole intersects diabase dykes, isotropic and layered gabbros as well as cumulate ultramafic rocks before terminating in serpentinitized peridotites at a depth of 2263m. Overall core recovery was about 98%.

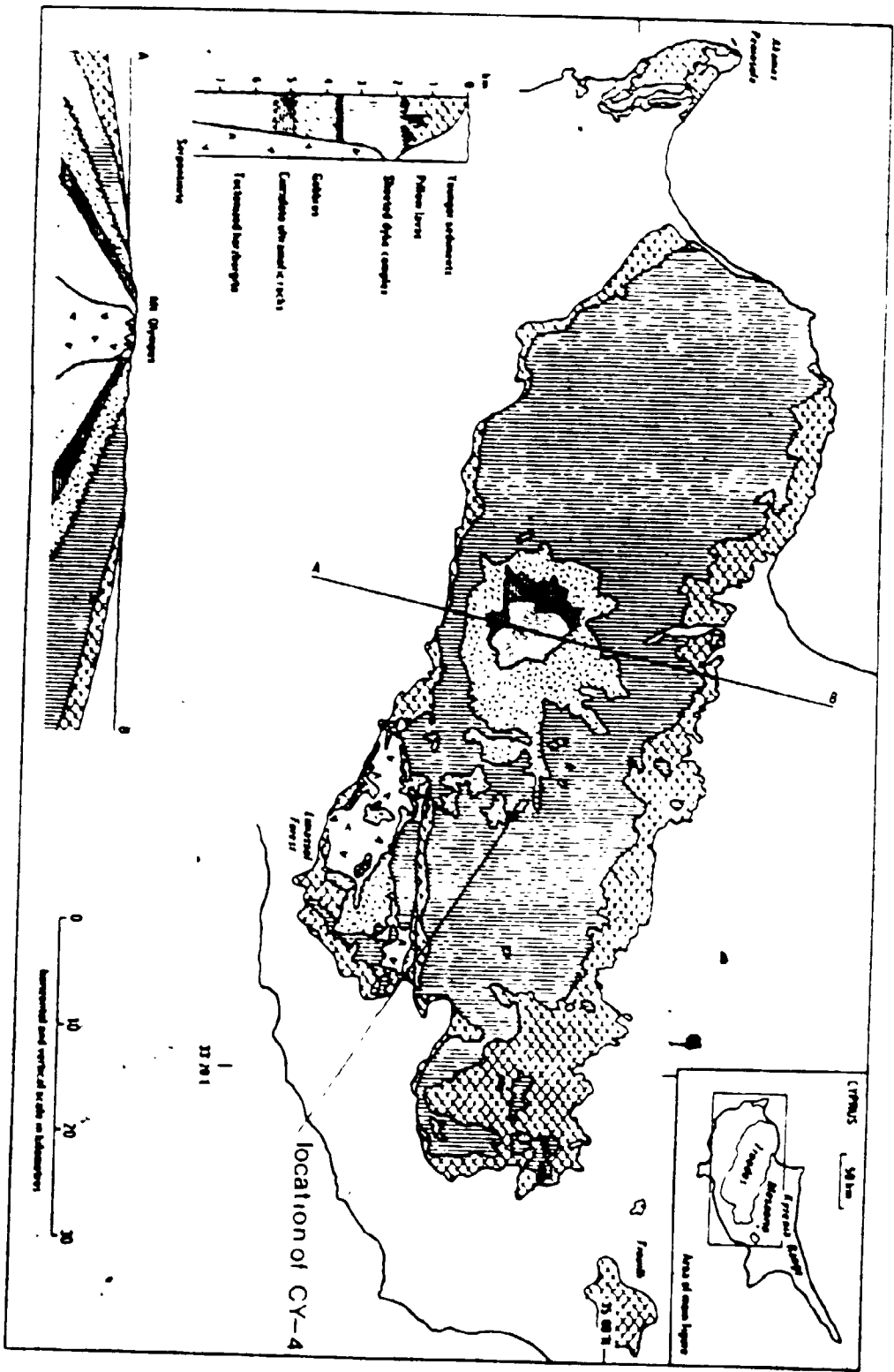


Fig.1.1. Location map showing site of CY-4.

In the current study, diabase dykes, isotropic and layered gabbros and the ultramafic cumulates were sampled from the drillcore with the intention of investigating the nature and extent of any postmagmatic alteration the rocks may have been subjected to and to ascertain to what degree, if any, such alteration could be ascribed to sub seafloor hydrothermal processes. The study also involved fieldwork in the isotropic gabbros occurring in the vicinity of the diabase dyke - plagiogranite - gabbro contact at Aylos Ioannis in the Pitsilia district of central Cyprus near Agros.

The main reason for the interest in sub seafloor hydrothermal processes as may or may not apply to the plutonic part of the oceanic crust is that such processes are now well known to be responsible for the extensive recrystallization of uppermost parts of oceanic crust, and in places are the direct causes of the formation of base metal massive sulphide deposits commonly occurring near the seawater/oceanic crust interface (MELSON and VAN ANDEL, 1966; CANN, 1969; SPOONER and FYFE, 1973; LIOU and ERNST, 1979; MUEHLENBACHS, 1979; ELTHON, 1981; BOHLKE ET. AL., 1984; ALT ET. AL., 1986). However, such processes are not as well constrained in the plutonic parts of the oceanic crust as they are in the uppermost parts. Studies in this field (e.g. BONATTI ET. AL., 1975; FOX and STROUP, 1981; VANKO and BATIZA, 1982; ITO and ANDERSON, 1983; STAKES and VANKO, 1986) have been mostly based on allochthonous dredge samples from the oceanfloor, thus often making it difficult to fully evaluate the nature and overall trends of post magmatic alteration as applicable to the deeper levels of oceanic crust.

The drilling at Palekhorl by the ICRDG through the plutonic part of the Troodos ophiolite sequence thus provided an opportunity to investigate the post magmatic alteration of the intrusive parts of ancient oceanic crust continuously

4

from the diabase dykes through to the serpentized peridotites free from the extensive weathering that dominates much of the Cyprian landscape.

Chapter Two

PREVIOUS WORK ON OPHIOLITES.

2.1. OPHIOLITES

The term ophiolite was originally used to describe serpentinites and was first used to describe the association peridotite-serpentinite, gabbro, diabase and associated sediments (radiolarian cherts, pelagic clays and deep foraminiferal limestones) by STEINMANN (1927). His impression was that the ultramafic and mafic rocks of this association had intruded into the overlying sediments (thus, the "STEINMANN TRINITY" of E.B. Bailey) and that the copper-bearing metalliferous veins associated with these rocks were a late magmatic phase injected into the surrounding and overlying rocks. His descriptions generally implied that ophiolites represented an early intrusive event in the formative stages of eugeosyncline development.

In 1972 the Penrose Conference on Ophiolites convened by the Geological Society of America defined ophiolites as a distinctive assemblage of mafic to ultramafic rocks and that in a complete ophiolite the rock types occur in the following order from top to bottom: PELAGIC SEDIMENTS: Cherts, red clays and minor limestones overlying the igneous complex. PILLOW LAVAS: Basalts and Spillitized Basalts interlayered with minor Mn-Fe oxide precipitates. SHEETED DYKE COMPLEX: A thick layer of vertically oriented parallel diabase dykes. GABBROIC COMPLEX: Isotropic and layered gabbros with minor plagiogranitic differentiates at the top grading downwards into cumulate peridotites with little deformation fabric. ULTRAMAFIC COMPLEX (commonly serpentinitized): Variable proportions of harzburgite, hercynite, wehrllite and dunite usually with a metamorphic tectonic fabric developed prior to serpentinitization (COLEMAN, 1977; GASS and SMEWING, 1981; HYNDMAN, 1985). A schematic profile of an ideal ophiolite sequence is presented in figure 2.

2.2. PETROGENESIS OF OPHIOLITES

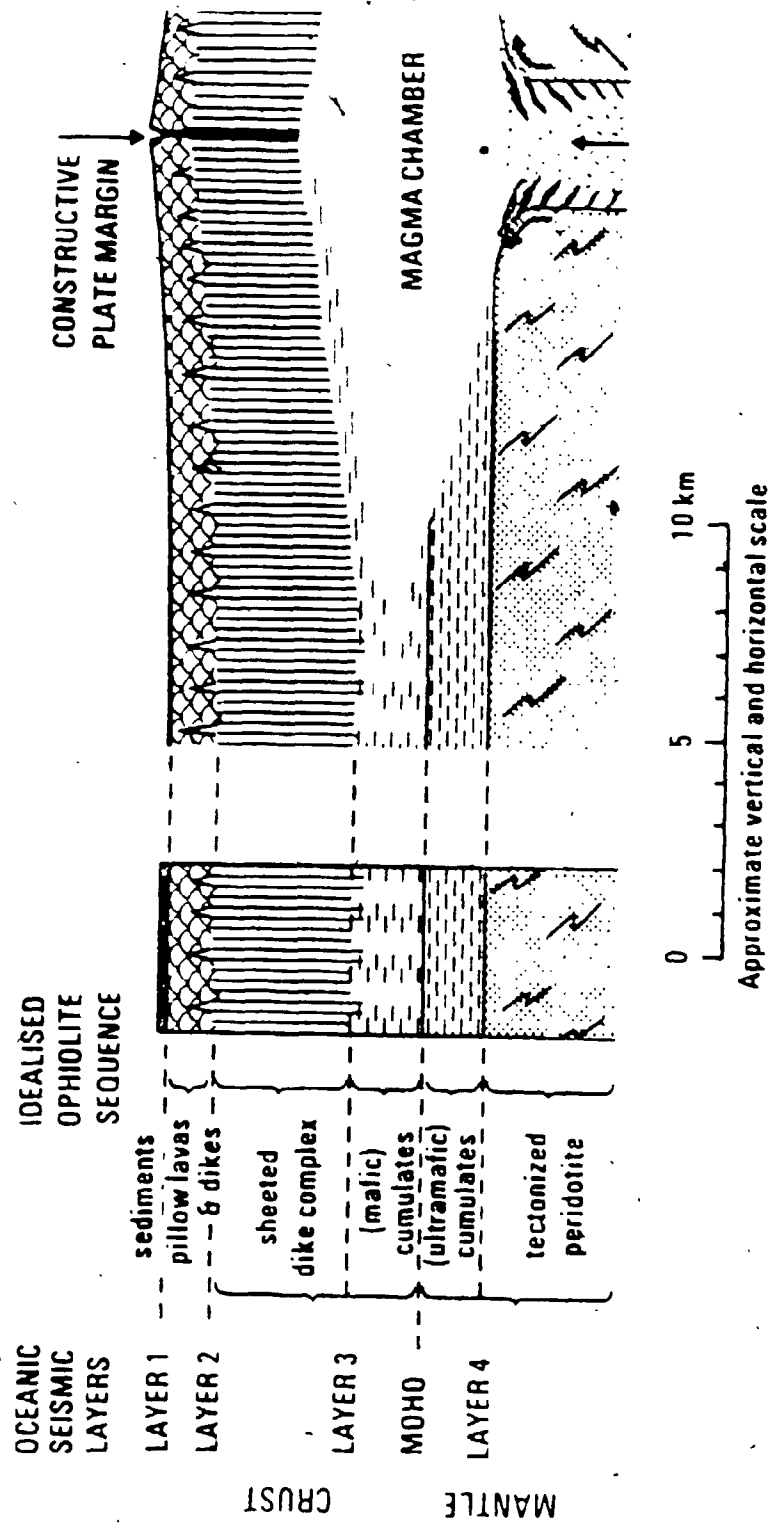
Chemical, structural and seismic studies (e.g. GASS, 1968; THAYER, 1969; CANN, 1970; COLEMAN, 1971; DEWEY and BIRD, 1971; MOORES and VINE, 1971; PEARCE and CANN, 1971; KHAN ET AL., 1972; SPOONER and FYFE, 1973; CHRISTENSEN and SALISBURY, 1975) considered that obducted ophiolites were similar to oceanic crust and upper mantle. The evidence these workers and others produced led to a wider acceptance of the hypothesis that ophiolites are fragments of oceanic crust (COLEMAN, 1977).

This was not a new hypothesis (see DE ROVER, 1957; DIETZ, 1963; GASS and MASSON-SMITH, 1963; HESS, 1965) but it gained wider acceptance because it fitted in with the newly developing theory of plate tectonics which showed that mid-oceanic rifts are divergent plate margins where oceanic lithosphere is formed and then spread out on both sides, only later to descend back into the mantle at ocean trenches (UYEDA, 1978). Presumably then, accidents could occur at ocean trench sites leading to the uplift and preservation of fragments of ocean crust, the process of obduction. Figure 2.2 is a model suggested for the ophiolites of the Middle East. It is an approximately true - scale sketch for the emplacement of Mideast ophiolites by the collision of a subduction zone with a continental margin.

2.3. COOLING OF OCEANIC LITHOSPHERE

Heatflow measurements near seafloor spreading centres (SCLATER and FRANCETEAU, 1970; LISTER, 1972) showed that the conductive thermal flux recorded could only account for less than half the expected flux based on theoretical calculations even though the decay of topographic height away from most of the ridges was in accord with lithosphere arriving at the ocean floor at its melting point (DAVIS and LISTER, 1974). Careful analysis of heat flow values over medium scale oceanic near-rift topography strongly suggested that

Fig. 2.1. Schematic section of an ideal ophiolite. after GASS, 1980.



convective hydrothermal circulation was occurring beneath the ocean floor rocks, and that this was the mechanism causing the difference between the expected and measured thermal flux. Utilizing this difference, the heat flow drawn by seawater convection per unit area of fresh ocean crust is estimated to be $15.1 \times 10^{-6} \text{ cal/cm}^2$ for slow spreading ridges and $11.5 \times 10^{-6} \text{ cal/cm}^2$ for intermediate to fast spreading ridges (WOLERY and SLEEP, 1976). Hydrothermal heat transfer has also been calculated experimentally by extrapolating the ratio between the concentration of ^3He and the fluid temperature measured in hydrothermal solutions discharging from the axial zone on an ocean ridge to the total oceanic flux of ^3He (JENKINS ET AL., 1978).

2.4. CONVECTIVE HYDROTHERMAL CIRCULATION AS AN OCEAN LITHOSPHERE COOLING MECHANISM

In addition to conduction, a heat transfer mechanism involving the gross displacement of matter becomes a viable possibility in situations such as mid-oceanic ridges where a heat source (magma) cools in a permeable environment saturated with fluid. The possibility of this occurrence has been shown by FYFE and LONSDALE (1981) to depend on the attendant geothermal gradient exceeding the adiabatic gradient:

$$-\delta T/\delta r = \theta g T/C$$

where θ is the coefficient of thermal expansion;

C is the specific heat at constant pressure;

g is the acceleration due to gravity.

STRAUS and SCHUBERT (1977) report that in a system where the matter being displaced is pure water, the adiabatic gradient is greatly exceeded whenever the geothermal gradient exceeds 25°C/km , meaning that thermal convection is

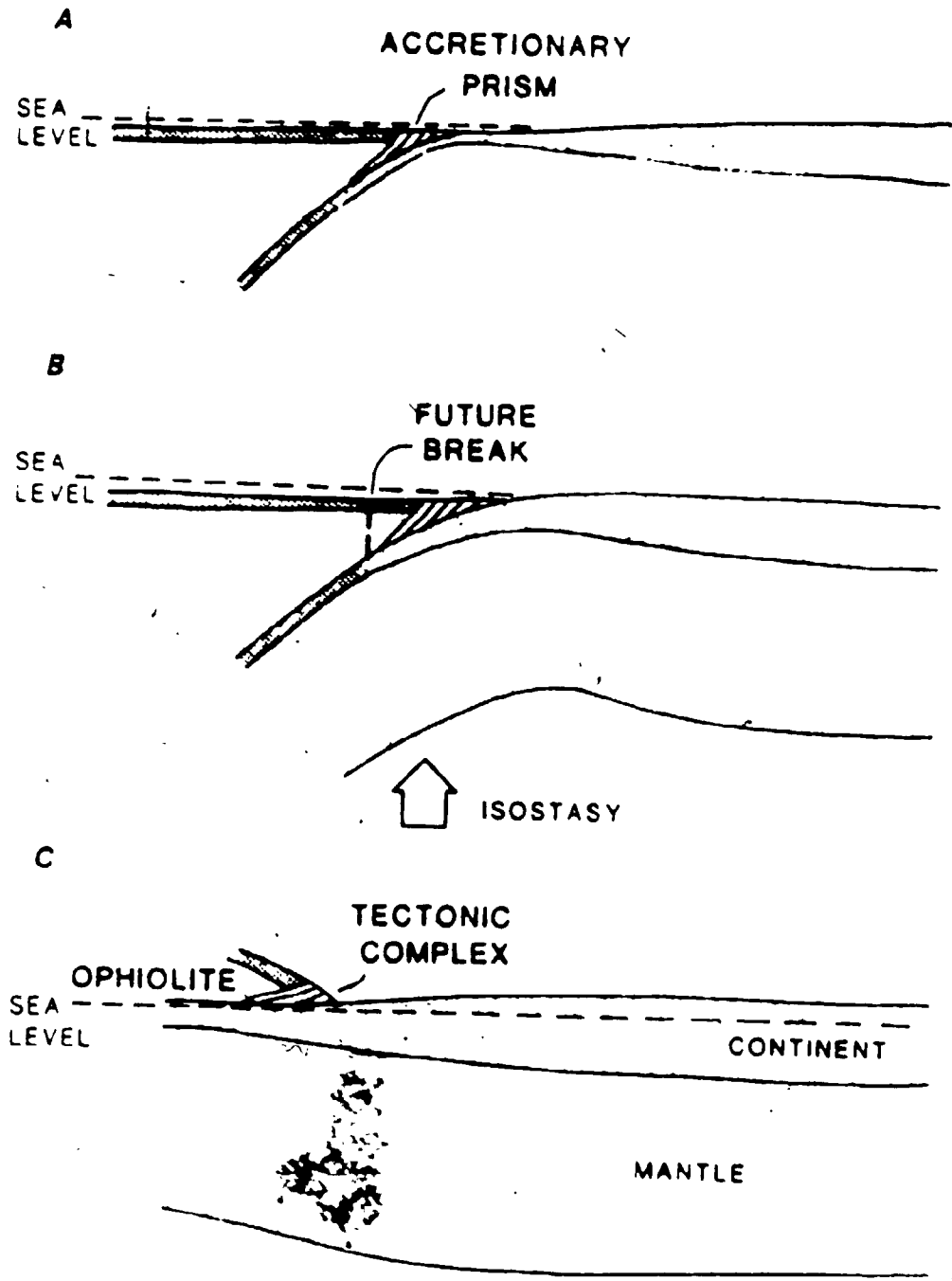


Fig. 2.2. Model for the formation of Middle East ophiolites. After MOORES ET. AL., 1984.

possible for almost all possible ocean floor gradients (FYFE and LONSDALE, 1981). Significant flow depends on a finite permeability and the onset of convective flow has been described by the Rayleigh number in the form:

$$R_s = \kappa \beta \Delta \theta g H / \kappa_\mu \eta$$

where κ is the permeability,

β is the coefficient of thermal expansion of the fluid,

$\Delta \theta$ is the temperature gradient,

g is the acceleration due to gravity,

H is the thickness of the permeable layer,

κ_μ is the thermal diffusivity of the saturated medium,

and η is the kinematic viscosity of the fluid.

$$\kappa_\mu = km / \rho \cdot C_p$$

where km is the thermal conductivity of the permeable medium, and

ρ is the fluid density.

C_p is the specific heat of the fluid.

$\eta = u / \rho$; where u is the dynamic viscosity.

Figure 2.3 illustrates a schematic model for the cooling of oceanic lithosphere by the convective mass transfer of seawater.

Actual convective flow depends on the Rayleigh number exceeding a critical value (ELDER, 1976) and the vigour of convection is directly proportional to the amount by which this value is exceeded.

LAPWOOD(1948), in his work on the onset of thermal instability in fluid-saturated porous material heated from below, determined the critical value to be:

$$R_s = 4\pi^2 (39.48).$$

A major problem with seafloor modelling is the issue of rock permeability at these sites (FYFE and LONSDALE, 1981). Initial permeability is created in the oceanic crustal rocks by brittle contraction and fracture as basaltic magma of density 2.7 - 2.8g/cm³ crystallizes to basalt with a density close to 3.0g/cm³ (DALY ET AL., 1986). This volume contraction in the sheeted dykes and gabbros creates a porosity in the range 5-10%. Several approaches have been taken to the question, and disregarding models which assume no convective heat transfer across the ocean floor (FEHN and CATHLES, 1978, 1979 ; PATTERSON and LOWELL, 1972), another class of models (BODVARSSON and LOWELL, 1972 ; LOWELL, 1975 ; SLEEP and WOLERY, 1978) assumes a permeability controlled by discrete, widely spaced fractures with convective heat loss (see fig. 2.3) These tend to fit the heat flow data (RONA and LOWELL, 1982), and typical calculations consider vertical fractures of a few mm width and separated distances of the order of km to yield permeabilities in the range 10⁻⁸ to 10⁻⁹ cm². Using this range for k in the compilation of Rayleigh numbers at seafloor sites, R_s greatly exceeds 4π² - indicating vigorous convection.

Calculations (SLEEP and WOLERY, 1978) show that a few continuous wide aperture fractures (flow is proportional to width³) can generate a large average bulk permeability.

2.5. CHEMICAL AND MASS ASPECTS OF SEAWATER-OCEAN CRUST INTERACTION

Chemical changes occurring in seawater and ocean floor crust due to their interaction depend on the flowrate, water/rock ratio and temperature of alteration (FYFE , 1978 ; SEYFREID and MOTTLE , 1982). Flowrate is proportional to rock permeability, while controlled by gradient; alteration temperatures are also a function of attendant geothermal gradients. Water/rock ratios are estimated using heatflow studies where it is known that about 12.5 km^3 of new oceanic crust must be formed each year at the ocean ridges to account for seafloor spreading (HEIRTZLER, 1972). Cooling of this magma eventually liberates between 25 to 50% of the global heat production (WILLIAMS and VON HERZEN, 1974 ; LUBIMOVA, 1977 ; SMITH, 1978 ; ANDERSON and SKILBECK, 1981) estimated at $2.4 \times 10^{20} \text{ cal/yr}$ (VERHOOGEN ET AL., 1970).

Assuming that this heat goes into raising the temperature of seawater to 100°C then 10^{18} g seawater/yr will cycle through ocean crust. Now depending on the average temperature to which the fluid is actually heated (50 to 300°C : SLEEP and WOLERY , 1978; 100 to 300°C : DAVIS and LISTER, 1977) and assuming circulation occurs through the entire thickness of ocean floor crust, the water/rock ratio will range 5-30 (see FYFE and LONSDALE, 1981). This is a range for "average" oceanic crust, and where flow is focussed in regions of high permeability, usually highly fractured and brecciated, very high water/rock ratios may be attained as shown by SPOONER (1977) whose calculated values reach 100 in the stockwork zones of the Troodos deposits.

2.6. EXPERIMENTAL WORK

Experimental work in this field has sought to duplicate the effects of natural hydrothermal activity on oceanic crust and seawater. The earliest experiments (HAJASH, 1975; BISCHOFF and DICKSON, 1975; HELGESON and KIRKHAM, 1976; SEYFRIED and BISCHOFF, 1977; BISCHOFF and SEYFRIED, 1978; MOTTLE and HOLLAND, 1978; SEYFRIED ET AL., 1978) were carried out before the 1979 discovery and sampling of hydrothermal fluids venting on the ocean floor at 21°N on the East Pacific Rise (RISE Project Group, 1979). These experiments showed that seawater is transformed from a slightly basic Na-Mg-Cl-SO₄ dominated solution to a slightly acidic Na-Ca-Cl dominated one during interaction with basalt. The experiments indicated that acidity and Mg uptake were important factors in the solution of metals.

Several workers also reported the discrepancy between the virtual absence of anhydrite in submarine rocks and its consistent appearance in all seawater-basalt experiments. BISCHOFF and SEYFRIED (1975) in their investigation of the behavior of heated seawater found that a magnesium-hydroxy-sulphate-hydrate (MHS) precipitates out early in seawater-basalt interaction, and that this hydrate plays an important role in the generation of acidity.

According to their findings, anhydrite precipitates out of seawater at 150°C thus reducing the concentration of Ca and sulphate in sea water. Above 250°C the Mg content begins to drop and the H⁺ content begins to rise. Magnesium hydroxy sulphate hydrate begins to precipitate out at this temperature till about 500°C. In the process of doing so, extracting sulphate from solution thus partially redissolves anhydrite. The incorporation of a Mg(OH)₂-like component into the MHS is responsible for the increase in H⁺. This increase in acidity of the heated seawater and related Mg depletion are crucial to metal extraction

during basalt-seawater interaction at elevated temperatures (ROSENBAUR and BISCHOFF, 1983).

Post 1979 experiments (e.g. SEYFRIED and BISCHOFF, 1981 ; SEYFRIED and MOTTLE, 1982 ; ROSENBAUR and BISCHOFF, 1983) acting on the basis of temperature and water/rock information obtained from the direct observation and study of venting fluids at 21° N EPR have been better constrained though yielding results in the same trend as earlier experiments. With regard to the most important factors regarding sub seafloor convective activity, direct observation and sampling at 21°N EPR and other sites investigated since then (e.g. EMBLEY, 1986) has revealed that the discharging fluids jet out of ocean crust at temperatures of up to 350°C and at flow rates of up to 100Kg/Sec and are particulate laden; their chemical composition is quite different from that of seawater (table 2.1).

Table 2.1: Composition of seawater and ventfluids in ppm from 21°N.

	FLUID pH	Mg	Ca	K	SO ₄	SiO ₂
Sea	7.9	1315	420	393	2755	10
Vent	3.6	0	862	978	0	1291

(After EDMOND, 1981.)

Concentrations of Ba, B, Li and K in the ventwater indicate that it is derived from basalt-seawater interaction at water/rock ratios of less than 3, thus indicative of a strongly rock dominated system (SLEEP, 1983).

However, a qualitative difference exists between water/rock ratios when dealing with heatflow and water/rock ratios in the case of chemical interaction.

In the former, the term relates the volume of seawater to the volume of rock from which the heat is extracted while in the latter it relates the volume of seawater to the volume of rock with which it reacts chemically. ROSENBAUER and BISCHOFF(1983) remind us that heat exchange can occur without chemical reaction.

Chapter Three

THE GEOLOGY OF CYPRUS.

3.1. INTRODUCTION

Located between 34° and 36°N latitude and 32° and 35°E longitude Cyprus is situated between the Anatolian Plateau to the north and the African Shield to the south. On the basis of geology and topography, the island is divisible into four main zones trending east-west and convex to the south (fig.3.1). From north to south these are: The Kyrenia Range consisting of a core of brecciated and recrystallized limestone and flanked on either side by sheared chinks and shales and intercalated with contemporaneous lava flows and sills. The Mesoria Plain, consisting of the northward dipping strata of the Mesoria group which lie with marked angular unconformity on tightly folded flysch. The Troodos Complex with a core of basic and ultrabasic rocks showing varying degrees of serpentinization surrounded by the Sheeted Complex and Pillow Lavas, occupying a roughly oval area of 3000km² in south western Cyprus with two small inliers, Troulli and the Akamas peninsula to the east and west respectively (BEAR, 1963).

The Mamonia complex to the south of Troodos, and separated from it by the east - west trending Arakapas fault belt that has been described as a fossil transform belt (MOORES and VINE, 1971). The complex is also known as the Limassol Forest Complex and is a severely deformed antiformal plutonic structure which is composed of a host rock of tectonized harzburgite and extensively serpentinized dunite and an intrusive suite of ultrabasic and basic plutons and dykes. Current studies suggest that the complex formed in an oceanic transform fault (MURTON and GASS, 1984), and is possibly a subduction melange (MOORES ET. AL., 1984). Figure 3.1. is a geologic map of the Troodos ophiolite complex. The inset map illustrates 3 main geologic regions of the island.

Fig. 3.1.
Geologic map of the Troodos ophiolite. After BEAR, 1963.



3.2. THE TROODOS OPHIOLITE COMPLEX

The Troodos ophiolite complex is the dominant geological feature of Cyprus. It occupies the central third of the island and is covered by one of the largest recorded positive gravity anomalies on the planet which attains a maximum of over 250 milligals over the center of the complex. The rocks of the ophiolite form the basement complex to sedimentary rocks of upper Maastrichtian -Tertiary age composed of deep to shallow abyssal marls and chalks which range 500-800m in thickness. No continental rocks are evident on Cyprus (WILSON,1959).

The complex has been divided into three parts for descriptive purposes (WILSON,1959; GASS and MASSON-SMITH,1963; GASS,1967). These are the Pillow Lavas the Sheeted Complex and the Plutonic Complex (fig.3.1). Extensive late Tertiary uplift of up to 2km (GASS and MASSON-SMITH,1963; ROBERTSON,1977) centres on what is believed to be a serpentinite diapir whose apex is Mt.Olympus which forms the topographic high point of the island and consists of the deepest rock type of the ophiolite. The combined effect of the serpentinite diapirism and erosion on Cyprus has been one of "reversed stratigraphy" where the summit of the ophiolite consists of the deepest lying rock type and the periphery is composed of pillow lavas locally overlain by Mn-Fe oxide chemical sediments-umbers.

The Plutonic Complex is exposed in the Mt.Olympus area and to the south in the Limassol Forest Area (MOORES and VINE,1971). It is composed of coarse to fine grained intrusives of gabbroic, dioritic, tonalitic and trondhjemitic composition collectively termed the High Level Intrusives which overlie the gabbros and ultramafics of cumulate origin. Tectonized harzburgites with a gneissic foliation and lineation which include lenticular dunite pods with accessory chromitite occur at the base. A dunite layer occurs above the harzburgites

(GASS,1980). The ultramafic rocks show extensive partial to complete serpentinization (BEAR,1960).

The entire complex is overlain gradationally by the Sheeted Complex, a massive dyke swarm consisting of 90 to 100% dykes intruded into screens of pillow lava in the upper part and plagiogranites and gabbroic rocks in the lower part.

Troodos harzburgites show a well developed tectonic foliation made prominent by the metamorphic segregation of olivine and orthopyroxene. The attendant texture is xenoblastic granular and the rock is composed of a minimum of 70% olivine and up to 30% orthopyroxene by mode. Clinopyroxene is also present as isolated grains of Cr-diopside, usually less than 5% of the mode. Cr-spinel consists of up to 2% of the mode.

Up to 20% of the total harzburgite outcrop at Troodos consists of irregular lenticular masses of dunite. Minor bodies of gabbroic and lherzollitic composition also occur. All these masses appear to have undergone similar deformation. The olivine of the dunites is of the same composition as that of the harzburgites. The chromite has high Cr/Al ratios and occurs as layered euhedral grains, suggesting that the dunite pods are of a cumulate origin (BEAR,1960 ; MOORES and VINE,1971 ; GREENBAUM,1977 ; GASS,1980).

The chemical and mineralogical homogeneity of the tectonized harzburgites has suggested to several workers (e.g. MOORES and VINE,1971 ; GREENBAUM,1972 ; MENZIES and ALLEN,1974 ; GEORGE,1975 ; KAY and SENECHAL,1976) that they represent the residue of a plagioclase lherzollite mantle from which basaltic liquid has been extracted to form the overlying cumulate plutonics, sheeted dykes, and pillow lavas. However, the recent work by

ROBINSON ET.AL.(1983) on fresh volcanic glass from Troodos leads them to the conclusion that the basaltic rocks of Troodos may represent liquids from an already depleted mantle source.

The tectonized harzburgites are overlain by one and two pyroxene and olivine bearing gabbros of a cumulate texture. These in turn are overlain by high level intrusives composed of isotropic gabbros and acidic, leucocratic rocks which also appear to be differentiates (ALDISS,1978). These high level intrusives range in thickness from 50 to 800m (GASS,1981) and form the base to the Sheeted Complex. They tend to be of subophitic texture and are typically composed of varying amounts of clinopyroxene, Ca-plagioclase, minor orthopyroxene and titanomagnetite (GASS,1980).

The Sheeted Complex is a N-S vertical dyke swarm that extends E-W across strike for more than 100km (BEAR,1980) and contains little or no host rock. It has been divided into an upper Basal Group composed of 90-100% dykes with screens of pillow lava and a lower Diabase Group composed of dyke swarms composed of 100% dykes (MOORES and VINE,1971). The mechanism of intrusion appears to have been one of multiple injections whereby a freshly extruded dyke intrudes into the centre of a preexisting dyke, only to be later intruded into by a later dyke itself (fig. 3.1). Multiple intrusive and extrusive episodes appear to have taken place over a period of time. The injection mechanism necessarily implies a tensile tectonic environment in an upwelling zone of mantle convection.

Individual dykes vary in width from 0.1- 5m and are fine to medium grained, mostly aphyric, non-vesicular with ophitic to variolitic textures. Though commonly affected by metamorphism, the igneous textures have not undergone significant transformation.

Pillow lavas and flows with sparse to abundant breccia relatively free from intrusives comprise the Pillow Lavas (WILSON, 1959 ; PANTAZIS, 1967). Only the uppermost pillow lavas contain olivine phenocrysts, which are commonly altered, and have been subjected to zeolite facies metamorphism. The lavas extend around the ophiolite complex at its periphery forming the uppermost 2-3km in the pseudostratigraphy.

Early workers at Troodos (WILSON, 1959 ; CARR and BEAR, 1960 ; GASS, 1960) recognised that the sequence could be divided into an upper and lower unit on the basis of field, petrographic and geochemical criteria.

The Upper Pillow Lavas are dominantly olivine and clinopyroxene phyrlic basalts with picritic units which in some locations lie unconformably on the oversaturated aphyric basalts of the Lower Pillow Lavas (GASS, 1980).

Later studies of the metamorphism of the lavas (GASS and SMEWING, 1973 ; SMEWING, 1973;1975) suggested that a metamorphic discontinuity separates the two lava units. Based on the spatial distribution and paragenesis of the metamorphic minerals encountered, GASS and SMEWING (1973) suggested that the Lower Pillow Lavas were metamorphically conformable with the underlying Sheeted Complex while all the Upper Pillow Lavas lay in a distinctly separate metamorphic facies. They suggested after BEAR (1960) that the Lower Pillow Lavas and the dykes of the Sheeted Complex were cogenetic and were metamorphosed at or near a spreading axis. They further suggested the term Axis Sequence to collectively describe these rocks, and the term Off-Axis Sequence for the Upper Pillows which they interpreted as being products of off-axis volcanic activity.

However, some of the more recent geochemical studies (ROBINSON

ET.AL.,1983 ; SCHMINCKE ET.AL.,1983 ; MALPAS and LANGDON,1984 ; RAUTENSCHLEIN ET.AL.,1985) working mainly with fresh volcanic glass still preserved from Troodos, and integrating this with field studies and petrographic work reject the thesis that the pillow lavas may have been pervasively altered as previous studies such as those of GASS and SMEWING,1973 and SMEWING,1975 have suggested. They point out that the large quantities of fresh glass preserved at Troodos is not consistent with a pervasive metamorphic event. These studies also have suggested the presence of two distinct volcanic suites, but state that they do not necessarily coincide with the earlier suites, and that in many instances the division is stratigraphically lower.

The upper suite is said to be a picrite-basalt-basaltic andesite assemblage of boninitic affinity while the lower suite is an andesite - dacite - rhyodacite assemblage of tholeiitic affinity.

The glass compositions reveal the existence of two major magma suites apparently corresponding to distinct stratigraphic intervals. The basal 400 - 500m of the sequence consists of the andesite - dacite - rhyolite assemblage containing abundant hyaloclastites. The remainder of the extrusives comprises a basalt - basaltic andesite assemblage with high MgO and low TiO_2 and low total iron. Neither of these two compositions is typical of mid - ocean ridge environments. The lower sequence most closely resembles and evolved arc - tholeiite while the upper sequence appears similar in some respects to boninitic lavas or high - Mg andesites. To date, there has been no field evidence to suggest that there is a structural or metamorphic discontinuity between the two suites, i.e. the two appear to be closely related in time. The close association in time and space of the two suites is similar to that observed in the Mariana and Bonin arcs (MEIJER, 1980; CRAWFORD ET. AL.,1981) and is suggestive of a genetic

relationship. The lavas have a higher than MORB volatile content, and it is this feature together with their geochemistry that suggests that they were erupted in a subduction zone environment, probably in an arc or fore-arc setting. However, the absence of pyroclastic rocks and the relative thinness of the crustal section at Troodos indicates that a mature island arc never developed (ROBINSON ET AL., 1983).

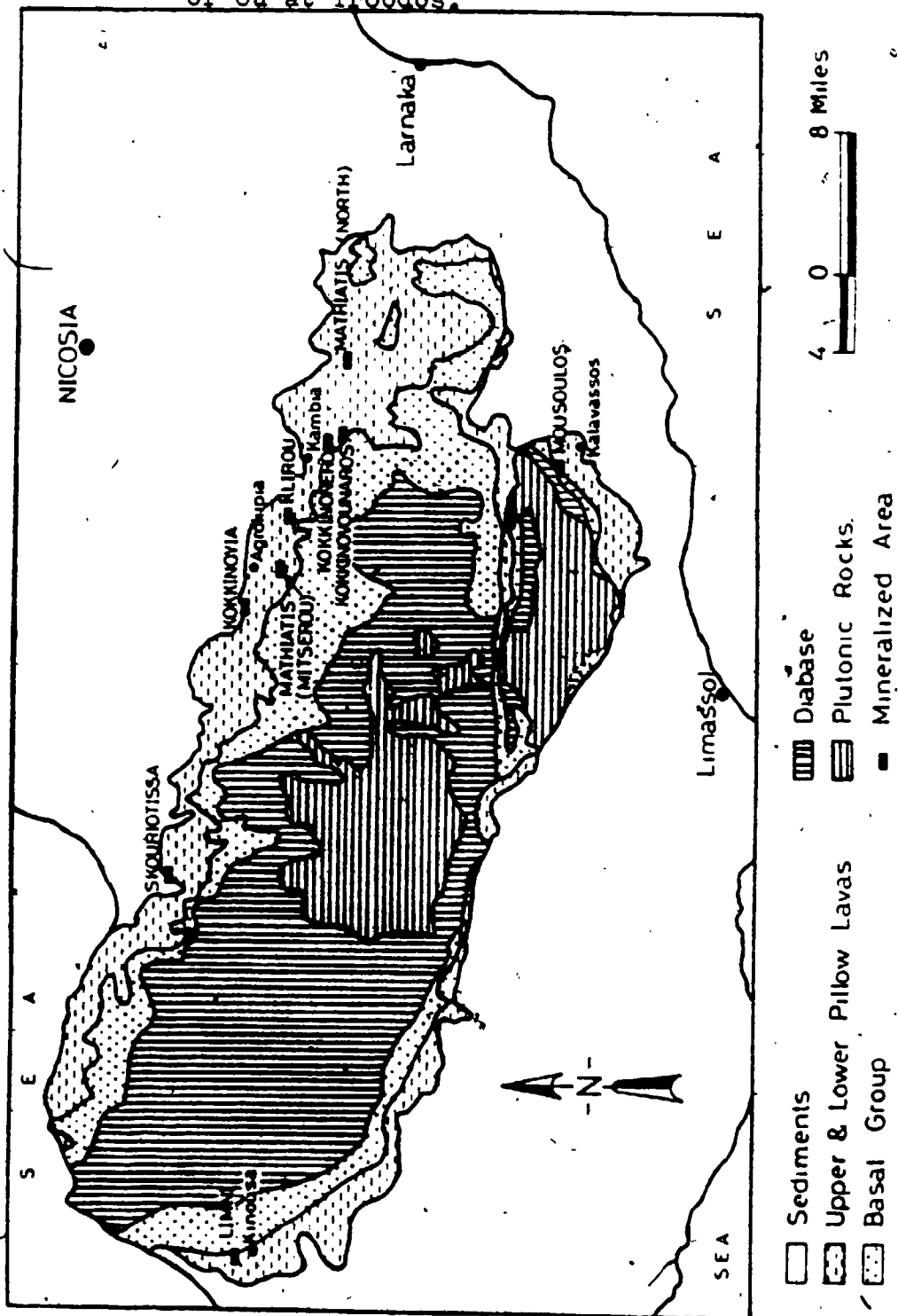
3.3. CYPRUS-TYPE MASSIVE SULPHIDES

Copper, or "Cyprian metal" as the ancients called it, was first mined on Cyprus 7,000 years ago by the ancient Egyptians who previously in neolithic times had mined the metal in the Wadi Magharah and from Sarabit at Khadim in the Sinai Peninsula (BUDGE, 1926).

Indeed, the name copper is derived from Cyprus, and the island is the type locality for massive and disseminated copper-bearing pyritic orebodies occurring in ophiolite complexes (COLEMAN, 1977). At Troodos, these orebodies occur in the pillow lavas close to the sediment/lava interface as massive and disseminated sulphide lenses underlain by funnel shaped stockwork zones (BEAR, 1963; SEARLE, 1972; CONSTANTINO and GOVETT, 1973). In general, the ore lenses are conformable with the pillow lava sequence and occur as disseminations in pillow lavas averaging 20% sulphur or as massive deposits with 40-50% sulphur and 1-4% Cu (BEAR, 1963). Pyrite and marcasite are the most abundant primary sulphides and are associated locally with small amounts of Cu and Zn ore of patchy distribution and include primary chalcopyrite and sphalerite. Quartz and chlorite are persistent gangue minerals (BEAR, 1963). The orebodies are typically zoned, and are located at the fringes of the ophiolite only because they are in the lavas (fig. 3.2).

Originally, they were of size range 1-10 x 10⁶ tons, the largest and richest

Fig. 3.2. Location map of the main sulphide deposits of Cu at Troodos.



having been the Mavrovouni deposit which contained about 15×10^6 tons of ore at between 3.5 and 4.5%Cu. (BEAR, 1963). Associated with these sulphide deposits are oxidized manganese and iron deposits, the "umbers", which represent late stage (post - sulphide deposits) waning hydrothermal activity whose exhalations underwent oxidation via mixing with seawater.

3.4. SUMMARY

Mineralogical, geochemical and structural evidence indicates that the Troodos ophiolite complex was extracted from pristine or depleted mantle in an extensional environment in an island arc or fore-arc setting. The presence of a well developed sheeted complex argues strongly for a major spreading component. The massive sulphide and oxide deposits of the complex occur in the uppermost pillow lavas and have a hydrothermal origin.

Chapter Four

TROODOS PETROLOGY

4.1. INTRODUCTION

Representative samples of sheeted dykes, gabbros and peridotites from the Troodos Ophiolite Complex were sectioned and examined petrographically to determine the igneous and metamorphic mineral assemblages and textural relationships. The mineral chemistry of the different phases studied was determined by electron microprobe analysis whereas X-ray diffraction analysis was used to identify very fine grained alteration minerals occurring in shear zones and veins.

4.2. IGNEOUS PETROGRAPHY

Troodos diabase dykes are of a dull grey colour, non-vesicular, aphanitic, uniformly textured and commonly exhibit one way chill margins of subhorizontal to vertical orientation. Later dykes at different orientations are commonly observed transecting earlier ones. Ca-plagioclase of labradorite composition is the dominant mineral phase comprising 50 to 60% of the mode. It occurs as clear, colourless subhedral to euhedral laths and exhibits characteristic albite and carlsbad twinning. Augite clinopyroxene is second in abundance to Ca-plagioclase. It is of subhedral to anhedral granular habit, colourless to pale green and occupies 30 - 40 % of the mode. Fe - Ti oxides, mainly titanomagnetite and ilmenite as well as a minor amount of orthopyroxene constitute the rest of the rock mass. The diabase dykes examined from Troodos exhibit a variety of textures which are related to the grain sizes of the constituent minerals. In the fine grained diabase, the dominant texture is microporphyrictic (plate 1.). In these rocks, the groundmass is composed of subcalcic augite, small amounts of orthopyroxene, Fe - Ti oxides and plagioclase.

Overleaf: Plate 1. All scale bars 100 μ m.

A. Microporphyrlic texture in diabase dykes with microphenocrysts of hydrothermal albite.

B. Contact between two varieties of Troodos diabase. Vein at contact is of chlorite.

C. Alteration of augite to actinolite in diabase. Remobilization of Fe - Ti oxides along actinolite cleavage.

D. Olivine alteration to serpentine in microporphyrlic diabase.

E. Same as B, with late zeolite vein bisecting chlorite vein.

F. Green actinolite forming as a retrograde phase in brown hornblende.

Ca-plagioclase (An60-50) is the major microphenocryst phase. Augite is also a microphenocryst phase but to a lesser extent. Both are of sub to euhedral habit when they occur as microphenocrysts. Olivine is the only other microphenocryst phase present. It occurs in very minor amount and is almost always altered to serpentine. With increase in grain size, usually traceable away from chill margins, the rock texture becomes intergranular, with subcalcic augite interspersed with Ca-plagioclase. In the lower parts of the Sheeted Complex, the rocks become coarser and the dominant feature of the texture here is that it is subophitic; with the subcalcic augite partially enclosing laths of Ca-plagioclase.

PLATE 1



Overleaf: Plate 2. A. Roddingitized gabbro from Troodos. Sample from CY-4 1073m. White zone predominantly anorthite and prehnite with dark patches of diopside and andradite. Diameter of drillcore is 4.7cm. Bar scale = 1cm.

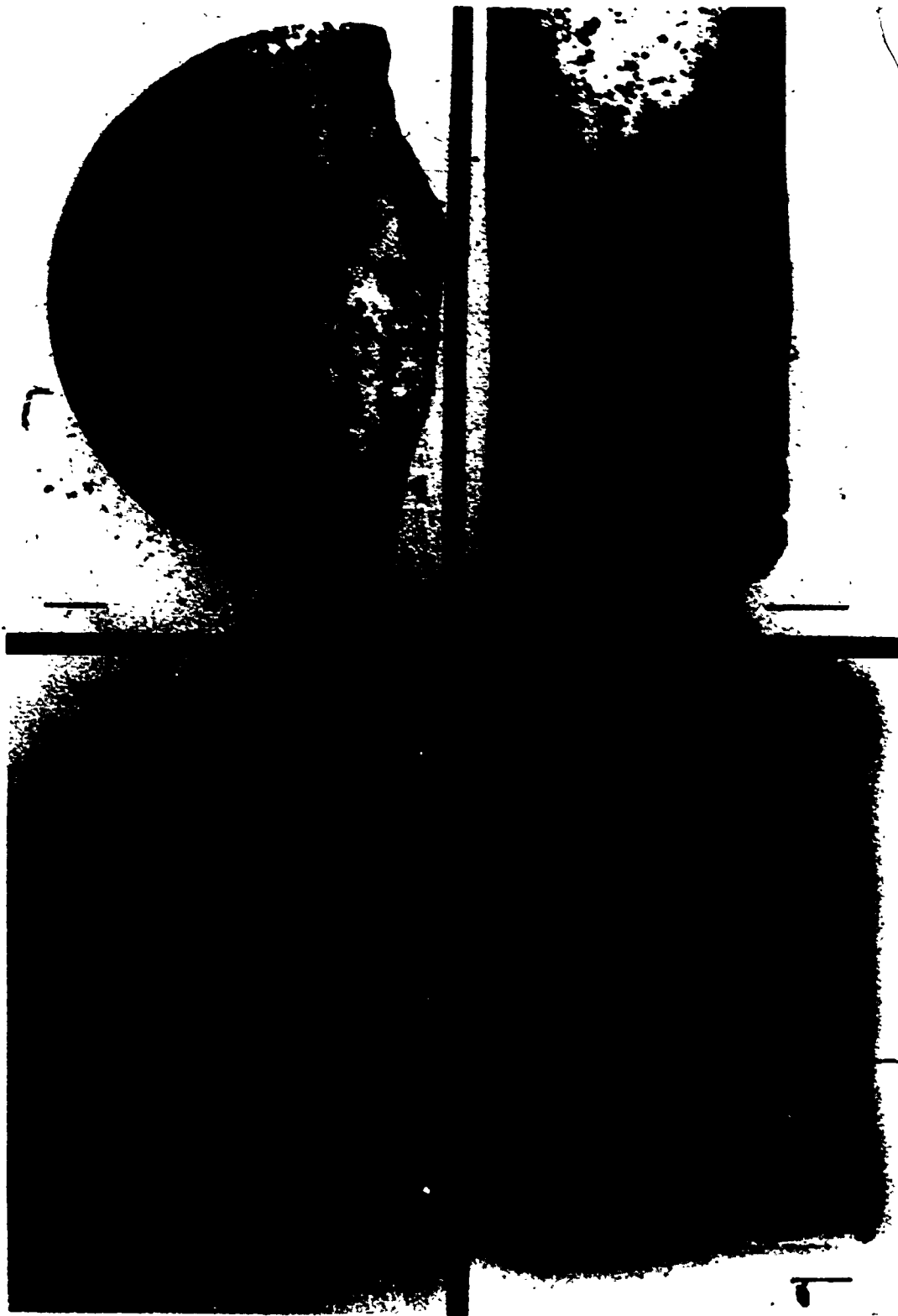
B. Leached, rodingitized gabbro from CY-4 at 1310m. Note porosity generated by hydrothermal fluids. Bar scale = 1.5cm.

C. Intensely altered rodingitized gabbro from CY-4. Dark mineral at top left is andradite garnet. Porosity generated by hydrothermal fluids. Bar scale = 1cm.

D. Epidote (dark patches at bottom), quartz (light areas), anorthite (milky zone bordering on dark diabase at top) alteration in diabase dykes occurring in gabbro at 1074m in CY-4. Bar scale = 0.5cm.

Petrographically the diabase dykes are hence classified as being tholeiitic on the basis of the presence of two Mg-pyroxenes especially in the groundmass as this "...is the hallmark of the tholeiitic basalt in the strictest sense of the term..." (WILLIAMS ET AL., 1982). Proceeding from a depth of about 900m and onwards in CY-4, screens or small bodies of gabbroic rock are encountered. With increasing depth larger and larger screens are encountered until at a depth of about 1200m where the transition to isotropic gabbro is apparently complete. However, that does not spell the end of the diabase dykes for these are still encountered, albeit sporadically, in the isotropic gabbro up to a depth of 1300m. What this shows is that the boundary between the diabase and the gabbros is not a sharp contact, but rather a gradational zone of transition. The presence of fine grained dykes well within and apparently wholly enclosed by gabbroic rocks is problematic and has been taken by some workers (e.g. GASS, 1980 ; 1981 ;

PLATE 2



MALPAS, 1984) to be evidence of the existence of several magma chambers, both spatially and in time, beneath active spreading ridges rather than the presence of one main magma chamber.

The initial gabbroic screens encountered at the base of the Sheeted Complex are light coloured or leucocratic rocks which are visually in high contrast to the dull grey coloured diabase. These rocks are plagiogranites or trondhjemites, so called because their mafic content as a whole is less than 10% of the modal composition. The proportion of these light coloured rocks is very small compared to the other rock types of the sequence; perhaps 2%. Mineralogically the trondhjemites consist of plagioclase and quartz, typically comprising 80 - 100 % of the modal composition. The plagioclase composition ranges An₃₀₋₆₀ with individual grains commonly displaying zoning. Modal quartz varies from 20 to 50 % with grains showing undulose extinction and embayed boundaries. Several textures are present in this rock type with the dominant one being quartz and plagioclase as equigranular aggregates. Graphic intergrowths of the two main minerals (plate 4) is common. The mafic components present, at most comprising 20 % of the mode, are augitic pyroxene commonly altered to fibrous actinolite and brown hornblende. Accessory minerals are iron-titanium oxides, zircon and sphene.

Medium to coarse grained, holocrystalline, isotropic, non-layered microgabbros and gabbros partially to wholly enclose the trondhjemitic rocks. They range in grain size from medium (microgabbros) to coarse grained undifferentiated isotropic gabbros. The medium grained microgabbros are commonly of subophitic texture while the coarser grained variety is of ophitic texture.

Overleaf: Plate 3. All bar scales = 100 μ m

A. Zoned epidote. Cores have higher Fe content than fringes. Groundmass of calcite (lower left) and anorthite (upper left). Section is from metadiabase.

B. Development of anorthite + carbonate + sphene from Ca-plagioclase (relict at lower left).

C. Quartz (lower left) + albite (upper left, white) + anorthite + epidote alteration assemblage in diabase dyke present in isotropic gabbro.

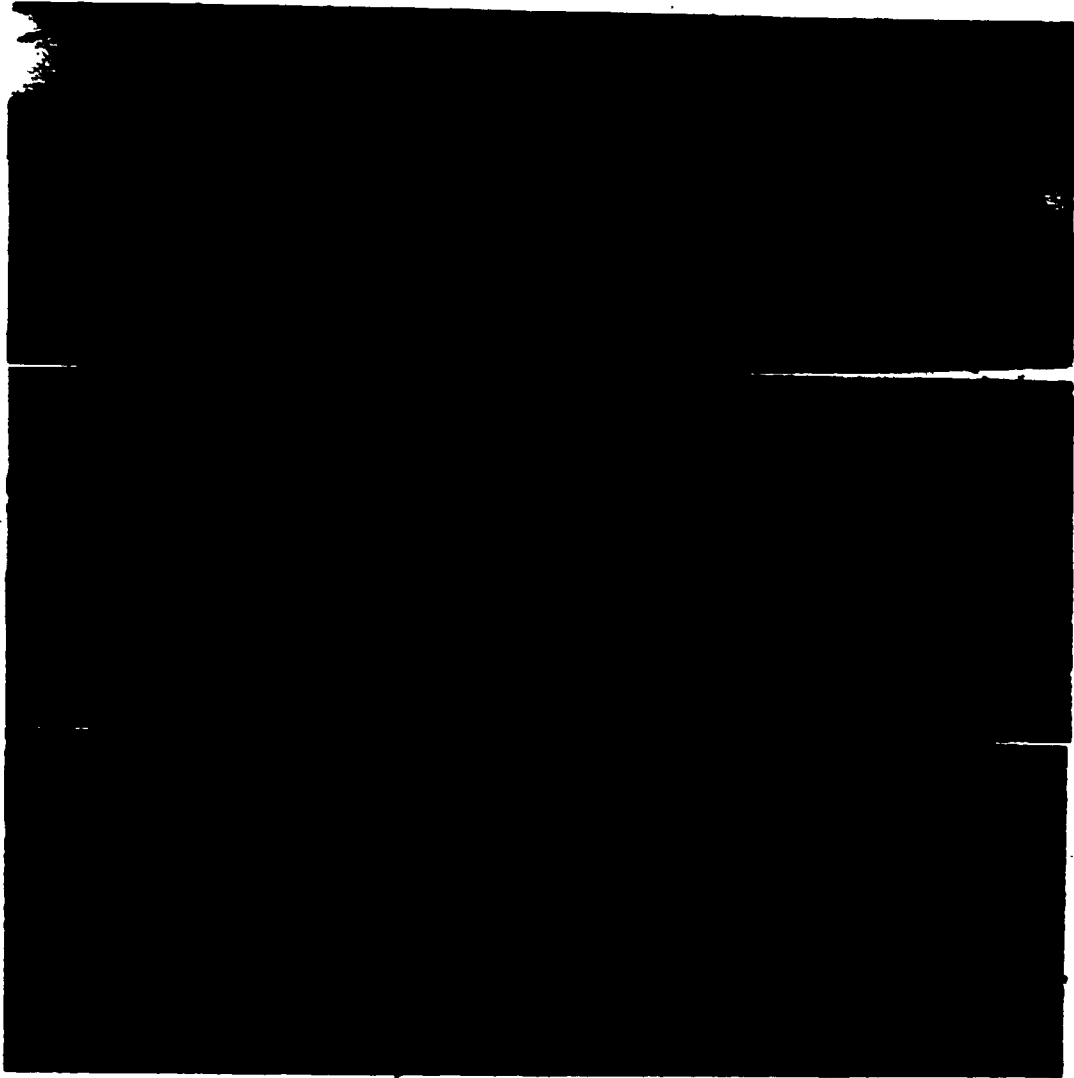
D. Hydrothermally altered plagioclase in amphibolite facies assemblage.

E. Late alteration of D. anorthite to prehnite and epidote.

F. Retrograde alteration of brown amphibole (hornblende) to green amphibole (actinolite) in amphibolite facies containing anorthite.

The plutonic rocks at Troodos have a number of other textures most notably anhedral granular and polycrystalline. The mineralogic make up of the plutonic rocks is essentially similar to that of the diabases with the major difference that they are more calcic in their composition. The plagioclase composition is An50-80, and plagioclase comprises up to 80% of the mode. Next in abundance is diopsidic augite, hypersthene, minor iron titanium oxides and apatite. The diopsidic augite displays exsolution lamellae of orthopyroxene. Hypersthene grains are also frequently observed (plate 8) displaying exsolution lamellae of diopside. The presence of exsolution phenomena indicates that cooling was a slow process in this part of the sequence.

PLATE 3



]

Layered gabbros and cumulate peridotites underlie the isotropic gabbros. Plagioclase steadily diminishes with increasing depth while olivine becomes more abundant. The dominant mineralogy is akin to that of the preceding gabbros. However, modal abundances vary greatly as a function of the layering. The dominant texture is poikilitic caused by coarse grained orthopyroxene enclosing olivine and plagioclase. The cumulate peridotites have cyclic sequences of pyroxenites, wehrlites, troctolites and dunites which are commonly serpentized. Core descriptions by the ICRDG(1985) provide a detailed description of the cumulate layering sequences and variations.

4.3. METAMORPHIC PETROGRAPHY

Rocks of the Sheeted Dyke Complex have been extensively fractured, sheared and brecciated. A detailed inspection of drillcore (CY-4) through 2200m of ophiolite, half of which intersects diabase dykes, leads this writer to conclude that at Troodos, the vein/fracture spacing is 0.1m and that the average aperture of fracture is 3mm. The composition of vein infill is estimated at 95 % laumontite with the remaining 5 % composed of chlorite, quartz, epidote, Fe-oxides, disseminated pyrite, gypsum and other Ca-zeolites such as stilbite and analcime.

The observed alteration at Troodos though extensive, has not been totally pervasive. It is closely related to fractures, shear zones and faults cutting through the diabase and as such the most affected parts are those in close proximity to the aforementioned features. Overall, apart from zones of shearing and brecciation, the igneous textures have not been obliterated though most of the minerals have been transformed.

The major changes involve the alteration of igneous calcic plagioclase to low temperature pure albite and the hydration of mafic minerals. Pyroxenes have been altered mainly to chlorite and actinolitic amphibole, while Ti-Fe oxides have

been altered to magnetite and sphene. Pyrite has been observed on fracture surfaces in the diabase dykes. The minor olivine that occurs as a microphenocryst phase in the microporphyrritic diabase has been replaced by serpentine. Plagioclase still retains its albite twinning and sub to euhedral lath form, but is of light to dark brown colour rather than colourless. Augitic pyroxene has mostly been transformed to chlorite and fibrous actinolitic amphibole (plate 5). It is commonly the last mineral to be transformed.

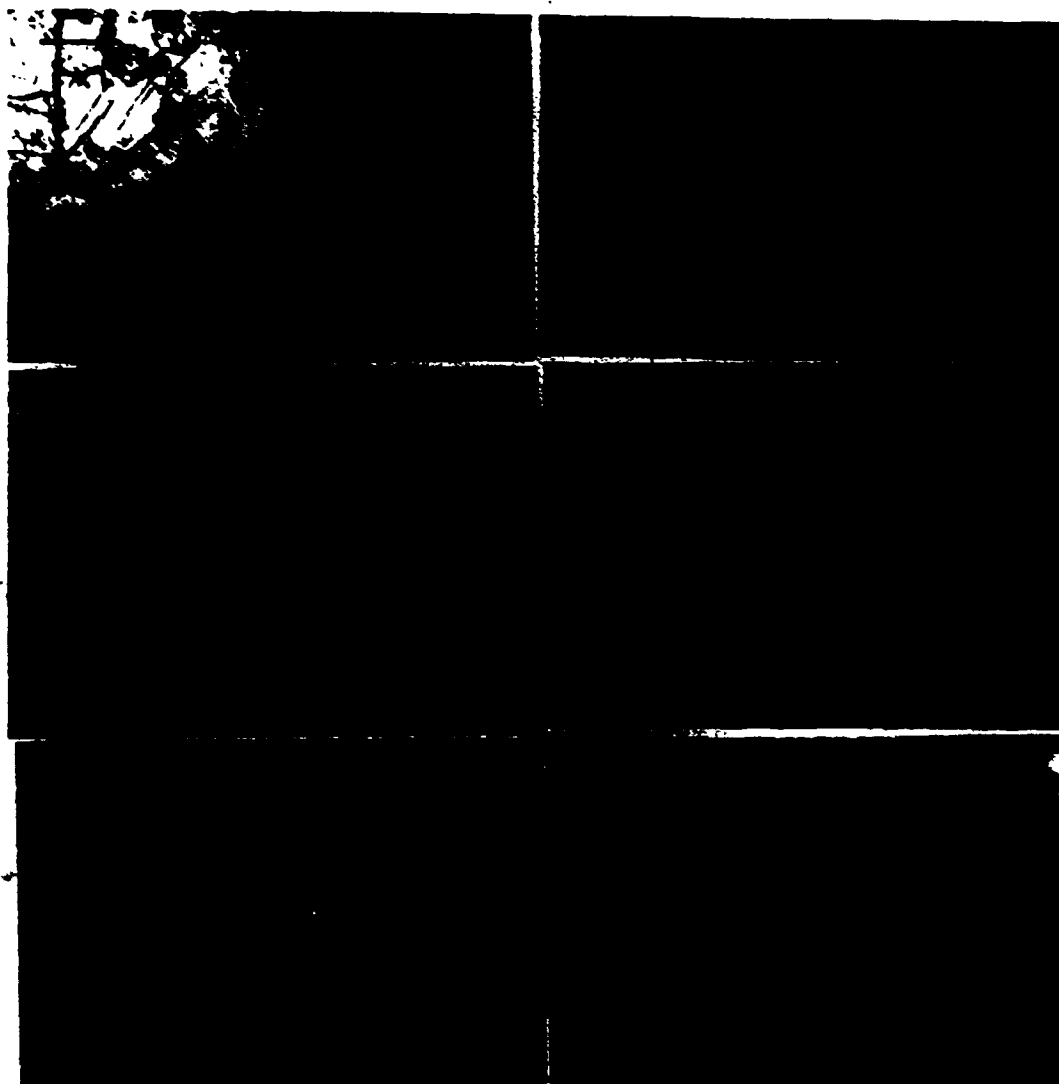
The characteristic post-igneous mineral assemblage for the diabase dykes is albite + chlorite + actinolite + sphene. The presence of zeolite group minerals in the diabase dykes is restricted to late veins and fracture fillings and is here considered as belonging to a late-stage event. The characteristic mineral assemblage for the late-stage event is laumontite + calcite + gypsum.

Quartz and epidote, also vein minerals, are associated together and are separate from the zeolite bearing fractures and veins. They appear to belong to the earlier alteration stage which is responsible for the overall metamorphism of the dykes.

Overleaf: Plate 4. All scale bars = 100 μ m.

- A. Amphibolite facies assemblage of anorthite and hornblende in metagabbro.
- B. Epidote + calcite + albite developed in metadiabase.
- C. Replacement of Ca-plagioclase by An_{95} and prehnite.
- D. Quartz + epidote + calcite assemblage. Fractures in quartz (lower right) filled by late Ca-zeolite (laumontite).
- E. Graphic intergrowth of quartz + plagioclase in trondhjemitic gabbro.

PLATE 4



2-

F. Hydrothermal texture of quartz + albite + opaques in quartz-albite vein in diabase.

The characteristic metamorphic features of the Troodos diabase dykes then, is the absence of penetrative deformation and the presence of a greenschist facies mineral assemblage and a later zeolite facies one most prominent in the fracture system. Metamorphic alteration of Troodos ophiolite gabbroic rocks is similar to that of the diabase dykes in that although it has been extensive, it has not been all pervasive. The major alteration trends observed consist of the extensive alteration or unalutization of clinopyroxenes to actinolite and minor chlorite (plate 5). The alteration is usually complete although in some instances, relict diopsidic augite is still visible. Kelyphitic rims of fibrous actinolite around augite are also observed (plate 7).

Chlorite is not as common in the gabbroic rocks as it is in the diabases. Where present it is usually in small amounts and interstitial to actinolite and plagioclase. Plagioclase (An50-80) has been transformed to more albitic forms (An15-30) and in parts to pure albite (see appendix A.11 for compositions of hydrothermal plagioclase). Plagioclase has also been altered to clinzoisite epidote and prehnite. Fe-Ti oxides have been altered to sphene. Relict titanomagnetite is commonly observed surrounded by sphene which it interpenetrates.

With increasing depth in the gabbroic sequence the composition of the plagioclase progressively becomes more calcic while the hydrothermal actinolite composition is replaced by magnesio - hornblende. The characteristic metamorphic mineral assemblage of the isotropic gabbroic rocks from the Troodos ophiolite is actinolite + chlorite + albite + epidote + sphene.

A change in the amphibole composition is noted with increasing depth and actinolite gradually gives way to hornblende as the major mafic hydrothermal mineral. Retrograde activity is observed via the presence of patches of pale green amphibole (actinolite) in plates of Tl (up to 1%) and Al(>5%)-rich brown amphibole (plate 1).

The alteration assemblage here is hornblende + chlorite + albite + epidote + sphene. This represents a transitional assemblage from greenschist facies to amphibolite facies.

In other words, the isotropic gabbros are characterized by greenschist facies metamorphism, and towards the base of these gabbros, epidote - amphibolite transitional facies are encountered, and lower still, in the region where faint layering becomes apparent, the characteristic metamorphic mineral assemblage is Ca-plagioclase (An70-95) + hornblende.

Overleaf: Plate 5. All bar scales = 300 μ m except A.

A. Relict Ca-plagioclase core in hydrothermal albite in metadiabase. bar scale = 100 μ m.

B. Albite + sphene + serpentized olivine in diabase.

C. Relict cores of igneous plagioclase in metagabbro surrounded by metamorphic phases.

D. Actinolite + Fe-Tl oxides + plagioclase in gabbro. Plagioclase still fresh although the original pyroxene is completely altered to actinolite.

E. Hydrothermal anorthite(top) + sphene + augite crystals + albite (white) in metasomatized gabbro.

PLATE 5



F. Fibrous actinolite + albite in splittized diabase.

This indicates that the transition from greenschist facies metamorphism to amphibolite facies metamorphism is complete and occurs within the isotropic gabbros. Further, though localized, alteration zones exist within the metagabbros and some appear to be due to calcium metasomatism. The zones occur as small patches (up to 1.5m) and some of them may be termed as having been rodingitized. Basically they are altered gabbros whose dominant feature is calcium enrichment in conjunction with silica depletion. They consist predominantly of the calcium-rich silicates diopside, prehnite, anorthite and sometimes andradite and typically occur in close proximity to serpentinized mafic to ultramafic rocks.

In the Troodos ophiolite rodingitized rocks occur as narrow alteration zones up to 0.5m wide in outcrop (pers.ob.) but are mainly exposed in the drillcore studied as narrow bands of an average size of 0.2m. They are of medium grain size and intergranular texture. The dominant mineral is anorthite which commonly tends to be pure, but usually ranges An90-98, interstitial prehnite and relict amphibole since altered to diopside. The Ca-Fe garnet andradite occurs as a coarse yellow-brown mineral which is characteristically fractured, with the fracture apertures filled by late Fe-rich prehnite which appears to be an alteration product of the andradite. Diopside in cases appears to be a dehydration product of actinolite although it commonly is a replacement of augite. Other minerals present include sphene with relict Ti-Fe oxides and leucoxene, with minor calcite. No hydrogrossular has been observed, although a previous study based deeper in the ultramafic pile (BARRISA ET.AL.,1983) at Troodos has identified the phase.

The ultramafic rocks of the Troodos ophiolite sequence have been extensively

serpentinized. Identification of the serpentine minerals carried out in this study indicates that antigorite is the major serpentine mineral present with minor chrysotile. Lizardite is rare. The main vein minerals in this part are prehnite + chlorite + laumontite + minor carbonate. Laumontite + calcite occur as vein minerals throughout the isotropic gabbros and well into the layered gabbros (see ICRDG, 1985). These minerals are also associated with albite and anhydrite, though the anhydrite tends to be localized in the lower sheeted dykes and upper gabbros. Anhydrite occurs locally as a vein mineral associated with calcite and prehnite and laumontite to depths of 1500m in drillhole. The mineral assemblages and nature of occurrence as late veins of this group of minerals suggests a low temperature retrograde metamorphism effected probably by seawater bearing sulphate, bicarbonate and calcium.

Overleaf: Plate 6.

All scale bars = 100 μ m.

A. Prehnite displaying characteristic imperfect columnar "bow-tie" form in metagabbro.

B. Prehnite displaying reniform globular masses, and occurring in contact with hornblende in metagabbro.

C. Serpentinized olivine (upper right). Note expansion fractures propagating into the adjacent amphibole. o D. Hornblende displaying "worm-eaten" texture together with cleavage in metagabbro.

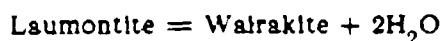
E. Anhydrite in metadiabase displaying characteristic cleavage. Note presence of prehnite (upper left).

PLATE 6



F. Greenschist facies assemblage of albite and fibrous actinolite developed from augite.

LIU(1971), has established the equilibrium curve of the assemblage:



at about 235°C at 0.5Kb, 255° +/- 5°C at 1Kb, 282 +/- 5°C at 2K fluid pressure.

Wairakite has not been identified at Troodos and hence it is assumed that the late stage alteration was well within the stability field of laumontite. However, the hydrothermal breakdown of natural laumontite above its stability range appears to be a very slow process and has been observed to persist as much as 80°C above its true stability limit (LIU, 1971).

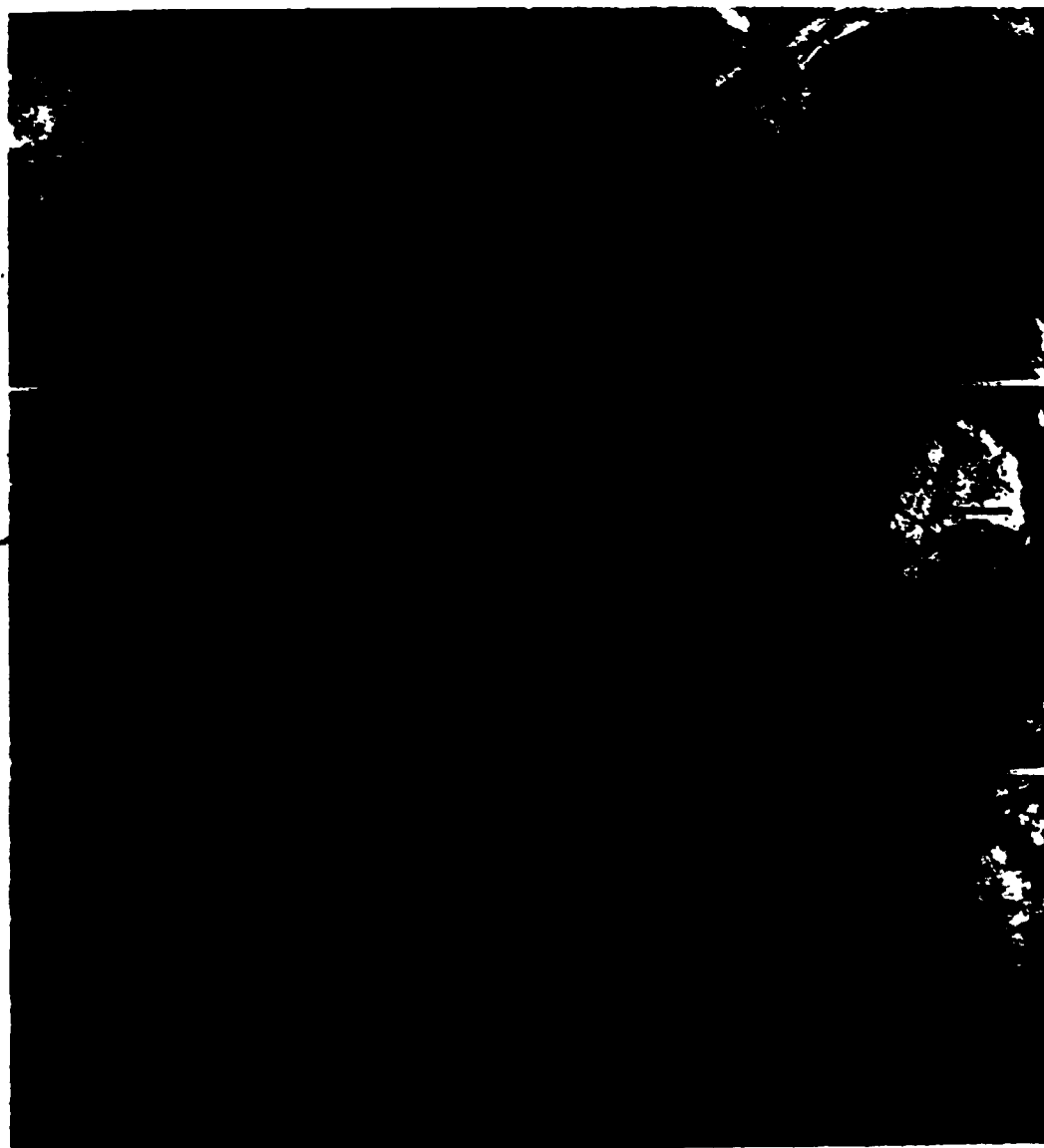
Alteration zones in which quartz and epidote are the predominant alteration minerals are noted sporadically in the lower diabase dykes and upper isotropic gabbros as veins 1-5cm wide, commonly with bleached aureoles usually devoid of ferromagnesian minerals.

One of the most profound manifestations of this type of alteration observed in this study occurs in CY-4 continuously between 1069m to 1074.5m. The extent of the zone, which occurs in diabase dykes which themselves occur in isotropic gabbros, suggests that this type of alteration represents a major effect of basalt-seawater interaction.

Overleaf: Plate 7. All scale bars 100µm.

A. Fibrous prehnite(right) in contact with quartz, sphene and hydrothermal plagioclase.

PLATE 7



B. Prehnite interstitial to anorthite in metagabbro.

C. and D. Alteration kelyphitic rim surrounds clinopyroxene in metagabbro.

C=XPOL, D=PPL.

E. Vein of prehnite + calcite in metadiabase.

F. Fibrous actinolite + altered plagioclase in metagabbro.

Core descriptions published by ICRDG(1985) describe the zone as predominantly white in colour with coarse grained aggregates (up to 5cm) of radiating green epidote crystals occurring in marked contrast to the dull grey colour of the host aphyric diabase whose mineralogy consists of 50% clinopyroxene and orthopyroxene, 40-45 % plagioclase and 5-10% Fe-Ti oxides.

The zone itself shows a mineralogical gradation at its contacts with the diabase. There is no evidence of a structural break between the units implying that the observed bleach zone (Plate 2) was originally an integral part of the diabase, now severely altered. At the onset, the diabase has been whitened by the extraction of the Fe-Ti oxides and their oxidation to coarser, granular sphene and the near total conversion of pyroxenes to the fibrous amphibole actinolite. The texture of the alteration zone contrasts with that of the aphyric diabase in that it is coarser grained and the original igneous textures appear to have been completely obliterated.

Mineralogically the zone consists of about 80% albite of a cloudy dark brown colour which generally shows no twinning except for the ghost outlines of former twins.

Overleaf: Plate 8. All bar scales 100 μ m.

A. Amphibolite facies grade hydrothermal anorthite in metagabbro.

B. Relict core of orthopyroxene surrounded by chlorite. Exsolution lamellae of clinopyroxene altered to actinolite.

C. Fibrous actinolite + plagioclase in gabbro.

D. Vermiform texture of amphibole in metagabbro.

E. Hydrothermal diopside in rodingitized gabbro.

F. Anorthite + hornblende in metagabbro.

Sphene, actinolite and relict clinopyroxenes constitute the rest of the rock. The sphene is of a coarser grain size further away from the diabase and commonly contains inclusions of ilmenite surrounded by coronas of leucoxene. The zone, which is milky white in appearance due to the albite runs parallel to the edge of the mesocratic diabase and grades into a clear white zone dominated by plagioclase, quartz and very coarse grained radiating aggregates of epidote. The plagioclase feldspar, of very coarse grain size, is determined by electron microprobe to be pure (>98%) anorthite composition.

Interstitial to the plagioclase crystals are varying aggregates of prehnite, epidote, quartz and calcite. The epidotes display zoning related to Fe-movement (see plate 3). The epidotes are intergrown with plagioclase and prehnite. The quartz occurs as an equigranular mineral and contains fluid inclusions which form the basis of a study included in this dissertation.

Of particular note is the occurrence of an epidote bearing alteration zone (see

PLATE 8



plate 9) observed deep in the ultramafic sequence of the of the complex in CY-4. To be specific, the zone occurs in medium grey, medium to very coarse grained, cumulate - textured, olivine - bearing websterites which consist of 85% clinopyroxene, 20-25% orthopyroxene and 10-15% olivine.

Overleaf: Plate 9. All bar scales 100 μ m.

A. Plagioclase + hornblende + orthopyroxene in metagabbro. Note retrograde actinolite developing in metagabbro.

B. Radiating clinzoisite + chlorite in ultramafic alteration zone.

C. Relict orthopyroxene core. Exsolution lamellae of clinopyroxene altered to actinolite.

D. Relict of labradorite in anorthite of amphibolite facies metagabbro.

E. (PPL) and F(XPOL). Andradite + retrograde prehnite from rodngitized zone in metagabbro.

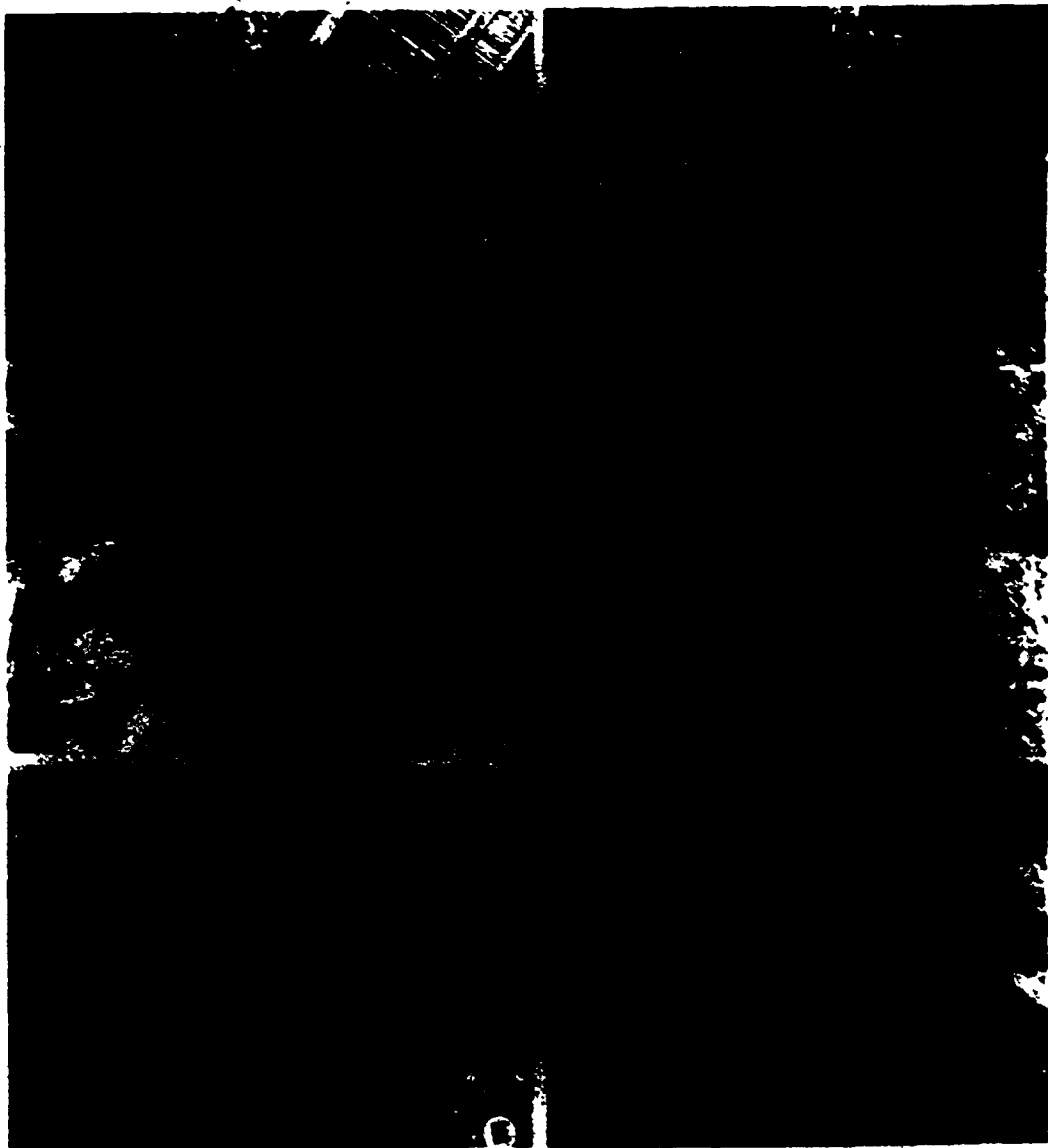
The alteration zone, about 15cm in drillcore, occurs at a depth of 1998.0m (see ICRDG,1985) and has an apple green and light grey colour. It is composed of 70-80% disseminated epidote. The remainder is composed of chlorite, calcite and minor sphene. Fracture planes dissecting the alteration zone are coated with a veneer of black serpentine.

4.4. MINERAL CHEMISTRY

FELDSPARS.

All feldspars in the plutonic rocks of the Troodos ophiolite complex encountered in this part of the study, by electron microprobe, are of the

PLATE 9



plagioclase series and exhibit a marked compositional variation according to their occurrence and extent of recrystallization. Analyses are presented in appendix A10 and A11. The igneous composition of the plagioclase occurring in the diabase and gabbro is dominantly labradorite (An50-80) which displays albite and carlsbad twinning and occurs in euhedral to subhedral lath form. Zoning is not common and hydrothermal alteration has produced a variation in the composition of the feldspars and its principal effect has been a shift in the plagioclase composition to more sodic values, producing albite (An0.5-2.0) and oligoclase in the altered rocks.

Overleaf: Plate 10. All bar scales 100 μ m.

A. Clinzoisite + chlorite in ultramafic alteration zone at 2000m in CY-4.

B. Chlorite + sphene in same zone as A.

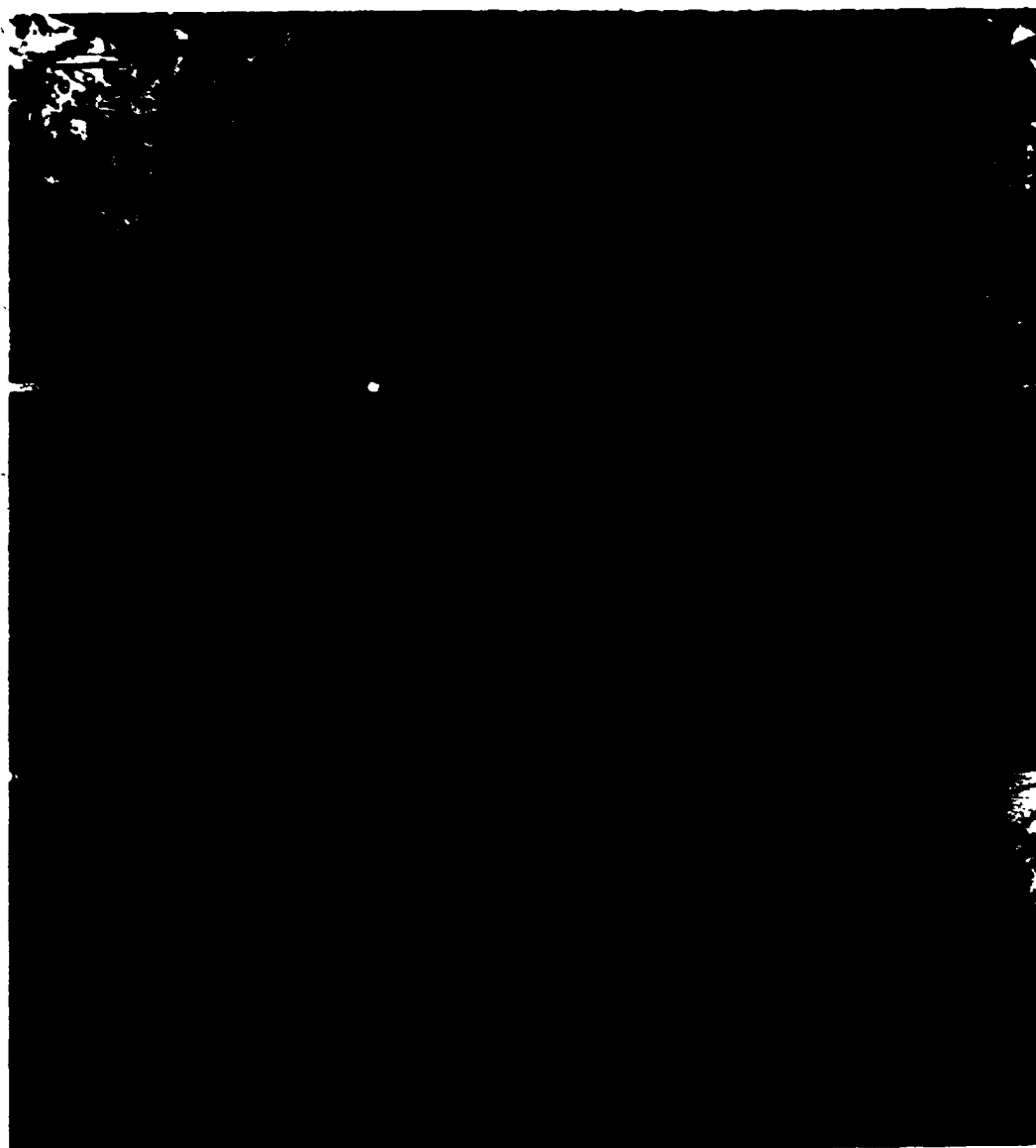
C. and D. Prehnite and carbonate of same zone which occurs in the websterites.

E. Plagioclase + chlorite of isotropic metagabbro..

F. Plagioclase + hornblende in metagabbro. Hornblende replaced by actinolite in patches.

Incomplete albitization is the more common form of Na-alteration and the composition of the altered feldspars in the dykes and upper gabbros ranges An6-17 in addition to the completely albitized feldspars (An content <5%). The albite is present as part of an alteration assemblage that is comprised of albite + actinolite + chlorite + sphene. In the isotropic gabbros the assemblage is albite

PLATE 10



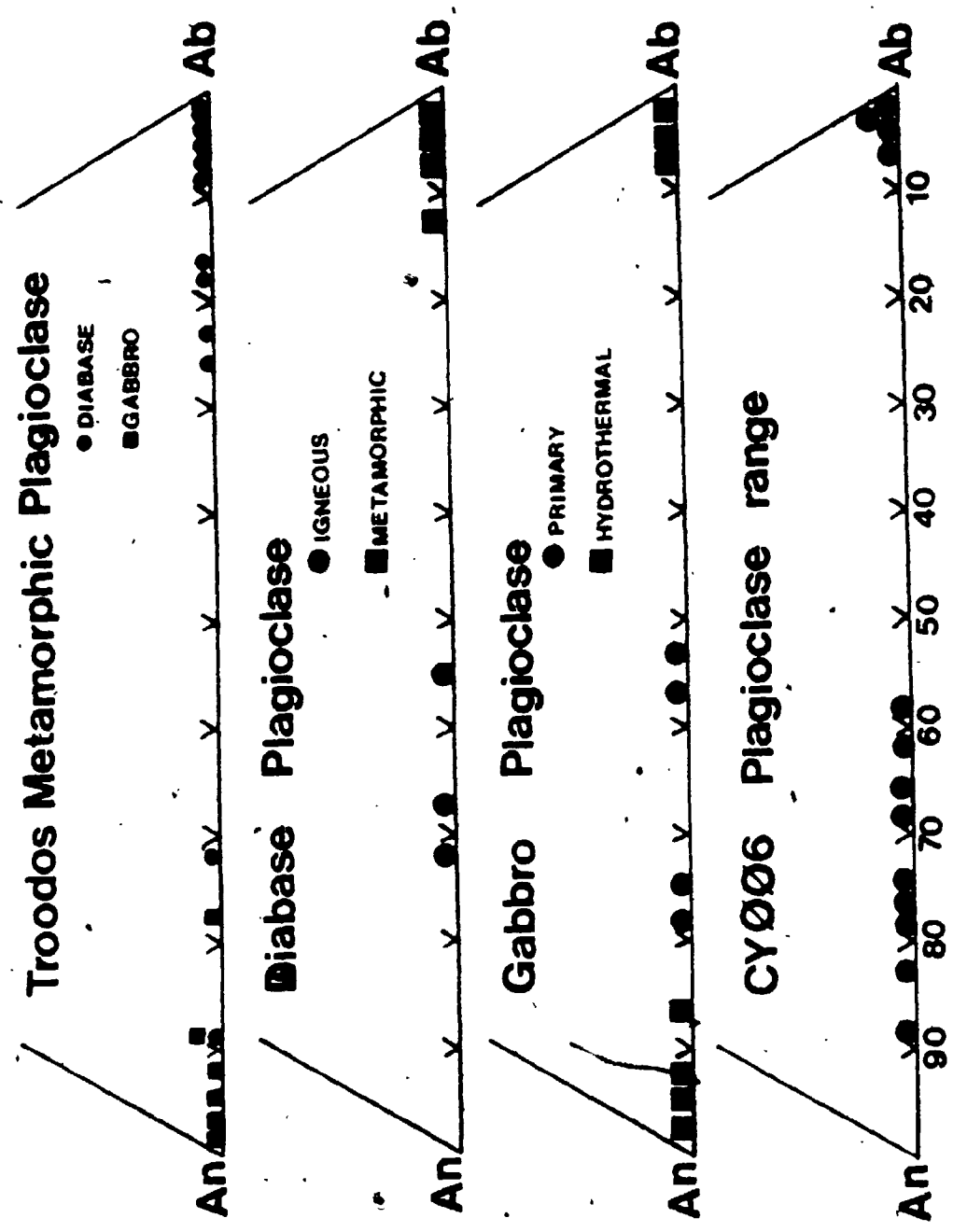


Fig. 4.1. Plots of the compositions of plagioclase from the Troodos ophiolite.

+ hornblende + chlorite + epidote +/- sphene. Fig.4.1 illustrates compositional variations for diabase and gabbro plagioclase as well as for a single diabase sample (CY 006) which appears to show the effects of two different alteration processes.

Increasing depth in the plutonic sequence affects the chemical composition of both the igneous and metamorphic feldspars, with the igneous feldspars ranging between An55-80 and the metamorphic feldspars ranging from the upper end of the labradorite range to An99. These very high Ca-feldspars occur with magnesio-hornblende and are also present in calc-silicate alteration assemblages of prehnite + epidote/clinozoisite +/- andradite +/- diopside in rodngitized gabbros. Table 4.2 illustrates the chemical composition of some of the Ca-rich feldspars from the gabbros. In general, the composition of the plagioclase in the gabbroic rocks is closely related to the bulk rock composition. Trondhjemitic gabbros occurring as small screens at the base of the sheeted dykes are comprised of albitic plagioclase (An30-80) commonly intergrown with quartz and thus producing graphic textured rocks (plate 4). Albite also occurs as a vein mineral in the dykes, and where the diabase is of microporphyritic texture, the microphenocrysts of plagioclase are predominantly albites although usually the groundmass plagioclase is fresh and more calcic suggesting that in part, the alteration has been a function of grain size.

CLINOPYROXENES.

Electron microprobe analyses of clinopyroxenes from the plutonic rocks of the Troodos ophiolite are presented in appendix A12. Many of the analyses represent several separate grains from the same rock. The grains occur as phenocrysts, intergranular aggregates, laths and cores (to retrograde amphiboles). Their similar compositions indicate that only minor chemical heterogeneity exists within the

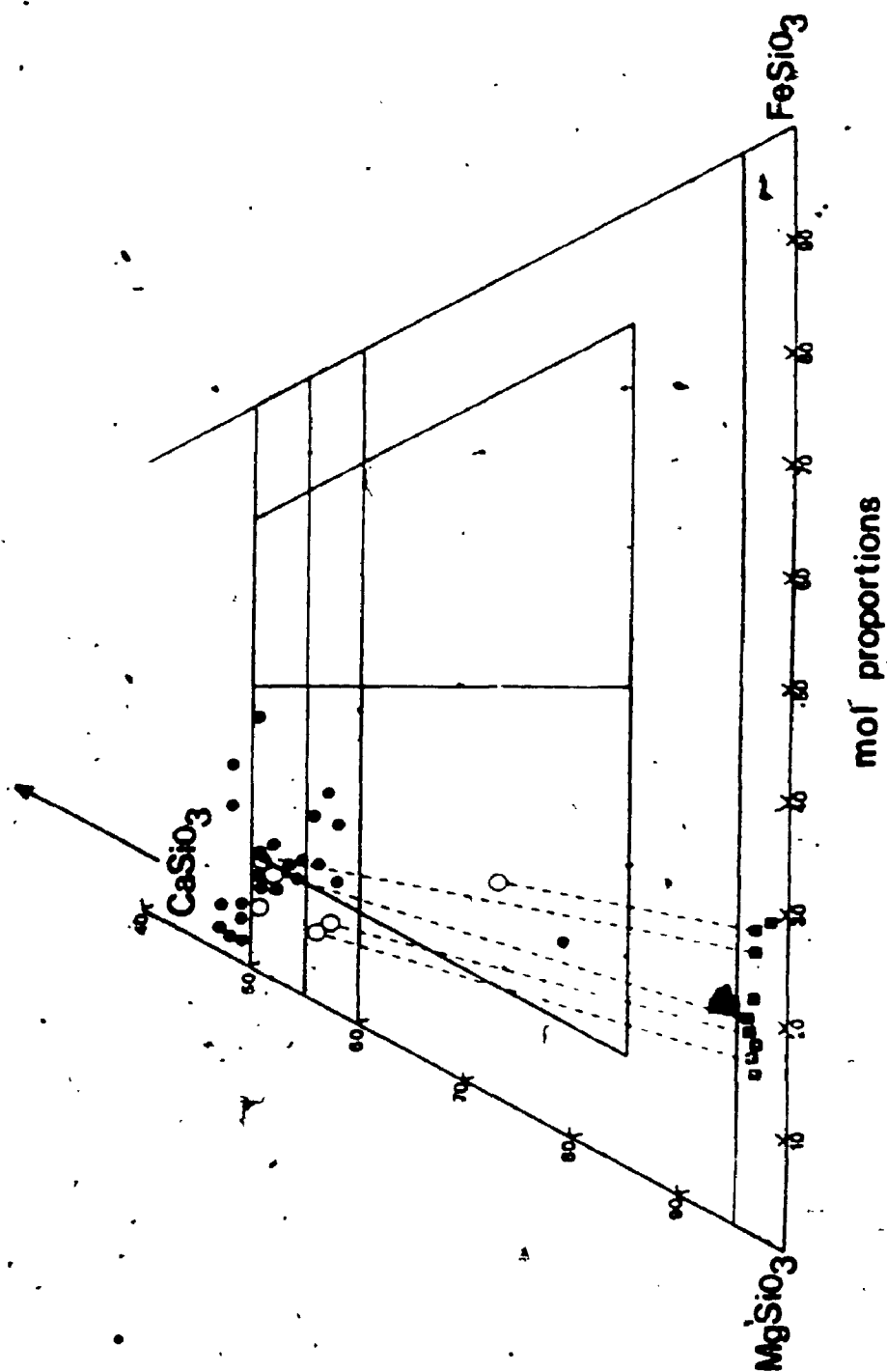


Fig. 4.2.. Plot of the composition of pyroxenes from the Troodos ophiolite •

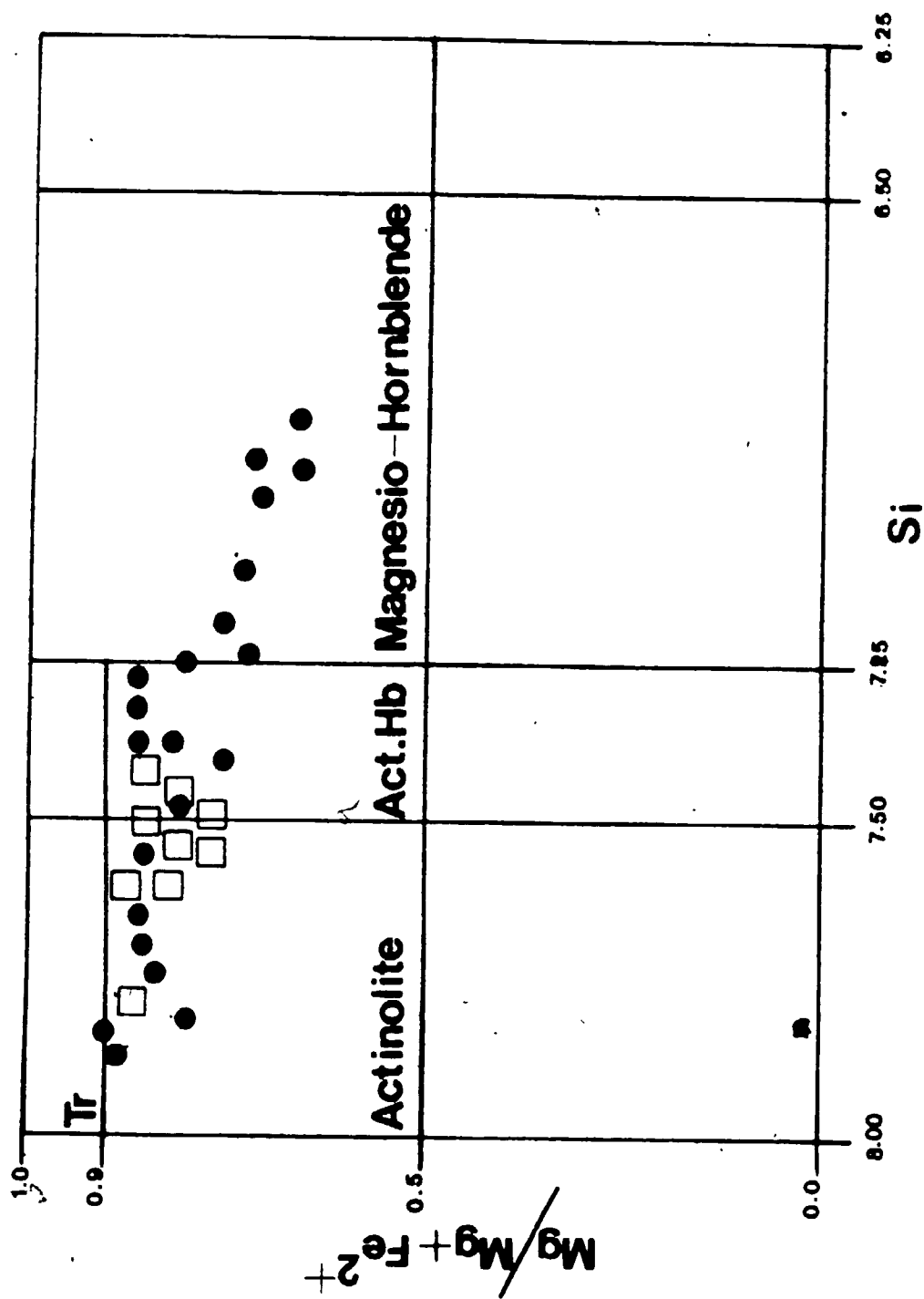
area of a microprobe section. When plotted (fig. 4.2.), most of the clinopyroxenes fall in the diopside - hedenbergite field, with some values plotting in the area of augite composition. The clinopyroxenes show only minor replacement of Si by Al in tetrahedral sites, with the range being from 0.0 to 0.084 cations per six oxygens although most analyses fall between ~~0.0~~ and 0.020 cations. The clinopyroxenes are characterized by evenly low Ti abundance with the average analysis for Ti ranging 0.0 to 0.1 wt.%, although up to 0.7 wt.% is recorded. The low Ti content appears to reflect igneous phenomena rather than later metamorphic events. The Ca contents of the clinopyroxenes are high and occupy the range Wo42-53. Most of the analysed pyroxenes (see appendix) have a Ca content in the range Wo45-51 corresponding to diopside-salite composition. Several workers (e.g. KUSHIRO, 1960; LE BAS, 1962) have suggested the use of clinopyroxene mineral chemistry to classify rocks of basaltic composition and in particular to distinguish tholeiitic from alkaline rocks on the basis of Al and Ti present in clinopyroxene.

CAMPBELL and NOLAN (1974) point out however, that silica activity in the melt as well as the actual crystallization conditions play an important role in the partitioning of Al and Ti into clinopyroxenes so much so that the Al and Ti contents of clinopyroxenes alone may not always lead to an accurate classification of the basaltic rocks in question. In the present case, the common occurrence of exsolution textures in the clinopyroxenes, high Ca and low Ti abundances as well as the Si/Al relations (fig. 4.2) all suggest the tholeiitic nature of the host rocks.

AMPHIBOLES.

Amphiboles are the chief alteration product of pyroxenes and range in colour from colourless through green to brown and exhibit a variety of textures, though most are fibrous (plates 5,6). The amphiboles replace clinopyroxene and minor

Fig. 4.3. Plot of Troodos ophiolite amphibole compositions.



olivine. They are associated with albite, anorthite, labradorite, epidote/clinozoisite, prehnite and sphene. In many instances amphibole is the only metamorphic mineral developed and occurs within the laths of former pyroxenes so that over all igneous textures are more or less retained. Amphibole classification is based on crystal chemistry as optical and physical determinative properties cannot differentiate unambiguously between different members of the group (LEAKE, 1978). Troodos Ophiolite amphiboles have $(Ca+Na)_B > 1.34$ and $Na_B < 0.67$ and have $Ca_B > 1.34$ in the amphibole formula where B represents the tetrahedral M4 site in the standard formula:

$A_{0-1}B_2C^VI_5T^IV_8O_{22}[OH,F,Cl]_2$ and can thus be classified as belonging to the calcic amphibole group (see appendix A14). Within this group, further classification is possible on the basis of Ti and Si content, and on the $Mg/(Mg + Fe^{2+})$ ratio. Since electron microprobe analysis does not differentiate between Fe^{2+} and Total Fe, the problem of the partial analysis has been solved following the method of LEAKE (1978) who recommends calculation of the number of ions on the basis of 23 oxygens followed by adjustment of the total cations, excluding $(Ca+Na+K)$ to $5+8=13$ by varying the Fe^{2+}/Fe^{3+} ratio. Pursuit of this procedure classifies the diabase dyke amphiboles as being actinolites primarily (fig. 4.3) with minor actinolitic hornblendes while the plutonic amphiboles occupy a wider compositional range that includes that of the diabase amphiboles and extends into the field of magnesio-hornblendes. It thus appears that the amphibole compositions of the ophiolite clearly distinguish the extent of metamorphism in the diabase dykes and gabbros, for while the diabasites have been subjected to greenschist facies P.T. conditions, fig. 4.4 shows that the gabbros have been subjected to greenschist as well as amphibolite facies conditions.

CHLORITE.

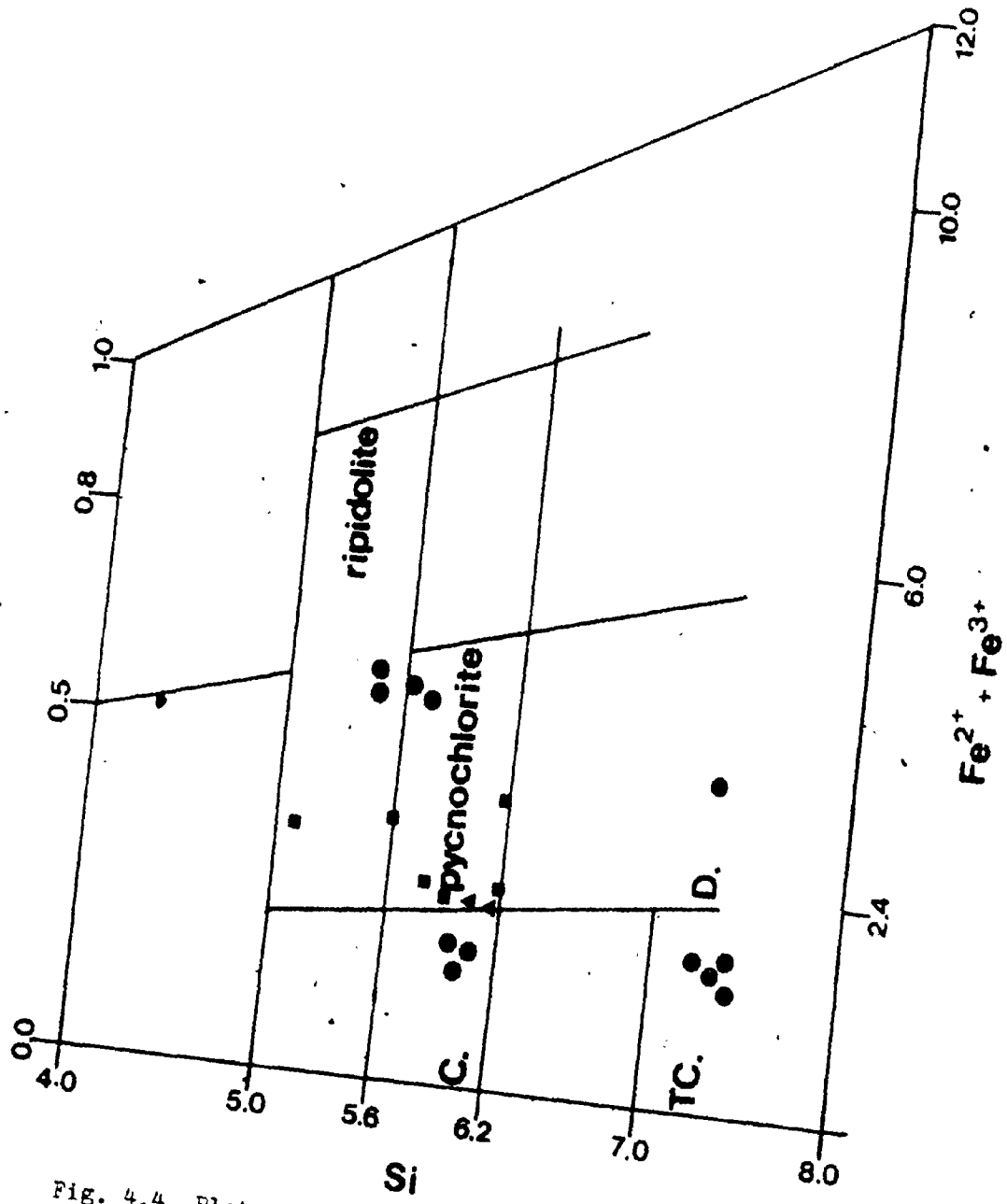


Fig. 4.4. Plot of chlorite compositions from the Troodos ophiolite.

Chlorite is primarily an alteration product of pyroxenes in the rocks studied. It is also a replacement product of Ca-amphiboles with which it is sometimes intergrown. As an alteration product it is observed in the diabase dykes, isotropic gabbros, layered gabbros and peridotites as irregular fine grained aggregates as well as in veins as massive aggregates usually occurring together with albite and quartz.

A classification of chlorites analysed in this study and based on the assumption that all the iron present is divalent (fig.4.4) shows a compositional variation with no apparent trend ranging between ripidolite, pycnochlorite and clinocllore with minor talc and diabantite. Such differences in composition may be due to differences in bulk rock composition, metamorphic intensity and degree of recrystallization. Bulk rock composition and the composition of the precursor assemblage appear to be the main controls of chlorite composition. Thus the chemical composition of chlorite developed from pyroxene and amphibole varies in composition although closely associated in space.

EPIDOTE/CLINOZOISITE.

Epidote/clinozoisite mineral analyses are listed in appendix A16. This mineral group is sporadically encountered in the diabase dykes, but is found mostly in the gabbros as part of the assemblage albite + chlorite + epidote + sphene + hornblende. In one instance the mineral group has been observed in the layered ultramafics. The group in general is of patchy occurrence and epidotes are commonly zoned (plate 3). Minerals commonly associated with this group in the diabase and metagabbros are quartz and sodic plagioclase and prehnite which is a late retrograde phase. Where present, they comprise a very minor percentage of the alteration assemblage except in quartz/epidote alteration zones where they constitute up to 10% of the assemblage. An observed alteration zone in the

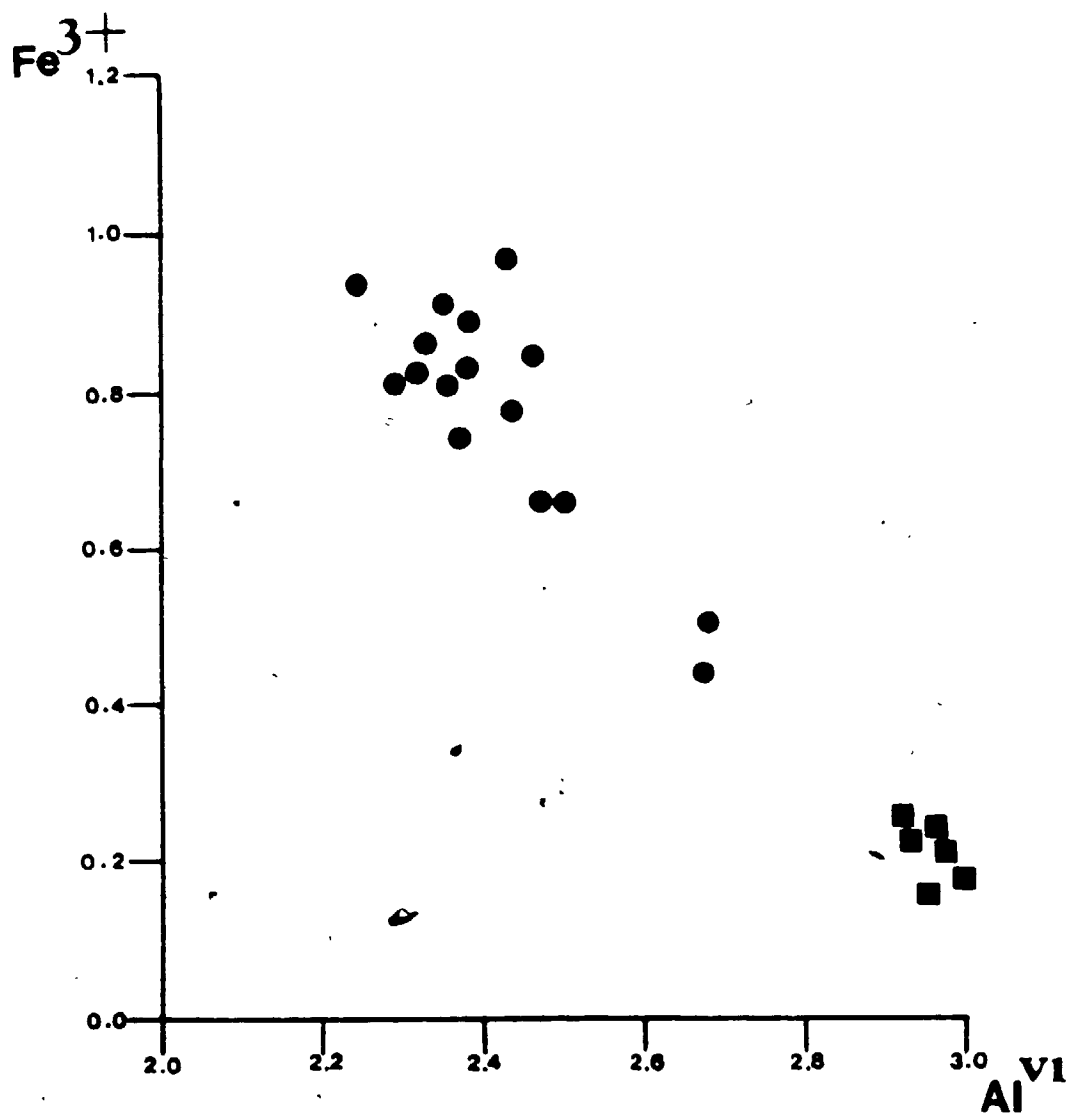


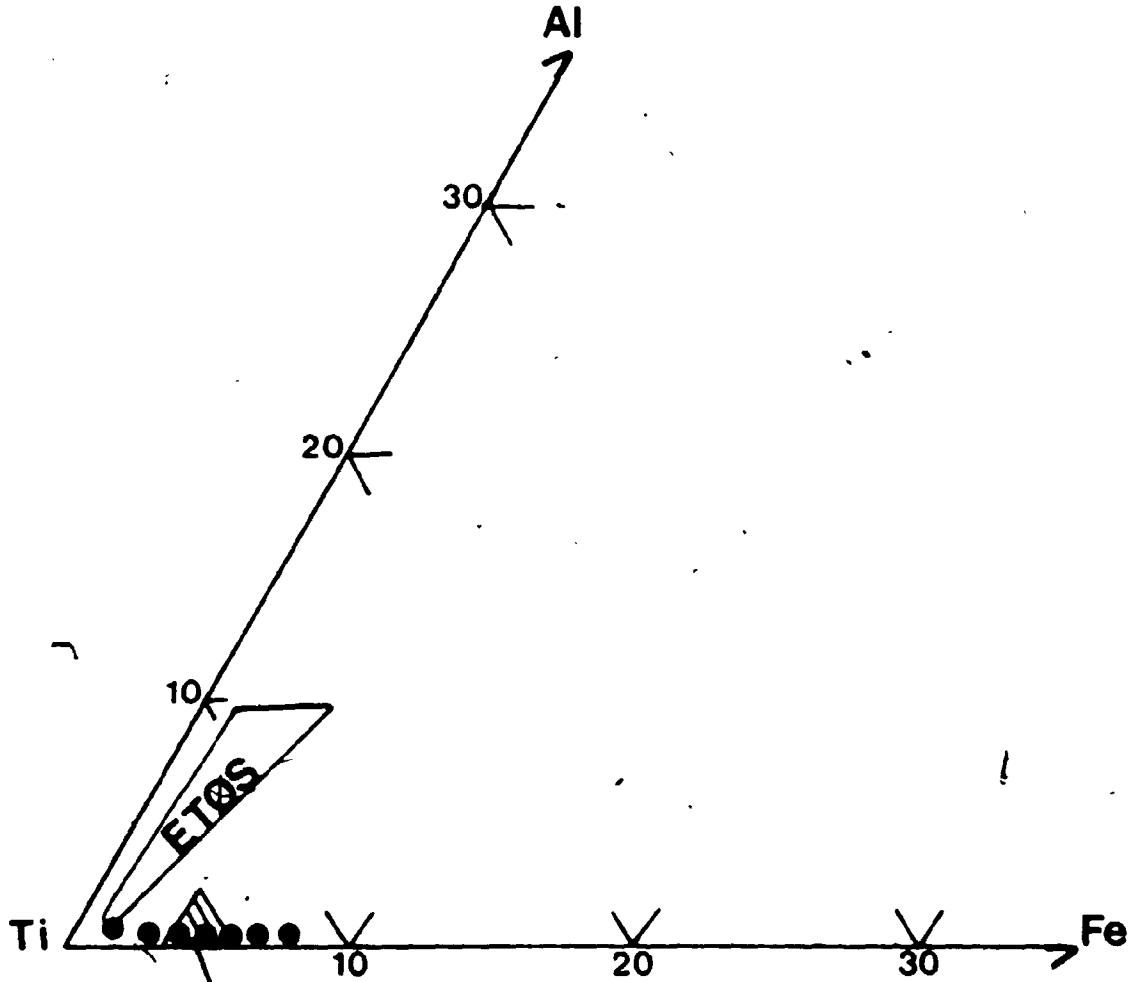
Fig. 4.5. Plot of proportions of octahedrally coordinated Al and Fe(III) in epidote and clinozoisite from the Troodos ophiolite.

websterites is composed of about 80% epidote/clinozoisite and chlorite + calcite. The mineral group is an alteration product from the breakdown of plagioclase and clinopyroxenes. The common forms are stubby prismatic crystals and spongy radiating aggregates. Zoning is common and the cores have a higher Fe content than the fringes. Fig.4.5 shows the major substitution of Fe_2O_3 for Al_2O_3 and indicates the range in composition which is also reflected in the varying degree of birefringence of the minerals. Most epidotes show a high birefringence, suggestive of high Fe^{3+} content.

PREHNITE.

Prehnite is not a common secondary mineral in the Troodos Complex, but is present as a late stage alteration product of zeolites and Ca-plagioclase. It occurs as crystal aggregates, in patchwork form and as a vein mineral. Bow-tie structure (plate 6) is common, though the usual form is anhedral prehnite with characteristic clear bright 2nd order interference colours. Analyses are presented in appendix A17. Variations of Fe^{3+} - Al^{VI} in the octahedral sites are presented in fig.4.6. Fe^{3+} shows a continuous variation for Al^{3+} corresponding to Fe_2O_3 ranging from 0.0 to 3.89%. The high Fe content of some of the analysed prehnites is reminiscent of the findings of KUNUYOSHI and LIOU(1976) who report that prehnites in low grade metabasaltic rocks commonly contain an appreciable amount of Fe^{3+} . SPHENE.

Sphene is a common alteration mineral in metamorphosed Troodos rocks, occurring in both greenschist facies rocks as well as amphibolite facies rocks, and the common form of occurrence is as cloudy aggregates in close association with opaque phases, Ca-amphiboles and chlorite. A plot of Al-Ti-Fe variation (fig. 4.7) indicates very limited substitution of Ti by Al and Fe and the analyses plot across the amphibolite facies field of SMITH(1970). Analyses are presented in appendix XII.



Amphibolite Facies

Fig. 4.7. Plot of sphene analyses from the Troodos ophiolite. ETOS represents sphene compositions from the East Taiwan Ophiolite after LIOU and ERNST, 1979; Amphibolite facies field after SMITH, 1970.

ANDRADITE.

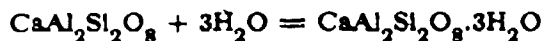
Andradite is the only garnet encountered in the rocks studied. It occurs only in the rodinilitized gabbros where it is associated with anorthite + diopside + prehnite. Prehnite commonly occurs replacing the andradite. Representative analyses are presented in appendix XII. Petrographic evidence suggests that most of the andradite is a replacement product of primary pyroxene.

ZEOLITES.

Ca-zeolites are present in all rock units of the Troodos Complex as veins and interstitial fill in breccia and shear zones. They comprise approximately 80% of all the vein minerals present, and are commonly associated with late calcite and anhydrite. The Ca-zeolite present is laumontite (about 95%). Other phases present in minor amounts are stilbite, thomsonite, analcime and heulandite. Analyses are presented in appendix A20. The nature of occurrence of the zeolites suggests that in the main, they are the products, together with calcite and anhydrite, of late stage hydrothermal activity; i.e. they represent the terminal stages of the activity responsible for the metamorphism of the host rocks.

4.5. METAMORPHISM

The submarine extrusion of pillow lavas and flows and the injection of diabase dykes at Troodos was followed by cooling dominated by the mass transfer of seawater through oceanic crust. The process has led to seawater - basalt reactions that have altered the mineralogy and chemistry of these former ocean floor rocks. At the low temperature high water/rock ratio seawater/seafloor interface, the rocks equilibrated with ocean water and became oxidized and hydrated forming minerals of the zeolite facies, primarily by the replacement of plagioclase via reactions such as:



Ca-plagioclase + water = thomsonite



Ca-plagioclase + quartz + water = laumontite

The palagonitization of glass, the partial replacement of the igneous minerals by K-Mg smectites and the oxidation of ferrous oxides are all part of this low temperature process.

In a recent study, GILLIS and ROBINSON (1985) examined the low temperature alteration of the extrusive sequence at Troodos and report non-pervasive zeolite facies grade metamorphism with the characteristic minerals analcime + phillipsite + natrolite + chabazite + mordenite + calcite + laumontite.

LIU (1979) reports that the basaltic rocks of the fragmented East Taiwan ophiolite have been subjected to ocean floor zeolite facies metamorphism and that depending on the bulk composition and mode of occurrence, various mineral assemblages occur. The best defined of these assemblages are: thomsonite + analcime + chabazite; pumpellyite + chlorite + laumontite in veins of the pillow cores; and pumpellyite + chlorite + K-feldspar; pumpellyite + laumontite + thomsonite; and Fe-rich prehnite + hematite in veins of the pillow matrices.

Other workers (e.g. AUMENTO ET AL., 1971; MIYASHIRO ET AL., 1971; ALT ET AL., 1986) report the presence of analcime, stilbite, heulandite, natrolite and mixed layer chlorite - smectites from metabasalts dredged from active oceanic ridges.

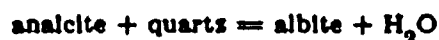
The diagnostic minerals of the zeolite facies identified in the current study from late stage alteration at Troodos in the lower diabase dykes and gabbros are laumontite + stilbite + calcite +/- anhydrite. Since laumontite forms at a higher temperature than most zeolites (COOMBS ET AL., 1959) and considering the nature of zeolites in the upper part of the Troodos stratigraphy (e.g. GILLIS and ROBINSON, 1985) the presence of laumontite in the lower diabase and gabbros indicates that retrograde zeolite facies metamorphism in the Troodos hyperbasal and plutonic rocks took place at a higher temperature than the metamorphism that prevailed just beneath the ocean crust / seawater interface.

The current study reports that the diabase dykes and isotropic gabbros have been altered to greenschist facies and epidote - amphibolite grade assemblages, and the upper layered gabbros to amphibolite facies grade assemblages.

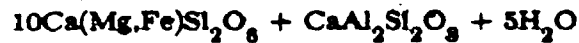
Locally, alteration extends into the ultramafic sequence causing extensive serpentinization and in places, epidotization. The minerals characteristic of the greenschist facies in the dykes are albite + actinolite + chlorite. Igneous labradorite has been transformed to albite by an exchange of sodium in the seawater for the calcium in the plagioclase:



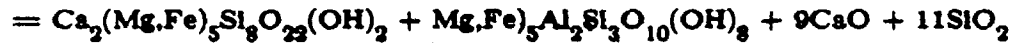
Vein albite present in the diabase may be a replacement product of zeolites via reactions such as



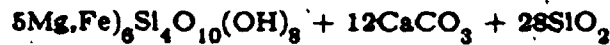
actinolite $(\text{Ca}_2(\text{Mg}, \text{Fe}^{2+})_3[\text{Si}_8\text{O}_{22}](\text{OH}, \text{F}, \text{Cl})_2$ and chlorite $(\text{Mg}, \text{Al}, \text{Fe}^{3+}, \text{Fe}^{2+})_{12}(\text{Si}, \text{Al})_8\text{O}_{20}(\text{OH})_{18}$ are hydration products of augitic pyroxene $(\text{Ca}, \text{Na}, \text{Mg}, \text{Fe}^{2+}, \text{Mn}, \text{Fe}^{3+}, \text{Al}, \text{Ti})_3[(\text{Si}, \text{Al})_3\text{O}_6]$ and may be formed using the calcic component of the plagioclase by reactions of the type:



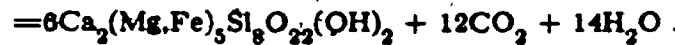
augite pyroxene + anorthite + water = actinolite + chlorite.



The greater abundance of actinolite relative to chlorite in these rocks suggests that the former may be forming at the expense of the latter by reactions of the idealized type :



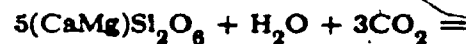
chlorite + calcite + quartz =



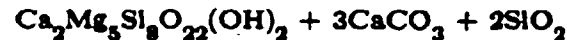
actinolite + carbon dioxide + water

where only the (Mg,Fe) component of (Mg,Fe,Al) chlorite is utilized (MUELLER and SAXENA, 1977).

HASHIMOTO, (1972) has shown that actinolite formation from clinopyroxene can also proceed under high fCO_2 conditions by the reaction:



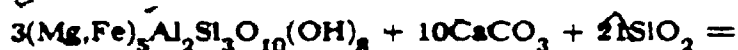
clinopyroxene + water + carbon dioxide =



actinolite + calcite + quartz.

Actinolite, commonly colourless to pale green is the most extensively occurring of the greenschist grade metamorphic minerals. Epidote/clinozoisite

group minerals are present in small amounts in the diabase, and more abundant in the isotropic metagabbros where they are commonly associated with a small amount of quartz. Minerals of this group occur in a wide range of metamorphic environments from prehnite - pumpellyite facies grade rocks through to amphibolite facies rocks:



chlorite + calcite + quartz =



epidote +



actinolite + carbon dioxide + water

In the gabbroic rocks examined, most epidote/clinozoisite is a replacement product of the hydrothermal alteration of plagioclase feldspar with a commonly observed textural feature being epidote occupying the laths of former feldspars which are survived by relict grains in the epidote.

The lower temperature stability limit of epidote has been estimated at $220^\circ \pm 50^\circ\text{C}$ for P_{total} of 1 - 6 kb and at 300°C at kKb (TOMASSON and KRISTMANNSDOTTIR, 1972; SEKI, 1972). However, in an oxygenated environment high f_{O_2} considerably decreases the temperature for the first appearance of epidote and the mineral has been observed in metabasalts of prehnite - pumpellyite facies (LIU, 1973).

At Troodos, as noted previously, epidote/clinozoisite is not a common alteration mineral despite the fairly high oxygen fugacity expected under seawater

dominated conditions. This may be a result of the low pressure conditions prevailing during metamorphism as suggested by MIYASHIRO(1971) who also notes a paucity of epidote group minerals in dredged ocean floor rocks. The elimination of epidote at low fluid pressures (2Kb P_{fluid}) via the reaction:

Epidote[Ps33] =

Grandite_m + Anorthite + FeO_x + Quartz + fluid

has been suggested at 670 +/- 40°C by FYFE(1960), 620°C by WINKLER and NITSCH(1963), 630°C by STRENS(1966), 620°C by LOOMIS(1966) and 645°C by HOLDAWAY(1967,1972).

LIU(1973) shows that the f_{O_2} - T location of the reaction crosses the Cu-Cu₂O buffer curve at 680 +/- 10°C at 3kb and 752 +/- 10°C at 5kb P_{fluid} . The Fe₂O₃ - Fe₃O₄ buffer curve is crossed at 635 +/- 5°C at 2kb, 678 +/- 5°C at 3kb and 748 +/- 5°C at 5kb P_{fluid} .

A chlorite decreasing reaction involving epidote for low pressure metamorphism of basaltic rocks expressed by:

albite + epidote + chlorite + quartz =

oligoclase + tschermakite + Fe₃O₄ + H₂O

has been shown by LIU, KUNYOSHI and ITO (1974) to occur at pressures below about 3kb and at temperatures lower than the chlorite eliminating reaction:

chlorite + sphene + quartz + actinolite = Al-amphibole + ilmenite + H₂O

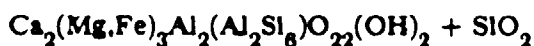
where the chlorite component breaks down at 550°C at 5kb P_{fluid}

(575°C/7kb) with oxygen fugacity set at the NNO buffer. Over the same temperature range in the chlorite eliminating reaction, the same workers note a rapid increase in the Al and Ti content of existing amphiboles - essentially a transition from actinolite to hornblende.

Troodos metagabbros affected by amphibolite facies metamorphism are characterized by the presence of anorthitic plagioclase (An 70+) and hornblende amphibole. The hornblende is a replacement of pyroxene and it may be produced by reactions of the type:



orthopyroxene + plagioclase + water =



hornblende + quartz

and also:



clinopyroxene + orthopyroxene + plagioclase

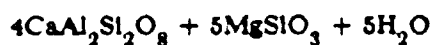


plagioclase + water = hornblende + quartz.

while anorthite may be derived from epidote by a reaction of the form:



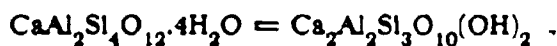
epidote + chlorite + quartz =



anorthite + enstatite + water.

(MUELLER and SAXENA, 1977).

Sporadic prehnite in these metagabbros appears to be a retrograde feature involving the breakdown of anorthite in whose interstices the prehnite commonly occurs. The occurrence of prehnite in veins may be due to the dehydration of laumontite via reactions of the sort:

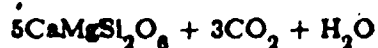


laumontite = prehnite + Al-silicates + water

(COOMBS ET AL., 1959.)

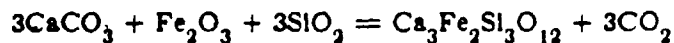
Troodos rodngitized gabbros, occurring as small patches in the lower gabbros, are characterized by the calcic assemblage prehnite + epidote/cclinzoisite + diopside +/- actinolite +/- calcite + andradite. + magnetite +/- quartz. The presence of andradite, epidote, magnetite and Fe - rich prehnite indicates that the hydrothermal fluids were locally rich in iron.

Relict actinolites are observed (by electron microprobe analysis) in the centre of diopsides. This shows that the diopside is a replacement of Ca-amphiboles probably by a dehydration reaction of the form:



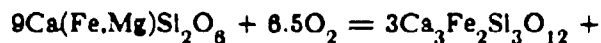
or else by Ca addition via Ca metasomatism.

Andradite is the only garnet mineral observed in the Troodos ophiolite rocks in this study, and apparently occurs only in the rodingitized portions of the gabbro. The presence of andradite may be a result of the reaction of calcite, a mineral also noted in the rodingitized rocks, with Fe-bearing phases including excess iron from the alteration of actinolite to diopside by a reaction such as:



(DEER, HOWIE and ZUSSMAN:1968).

Petrographic evidence suggests, however, that most of the andradite is a replacement product of primary pyroxene, and the association of quartz and Fe-oxides with andradite suggests that a reaction of the following kind may have taken place:



clinopyroxene + oxygen = andradite + quartz + magnetite



The experimental work of KURSHAKOVA (1971) indicates that the formation of andradite is favored by an increase in oxygen fugacity at constant P and T.

The common form of the andradite observed in the rodingitized rocks shows it is criss-crossed by fractures and that the fractures are mostly filled with Fe-bearing prehnite.

Troodos ophiolite peridotites have been subjected to extensive serpentinization. The metamorphic mineral assemblage of the peridotites is mostly antigorite + lizardite (minor) + chrysotile (minor) + talc + chlorite + calcite.

Late stage veins of laumontite, calcite and prehnite are also present. In one instance, epidote/clinozoisite is also present in an alteration zone associated with calcite + chlorite in close proximity to a fracture plane coated with a veneer of antigorite. The assemblage occurs in Al deficient websterites (at 1996.0m in CY-4) and must imply that the hydrothermal fluids responsible for the alteration assemblage transported Al^{3+} -an element usually thought of as being immobile under low to medium metamorphic conditions.

Continued hydrothermal activity at Troodos at a lower geothermal gradient than that pertaining to the main metamorphic episode has resulted in retrograde zeolite facies grade metamorphism in the diabase dykes and upper gabbros and prehnite - pumpellyite facies metamorphism in the lower gabbros. The effects of the metamorphism (i.e. development of retrograde minerals) is essentially confined to fracture walls, shear zone gangue and other fluid pathway sites. This is indicative of the hydrothermal nature of the alteration. Laumontite is the chief hydrothermal mineral with minor calcite and anhydrite of the zeolite facies in the dykes and gabbros. Prehnite - pumpellyite grade metamorphism is represented by prehnite + chlorite + calcite. Reactions transitional to this facies include:



and



(COOMBS ET. AL., 1959).

4.6. METAMORPHISM AT AYIOS IOANNIS PITSILIA

A mineralized area of Fe - stained, rust coloured gabbros covering an area of about 3 km² on the outskirts of Ayios Ioannis village in the Pitsilia district of central Cyprus was investigated as a part of this study.

In the ophiolite sequence, the zone occurs about 1km below the base of the sheeted dyke/gabbro transition, well within the isotropic gabbros. The Fe - staining of the area is due to mineralization centered around several massive NE trending, near vertical to vertical quartz - sulphide veins that form ridges on the hillsides and crop out for over 500m.

Reconnaisance work by the Cyprus Geological Survey (CONSTANTINO, 1973) indicates that the mineralization at Ayios Ioannis consists of Cu and Fe sulphides (pyrite, chalcopyrite, pyrrhotite) as well as Ni, Co, Au (up to 100ppm), and Ag (up to 20ppm). The veins have been mined in antiquity, presumably at least by the Romans, as adits into the hillsides attest.

3 major veins outcrop in the area; the veins have an average aperture of 0.5m and are roughly parallel to each other. They consist of vuggy quartz with well formed coarse grained crystals up to 0.10m long, patches of sulphides of Cu and Fe, and xenoliths up to 0.5m long of very fine grained chloritic material.

Post quartz-sulphide vein diabase dykes are in contact with the quartz veins in several parts of the outcrop. The isotropic gabbros have been Mg-metasomatized in a wide aureole up to 500m on either side around the veins causing the extensive development of chlorite. Other metamorphic minerals developed in the area are epidote, albite and brown hornblende. In the gabbro which is closest to the quartz veins, chlorite is absent and the mineralogy here is albite + hornblende. The chlorite in this part of the gabbro appears to have been eliminated at high temperature by a reaction with the quartz of the sort:

chlorite + actinolite + epidote + quartz = hornblende + H₂O

(COOMBS ET AL., 1959).

The following tables present electron microprobe analyses performed by the present writer from the metagabbro which constitutes the wallrock of one of the quartz - sulphide veins:

Table 4.3. Amphibole from A. Ioannis.

	1	2	3	4	5	6
SiO ₂	50.34	49.20	51.63	51.50	50.64	50.37
TiO ₂	0.94	0.89	0.72	0.79	0.99	0.82
Al ₂ O ₃	4.91	6.37	5.05	4.29	4.62	5.05
FeO*	12.47	12.64	11.48	11.40	12.23	12.59
MnO	0.36	0.27	0.24	0.25	0.29	0.29
MgO	16.22	15.26	15.86	17.20	16.23	16.00
CaO	11.19	11.41	11.31	11.69	11.30	11.40
Na ₂ O	1.10	1.14	0.72	0.64	1.00	0.80
K ₂ O	0.29	0.22	0.23	0.13	0.29	0.21
Total	97.82	97.45	97.24	97.89	97.59	97.63
NO. OF IONS ON THE BASIS OF 23(O, OH, F, Cl)						
Si	7.285	7.189	7.437	7.385	7.332	7.297
Al	0.715	0.841	0.563	0.615	0.688	0.703
Al	0.123	0.251	0.294	0.110	0.120	0.159
Ti	0.102	0.097	0.078	0.085	0.108	0.089
Mg	3.499	3.309	3.405	3.676	3.502	3.455
Fe	1.509	1.538	1.383	1.367	1.481	1.525
Mn	0.044	0.033	0.029	0.030	0.036	0.036
Ca	1.735	1.779	1.745	1.796	1.753	1.769
Na	0.309	0.322	0.201	0.178	0.281	0.225
K	0.054	0.041	0.042	0.024	0.054	0.039

* Total Fe as FeO

Table 4.4 Plagioclase from A.Ioannis.

	1	2	3	4	5	6
SiO ₂	70.32	71.22	70.59	68.45	68.80	68.18
Al ₂ O ₃	21.19	20.20	20.17	22.63	20.72	20.48
FeO	0.00	0.00	0.00	0.05	0.00	0.00
MgO	0.00	0.00	0.00	0.00	0.00	0.00
CaO	0.98	0.10	0.43	1.30	1.45	1.38
Na ₂ O	8.22	8.59	9.34	8.55	7.86	10.79
K ₂ O	0.02	0.00	0.00	0.04	0.01	0.02
Total	100.73	100.11	100.53	99.02	98.84	100.83

NO. OF IONS ON THE BASIS OF 32(O)

Si	12.024	12.214	12.121	11.858	12.003	11.825
Al	4.270	4.082	4.081	4.619	4.260	4.186
Fe	0.000	0.000	0.000	0.000	0.000	0.000
Fe	0.000	0.000	0.000	0.000	0.007	0.000
Mg	0.000	0.000	0.000	0.000	0.000	0.000
Na	2.725	2.856	3.109	2.200	2.659	3.628
Ca	0.180	0.018	0.079	0.241	0.271	0.253
K	0.004	0.000	0.000	0.009	0.002	0.004
AB	93.68	99.36	97.52	89.79	90.68	93.38
AN	6.17	0.64	2.48	9.85	9.24	6.50
OR	0.15	0.00	0.00	0.36	0.08	0.11

The metamorphic assemblage present at Ayios Ioannis Pitsilia indicates that epidote - amphibolite facies metamorphism occurred in the isotropic gabbros. The massive quartz veins are thus most probably fossil remnants of the output discharge conduits of giant hydrothermal convection cells of the type that are responsible for massive sulphide ore formation higher up in the stratigraphy at the original pillow lava/seawater interface.

The presence of very coarse grained Al-Ti rich hornblende (table 4.3) indicates that the discharge temperature of the hydrothermal fluids deep in the plutonic sequence had attained temperatures in excess of 500°C. The chemical composition of the fluid is constrained by the extensive chloritization (Mg - metasomatism) of the gabbros which was accompanied by widespread albittization (table 4.4) of feldspars. Taken together, this implicates seawater.

The mineralized quartz veins in the gabbros at Ayios Ioannis Pitsilia are thus important in that they are the fossil remnants of the focused discharge part of a convective flow hydrothermal system, and situated deep in the plutonic sequence give a clear indication as to how deep seawater may convect into oceanic crust.

4.7. PHYSICAL CONDITIONS OF HYDROTHERMAL METAMORPHISM

Zeolite, greenschist, and amphibolite facies metamorphism has occurred in the volcanic and igneous rocks of the Troodos ophiolite. The grade of metamorphism is directly related to rock position in the pseudo - stratigraphy corresponding to increasing temperature of fluids with depth.

The metamorphism is not pervasive and is predominantly related to fractures, faults, shear zones, veins and other discontinuities in the rock that were utilized as fluid pathways by convecting fluids. This feature, together with the fact that the rocks have not developed any foliation and that overall igneous textures have been preserved characterizes the type of metamorphism at Troodos.

The minimum temperatures for the development of zeolite facies metamorphism, judging from diagnostic minerals, at fluid pressures relevant to deep ocean floor surfaces, are 170° to 260°C for laumontite at about 2Kb and even less for other Ca - zeolites.

Laumontite is only stable below 3kb; at higher fluid pressures it breaks down to lawsonite + quartz + H₂O (LIOU, 1971). At decreased H₂O activities such as in seawater, the observed zeolite minerals will occur stably at even lower P- T conditions than those deduced from experiment; laumontite will form in a CO₂ bearing fluid at 1Kb P_{fluid} and 260°C with a maximum mole fraction of CO₂ of 0.023 (THOMPSON, 1971). The temperature range 100 - 300°C and pressures to a maximum of 3kb has been suggested from observations of burial metamorphic sequences and experiments (COOMBS ET. AL., 1959). Furthermore, minimum temperatures of formation for laumontite and prehnite have been estimated to be about 50°C and 90°C, respectively (BOLES and COOMBS, 1975).

From the zeolite facies minerals present in the pillow lava sequence at Troodos (e.g. GILLIS and ROBINSON, 1985) and other experimental and observational data (e.g. COOMBS ET. AL., 1959; LIOU, 1971; LIOU, 1979; LIOU and ERNST, 1979) it is concluded that the zeolite bearing volcanic rocks at Troodos were metamorphosed at temperatures between 50 and 100°C and pressures of up to 1.5kb.

The development of albite + actinolite + chlorite + sphene in the metadiabase and metagabbros at a depth proceeding from 1km below the inferred seawater/oceanic crust interface, and the presence of Ca - plagioclase and hornblende in deeper metagabbros indicates the advance of metamorphism to amphibolite facies grade in the ophiolite sequence over an interval of about 3km.

NITSCH (1971) has shown experimentally that the assemblage actinolite + chlorite + epidote + quartz of the greenschist facies is stable at temperatures above 350°C and P_{total} 2kb. The assemblage albite + chlorite + epidote + sphene + hornblende indicates the epidote - amphibolite facies which represents an intermediate zone assemblage between the greenschist and amphibolite facies. The presence of such a transitional zone is indicative of very low pressure metamorphism (LIOU ET. AL., 1974 ; KUNYOSHI and LIOU, 1976). An experimental study of phase relations among greenschist, epidote - amphibolite and amphibolite assemblages by APTED and LIOU (1983) using natural basaltic glass at 5 and 7 Kb P_{fluid} and an oxygen fugacity determined by hematite-magnetite and quartz - feldspar - magnetite buffers confirms the existence of a high pressure epidote - amphibolite facies consisting of the assemblage epidote + hornblende + albite + quartz +/- Ti-phase. The facies is related at lower temperatures, about 500°C , to the greenschist facies by a chlorite eliminating reaction and at higher temperatures to the amphibolite facies by an epidote eliminating reaction.

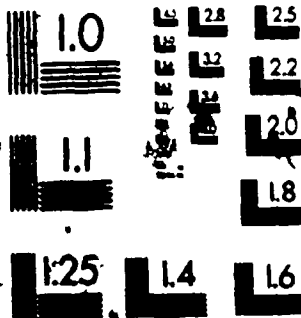
At lower pressures of 2Kb_{total}, LIOU ET.AL.(1974), using natural basalts as seeding material and oxygen fugacity determined by the QFM buffer, find that the upper boundary for the greenschist assemblage albite + epidote + chlorite + actinolite is located at 475°C and the lower limits of the amphibolite assemblage Ca-plagioclase + hornblende at 550°C .

A consideration of the above mentioned experimental results and of the possible effects of variable oxygen fugacity and fluid pressure as well as the bulk composition leads the current writer to infer that Troodos hyperbasal and plutonic rocks were metamorphosed at temperatures between 300° - 600°C and total pressure up to 1.5kb at a depth of 1 - 3 km and over a geothermal gradient of 150 - $250^{\circ}\text{C}/\text{km}$.

The last stage of the recrystallization of Troodos plutonic rocks occurred under conditions of zeolite and prehnite - pumpellyite facies grade in the hyperbasal and plutonic portions respectively. This was primarily due to the gradual relaxation of the geothermal gradient as the ocean crust spread away from the ridge axis and as it lost heat due to the effects of the fluids convecting through it. This waning stage of hydrothermal activity is best evident along former fluid pathways due to the development of the vein assemblages laumontite + calcite and prehnite + development of vein assemblages of laumontite + calcite and prehnite + chlorite. Laumontite replacement of albite in upper level shearzones and the presence of actinolite surrounding hornblende in metagabbros is also supporting evidence for this phenomenon.

2

MICROCOPY RESOLUTION TEST CHART
NBS 1910a
ANSI and ISO TEST CHART No. 2



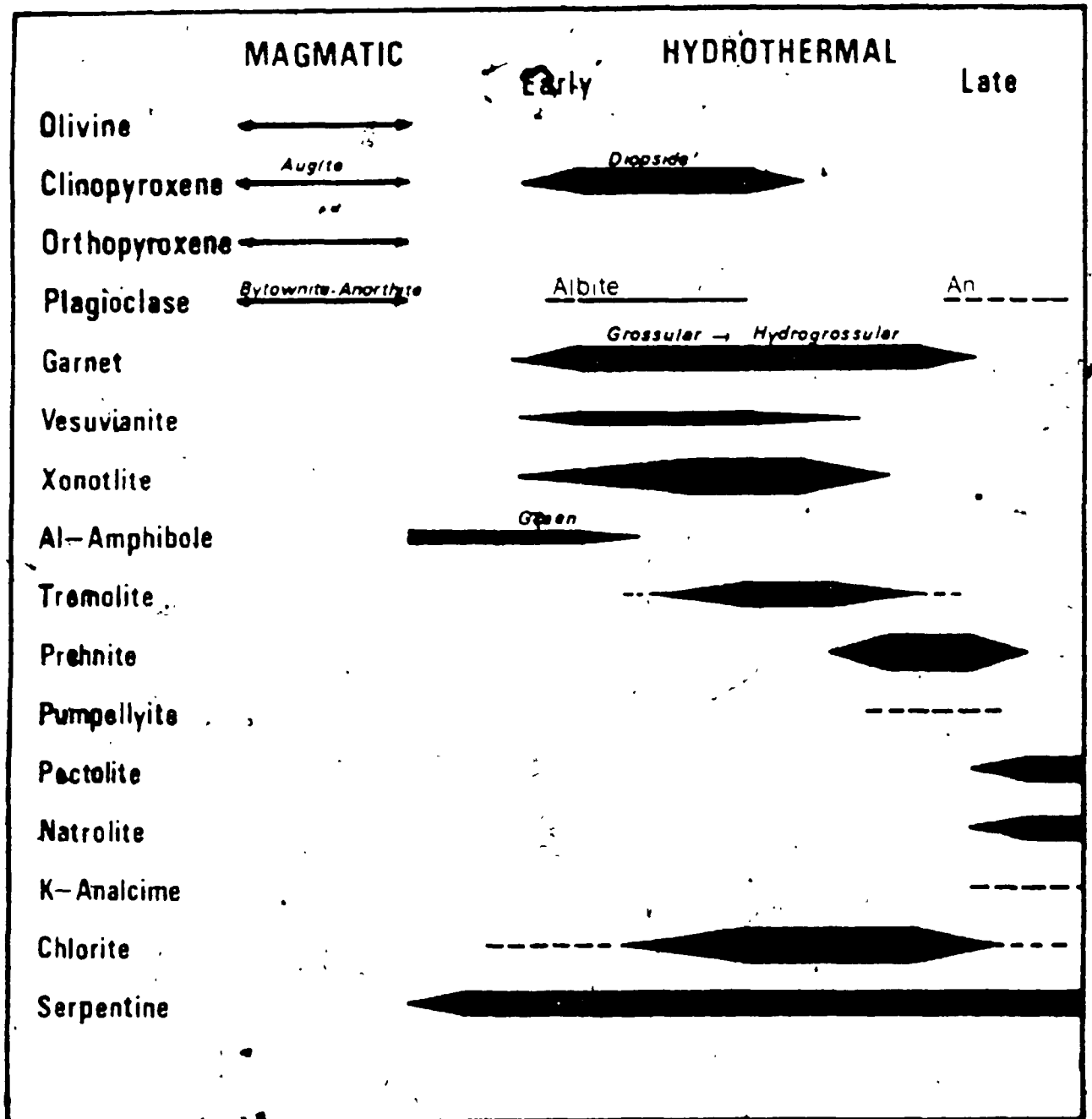


Fig. 4.8. Summary diagram showing the major magmatic and hydrothermal minerals of the Troodos ophiolite.

Chapter Five

GEOCHEMISTRY

5.1. WHOLE ROCK GEOCHEMISTRY

Major element oxides, the rare earth elements and the trace elements S, V, Cr, Co, Ni, Cu, Zn, Ga, Rb, Sr, Y, Zr, Nb, Ba, U, Th, Au, Pb, B were determined on samples representing lower sheeted dykes and gabbroic rocks via X-ray fluorescence analysis and spark source spectroscopy. The greater part of the analyses were performed in house at UWO by the present writer. Backup analyses were performed at X-ray assay laboratories in Don Mills, Ontario. In addition, ferrous/ferric iron ratios were determined by analysing for Fe^{2+} for select samples using the method of WILSON (1955). The analytical methods employed and the full results are presented in the appendix.

Of 88 samples analysed, 35 represent various diabase and 45 represent all gabbros encountered including rodngitized varieties. Fresh samples were selected at a regular interval whilst altered rocks were sampled preferentially in order to be able to determine the nature of the alteration with increasing depth in the ophiolite.

5.2. MAJOR ELEMENTS

Results obtained of major elements were plotted on the various diagrams that follow to show relationships and trends more clearly than would be apparent from the visual inspection of the tables of chemical data. Normative compositions have not been utilized as an index of classification because of the extensive nature of hydrothermal activity that has affected most of the major elements.

A chemical index utilizing only the petrographically freshest of samples which

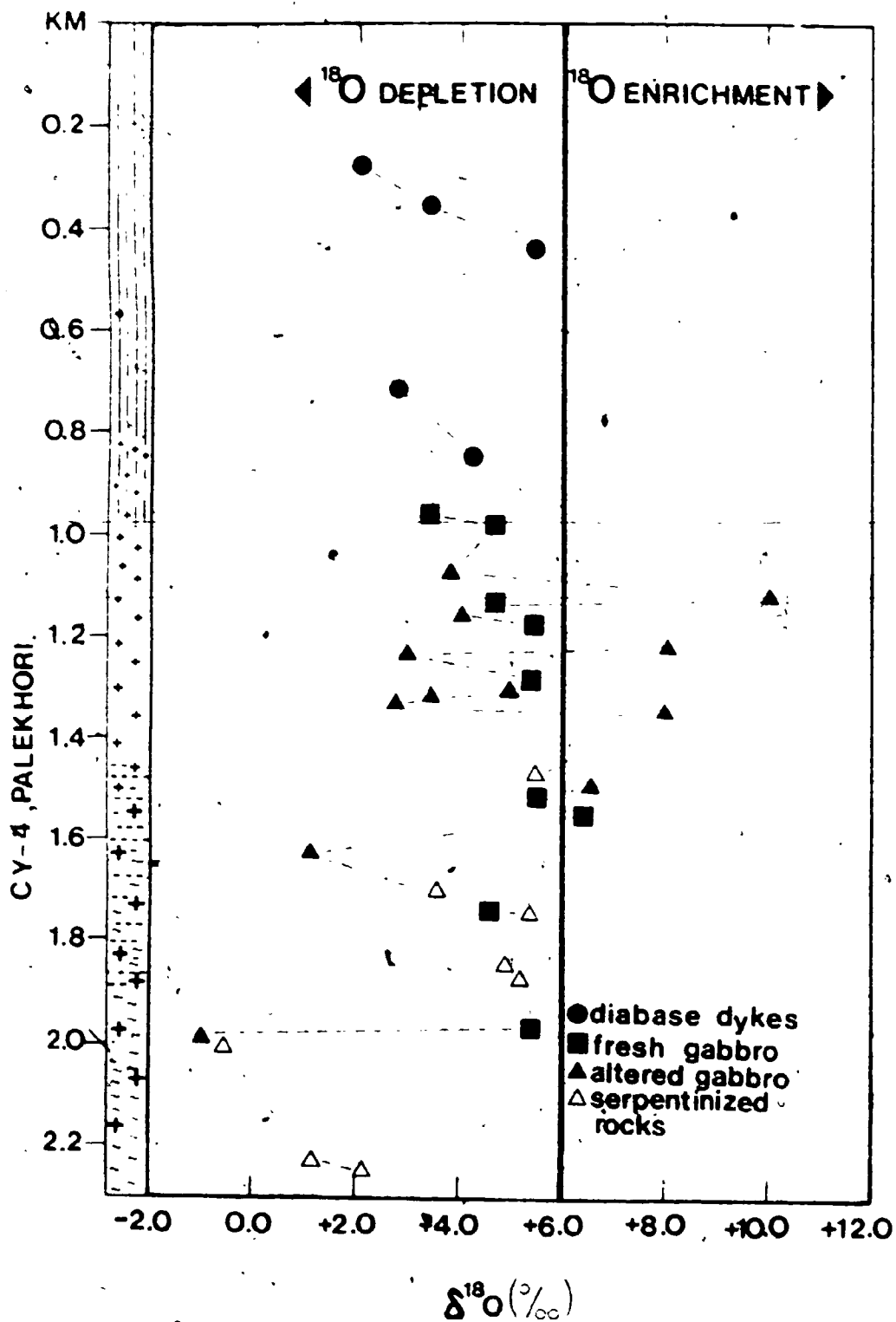
plots $\text{Na}_2\text{O} + \text{K}_2\text{O}$ vs. SiO_2 in wt. % classifies the rocks as being of tholeiitic composition with a high concentration of SiO_2 (fig. 5.1a), thus placing the majority of samples in the intermediate field.

The trends of certain major elements against the volatile content or LOI (loss on ignition) which is mostly the volatile content ($\text{OH}, \text{Cl}, \text{F}, \text{CO}_2$) of secondary hydrous minerals shows a broadly positive correlation for MgO and Na_2O and a negative one for CaO (fig. 5.1b,c,d) indicating that these elements have been mobile during metamorphism.

This matches petrographic observations of the development of albite from calcic plagioclase and the alteration of pyroxenes to chlorites and amphiboles. Fresh diabase analysed has a LOI range of 0.1 - 0.8 wt.% while altered diabase ranges 1.1 - 13.0 wt.% (see appendix) BEST(1982) gives an average volatile content ($\text{H}_2\text{O}^+ + \text{H}_2\text{O}^- + \text{CO}_2$) value of 2.3 wt. % for fresh diabase.

Figs. 5.1 and 5.2 show the trends of several major elements against MgO . The plots emphasise the very low contents of MgO in both the dykes and the gabbros. The broad ranges of SiO_2 , CaO and Na_2O probably indicate that alteration has affected even those rocks which appear to be petrographically fresh while Al_2O_3 variation may be related to the differing plagioclase contents of the various rocks. Figure 5.1. presents the following major element variation diagrams: A: Plot of $\text{Na}_2\text{O} + \text{K}_2\text{O}$ vs. SiO_2 in wt.% for fresh diabase. ALK = alkaline field, TH = tholeiitic field. B, C, D: Trends of the major elements MgO , CaO and Na_2O against volatile content (LOI) of samples. Open circles represent diabase. Squares (in B.) and triangles (in C, D) represent gabbro samples. E. SiO_2 v/s MgO and Al_2O_3 v/s MgO . Squares represent diabase samples. Triangles represent gabbros.

Fig. 5.7. $^{18}\text{O}/^{16}\text{O}$ whole rock profile for the Troodos ophiolite as observed in drillhole CY-4.



The plot of TiO_2 vs. MgO shows very low contents of TiO_2 in all the dykes and gabbros. The dykes have a marginally higher TiO_2 content than the gabbroic rocks. TiO_2 is restricted between 0.2 and 1.4 wt. % over a range in SiO_2 of 46 to 64 wt. %. That some of the dykes have an overall higher TiO_2 content indicates the presence of more than one type of magma and their relatively higher abundance of SiO_2 when compared to the gabbros is consistent with this. It is of note that TiO_2 is considered an immobile element during low to medium temperature metamorphic processes (PEARCE AND CANN, 1971). K_2O is of low abundance throughout the entire sequence. Values are commonly below the detection limit of 0.01 wt. % and reach a high of 0.2 wt. % in the diabase and 1.6 wt. % in the gabbroic sequence. The latter figure is abnormally high considering the range of values obtained, and may be due to alteration effects. Low K_2O values are typical of tholeiites (HYNDMAN, 1985). Mass considerations of seawater-basalt interaction (see HONNOREZ, 1981 ; THOMPSON, 1983) show that in the sub-oceanic environment, the behaviour of K is temperature dependent and initially in the low temperature, high water/rock ratio environment typical of the upper few meters of oceanic crust, K will be extracted out of seawater, where it is at a concentration of 400ppm, and fixed in phases such as K-rich smectite. Figure 5.2. shows the following major element variation diagrams:

A., B., C.: Trends of the major elements Na_2O , CaO and TiO_2 against MgO in wt. %. Triangles represent diabase analyses, open circles represent gabbro samples. D. TiO_2 v/s SiO_2 wt. % for Troodos diabase (diamonds) and gabbros (open circles). The situation is reversed during high temperature alteration in deeper parts of the oceanic crust where K, Si, B and Li are leached from the rock, but may be reprecipitated locally. Overall, the net effect of seawater-basalt interaction as regards K is that the K content of oceanic crust is increased. The low K values reported in this study seem to indicate that the element has been stripped from the diabases and gabbros of the ophiolite.

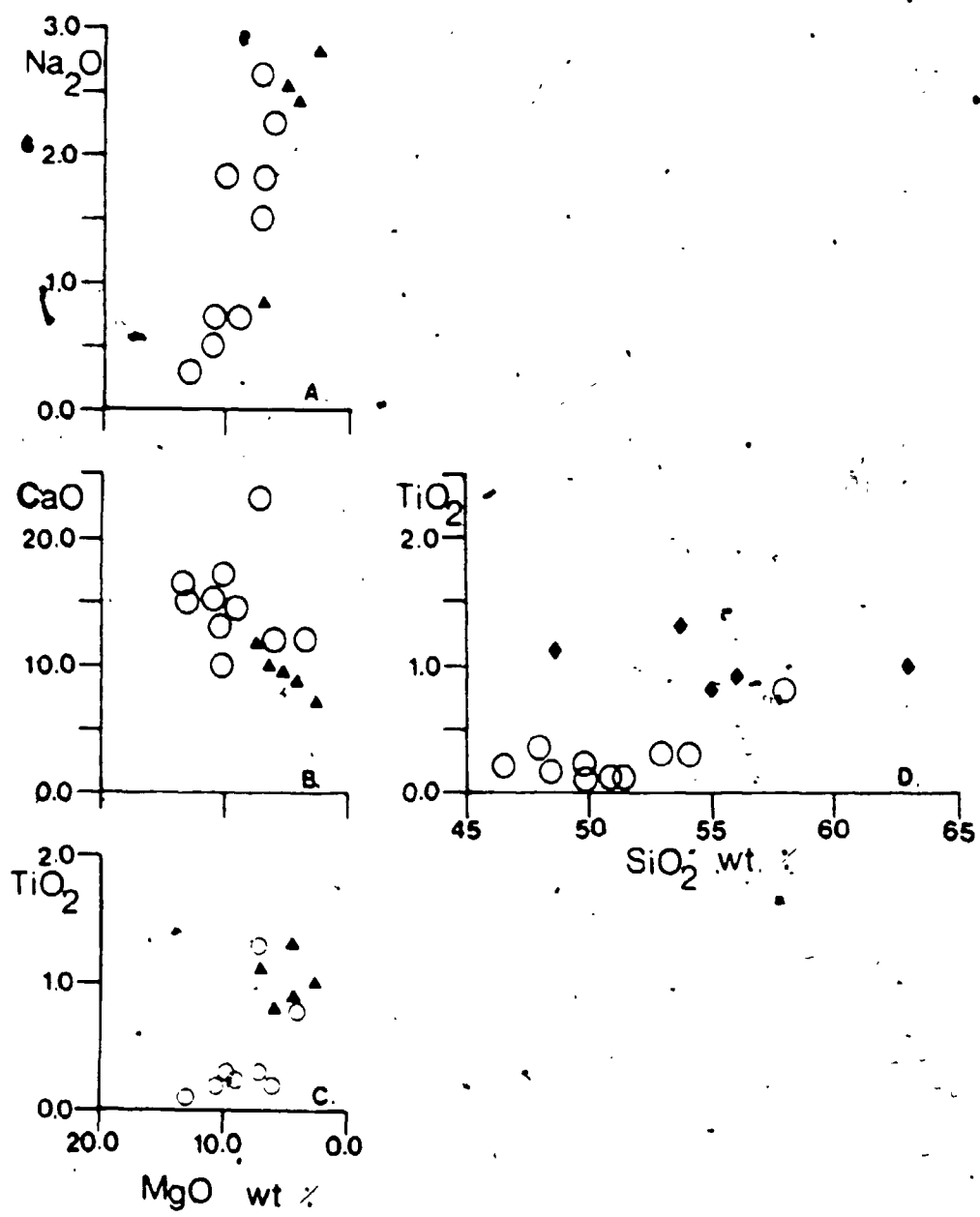


Fig. 5.2. A., B., C., D. Major element variation diagrams for plutonic rocks of the Troodos ophiolite. Open circles represent diabase dyke samples. Triangles and diamonds represent gabbro samples.

Quite the opposite conclusion can be observed from the work of MOORES and VINE(1971) who report K_2O values of up to 5 wt. % for presumably altered basalts and trachybasalt dykes from the top of the Troodos sequence. RAUTENSCHLIEN ET AL. (1985) report K abundances averaging about 1500ppm from glass preserved in Troodos pillow lavas and flows.

CaO shows a broad positive correlation with LOI in the gabbroic rocks. Petrographic work indicates that this can primarily be attributed to the development of Ca-rich phases such as Ca-zeolites and amphiboles in metamorphosed rocks which coexist with major amounts of chlorite, epidote/clinozoisite and prehnite. Where intensive alteration has occurred, the calcium metasomatism occurs together with silica leaching. The end result is commonly the development of rodngitized gabbros.

Fe^{2+} was determined by the titration using the method of WILSON(1955). The results are presented in the appendix and illustrated graphically in fig.5.3.

The ratio Fe^{2+}/FeO_{Total} varies from 0.8 (+/- 0.01 1σ) in fresh diabase to 0.6 in incipiently altered diabase, through to 0.4 in completely altered diabase. This corresponds to progressive trends of increasing alteration with proximity to the original ocean floor and confirms that the alteration observed is primarily an oxidation process.

Figure 5.3 presents the Ferric/ferrous data in graphic form: FeO wt. % vs. Fe^{2+}/FeO_{Total} wt. % for Troodos diabase (filled triangles), metadiabase (filled circles), fresh gabbro (open triangles) and metagabbro (open circles).

The Solid bar at 0.7 Fe^{2+}/FeO_{Total} wt. % represents average value for igneous mafic rocks (after HYNDMAN, 1985).

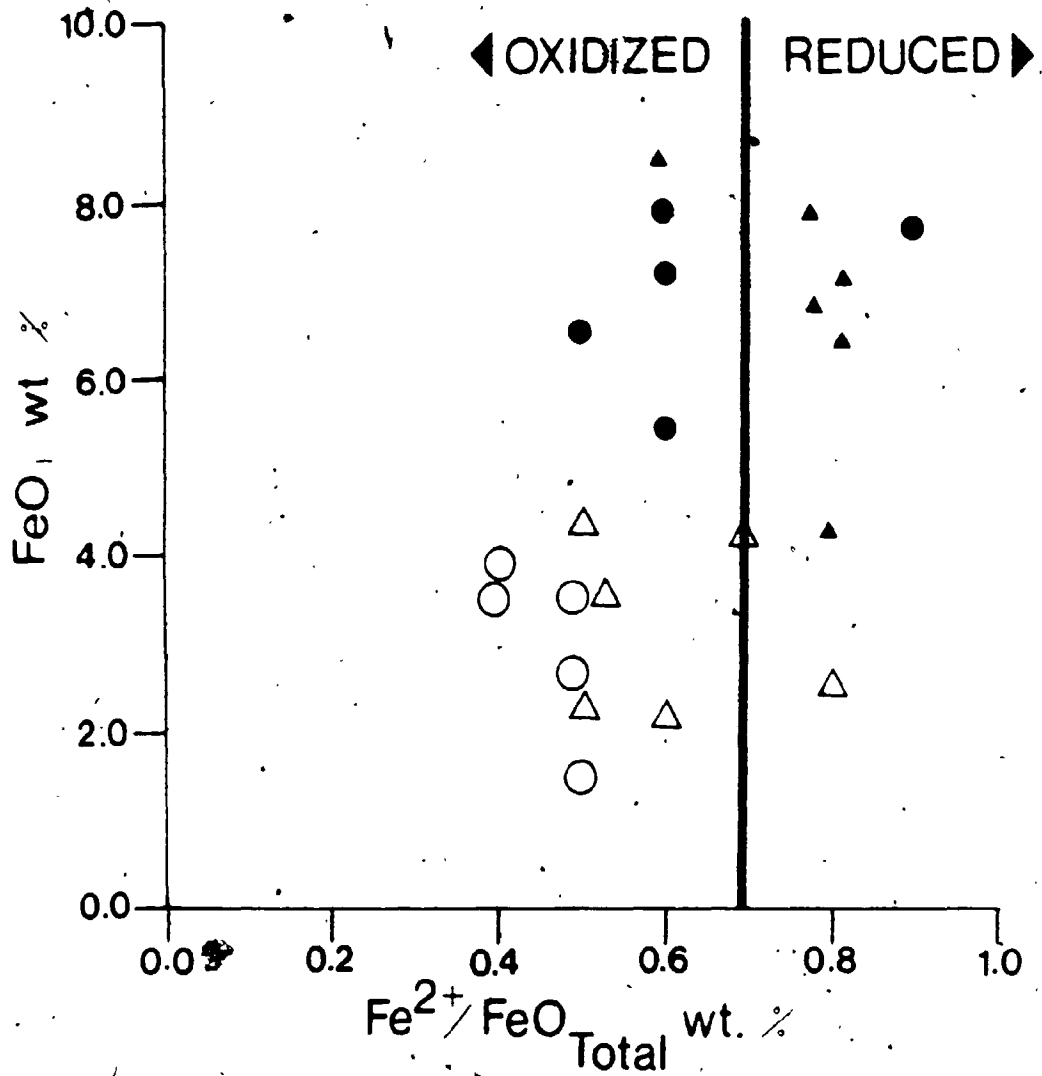


Fig. 5.5. FeO wt. % vs. Fe²⁺/FeO total wt. % for plutonic rocks of the Troodos ophiolite. Filled symbols represent diabase samples, open symbols represent gabbro samples. Triangles represent fresh rocks while circles represent altered rocks.

Some altered gabbros have not been oxidized ; this indicates that they probably interacted with reducing rather than oxidising fluids. Fresh mafic rocks have an average Fe^{2+}/FeO Total ratio of 0.7 (HYNDMAN, 1985). In general, oxidation-reduction processes in most rocks will not occur unless subjected to high water/rock conditions (EUGESTER, 1959).

5.3. TRACE ELEMENTS

Even though Troodos rocks are not typical Mid - Ocean Ridge type rocks (see ROBINSON ET AL., 1983), a comparison between them and MOR rocks is useful in as far as their alteration geochemistry may be able to characterize the main trends of what is essentially similar cooling histories.

A comparison between trace element data obtained in this study and trace element abundances in basalts from the mid-ocean ridges (see HAWKESWORTH, 1981) reveals fluctuations, deviations and similarities caused by a variety of factors:

In hydrothermally altered diabase dykes and gabbro, the abundance of Sr shows a wide variation (fig. 5.4) which has a median equivalent to mid-ocean ridge basalt (MORB) of 90 ppm. Apart from the fact that calcic plagioclase is a major constituent of basaltic rocks (thus allowing a large number of sites into which Sr can enter with a low potential energy) the data appears to reflect the variation in plagioclase content among the various rock types as well as the influence of seawater Sr. The exact influence of these various factors is indeterminate as the data obtained shows a roughly normal distribution about the average for MORB. What appears certain is that Sr is very mobile in this environment and has undergone extensive redistribution.

A previous trace element study of Troodos pillow lavas and flows by GUILLEMOT AND NESTEROFF (1980) gives an average Sr content of about

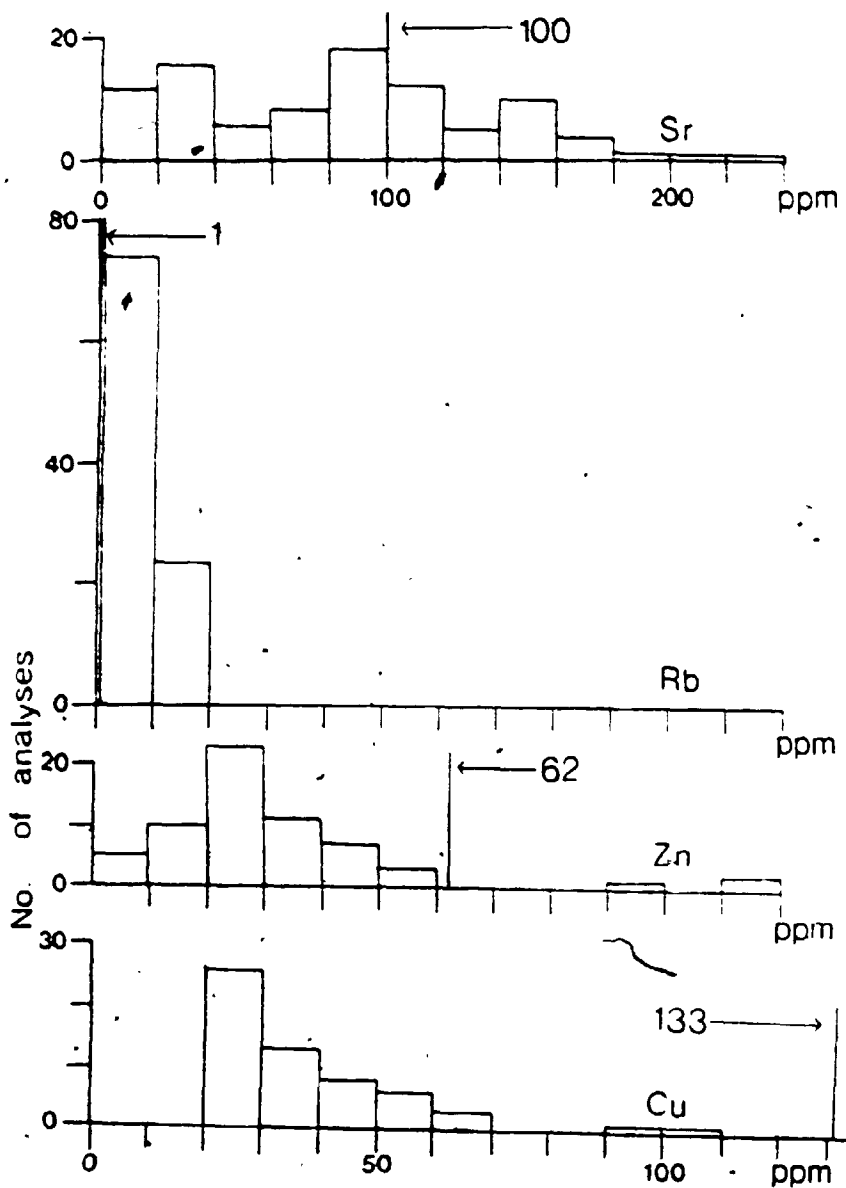


Fig. 5.4. Histograms for the abundances in ppm of Sr, Rb, Zn and Cu from diabase dykes of the Troodos ophiolite.

500ppm. This indicates an increase of five fold in Sr content in the extrusive part of the ophiolite. However, the Rb content shows a large variation to a maximum of 20 ppm as compared to an average MORB value of 1 ppm. This major difference in abundance of two elements whose geochemical behavior is in most cases identical is clear evidence of the genetic difference between the two rock types i.e. Troodos rocks, although complete with a Sheeted Complex, were not formed at a major ocean ridge.

Several workers (e.g. AUMENTO, 1979) have shown that U is enriched in altered oceanic crust relative to the pristine unaltered magmatic state and that some of the most altered varieties of ocean crust have values typical of granites, about 5 ppm. In the present study, U has been found to range between <0.1 ppm - 0.3 ppm. Since the value of U has been clearly shown to increase with age whenever massive seawater influx occurs for basalts (MITCHELL and AUMENTO, 1977) with values reaching 1 ppm in the most altered samples at large distances from the Mid - Oceanic Ridges, the case can be made that the abundance data of U at Troodos indicates that the ophiolite was obducted or exposed at a site only 10's of km away from its incipient spreading centre. This observation is compatible with the view of other workers (e.g. ROBINSON ET AL., 1983 ; RAUTENSCHLEIN ET AL., 1985) who, from the glass chemistry of the different pillow lavas, show that the formational environment of the ophiolite was a small spreading centre in a supra subduction zone environment.

The abundances and ratios of certain alteration insensitive elements may be diagnostic of the tectonic site of magma genesis (RAUTENSCHLEIN ET AL., 1985). For example, Zr and Y are among a small number of High Field Strength elements not readily affected by low grade metamorphism and hence may be used to deduce the tectonic environment of formation of rock suites whose

geochemistry would otherwise be suspect because of metamorphism and metasomatism. In the case of Zr and Y, the variation in Zr/Y is characteristic of magma source regions in the lower crust and upper mantle while the Zr content reflects the concentration in the source rocks as well as the degree of partial melting and fractional crystallization.

In the current study, a plot of Zr/Y vs. Zr (fig.5.5) for diabase dyke data reveals a distribution of points in both island-arc basalt and MORB fields i.e. yielding equivocal data as to the formational environment of Troodos. This finding is of significance in the light of other geochemical work at Troodos (see for example RAUTENSCHLEIN ET. AL., 1985).

Unequivocal trace element data case for the interaction of seawater with the rocks studied comes from the abundances in select samples of B and Cl (table 5.2) which are enriched in seawater with respect to oceanic mafic rocks.

Table 5.2. Boron abundance for select diabase(d) and gabbro(g) from the Troodos Ophiolite.

Sample #	Rock type	B(ppm)
CY130	d	30
CY024	g	30
CY030	g	20
CY039	g	20
CY088	g	20
CY078	g	20
CY093	g	20
CY098	g	20
CY108	g	20
CY107	g	20

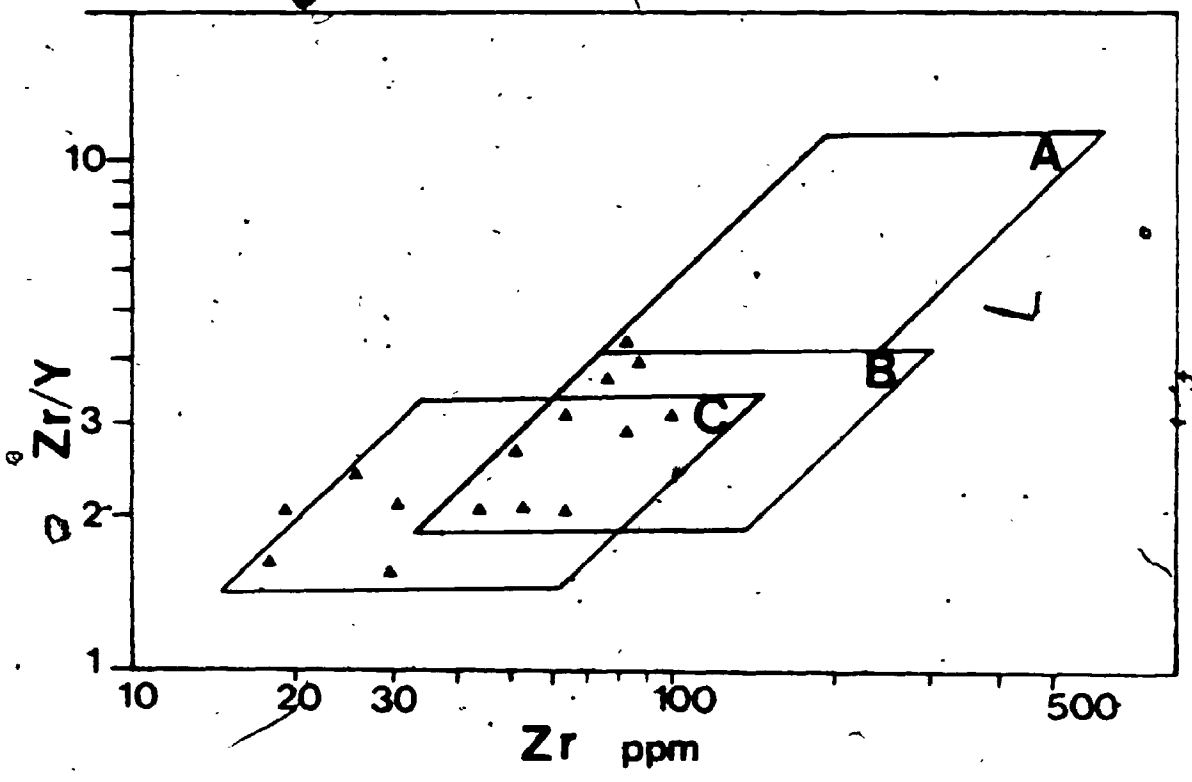


Fig. 5.5. Plot of Zr/Y vs. Zr for Troodos ophiolite diabase dykes. A represents field of Continental Basalts, B represents field of Mid Ocean Ridge Basalts while C represents field of Island Arc Basalts.

Table 5.3. Boron abundance for select diabase(d) and gabbro(g) from the Troodos Ophiolite.

Sample#	Rock type	B(ppm)
CY130	d	30
CY024	g	30
CY030	g	20
CY039	g	20
CY088	g	20
CY076	g	20
CY093	g	20
CY098	g	20
CY106	g	20
CY107	g	20

On average, the rocks have been enriched about 10 fold from igneous values of 2.0 ppm B for gabbros, and 2.7 ppm for basalts (FAIRBRIDGE, 1972). Cl abundances (see appendix) average 500 ppm a value representing a 5 fold enrichment over the igneous value of 100 ppm (FAIRBRIDGE, 1972) which itself may already indicate contamination.

5.4. STRONTIUM ISOTOPE GEOCHEMISTRY

Twenty samples representative of the rock suite had their $^{86}\text{Sr}/^{87}\text{Sr}$ ratios determined by thermal ionization spectrometry and these were used as petrogenetic indicators and alteration tracers (table 5.3):

Table 5.3. Present day $^{86}\text{Sr}/^{87}\text{Sr}$ ratios for Troodos rocks.

Sample #	Depth(m)	Rb(ppm)	Sr(ppm)	$^{86}\text{Sr}/^{87}\text{Sr}$
CY292(d)	20.8	2	100	0.70526+/-3
C251(mg)	279.8	6	120	0.70492+/-3
CY118(ag)	983.6	10	90	0.70444+/-2
CY109(g)	1036.0	5	30	0.7053+/-2
CY012(ag)	1115.5	15	90	0.70560+/-5
CY030(g)	1245.3	5	100	0.7051+/-5
CY039(ag)	1313.8	5	205	0.70583+/-1
CY042(ag)	1347.3	2	35	0.70513+/-6
CY057(ag)	1470.6	10	180	0.7082+/-1
CY059(sg)	1478.5	5	30	0.70594+/-3
CY064(g)	1503.1	1	20	0.7053+/-3
CY066(g)	1536.7	5	20	0.70536+/-5
CYB61(sg)	1550.0	3	100	0.7056+/-5
CY073(ag)	1618.4	5	90	0.7059+/-3
CY084(sg)	1708.3	10	100	0.70545+/-2
CY089(sp)	1742.7	5	100	0.7149+/-3
CY099(sp)	1808.9	3	50	0.7043+/-5
CYB70(sp)	1977.2	1	10	0.7062+/-3
CYB80(sp)	1981.3	2	15	0.7054+/-3

d = diabase; mg = microgabbro; a = altered; g = gabbro; s = serpentized. p = ultramafic rock.

The use of Sr isotopes as natural tracers in geological processes stems from Rb - Sr geochronology, and the use of Sr as a petrogenetic indicator is facilitated by its having four stable isotopes, ^{88}Sr - ^{81}Sr , with fixed relative abundances of 0.55% for ^{81}Sr , 9.75% for ^{86}Sr , 6.96% for ^{87}Sr and 82.74% for ^{88}Sr .

^{87}Sr is a decay product of ^{87}Rb while the remaining isotopic abundances are constant in nature as the species are neither radioactive nor the decay products of any naturally occurring radioisotope. What this means is that the abundance of ^{87}Sr depends not only on the amount of ^{87}Sr present at the time of formation of the material, but also upon the concentration of Rb and the age of the material.

As isotopic ratios are more accurately measured by a mass spectrometer than actual amounts, the abundance of ^{87}Sr is expressed as the ratio $^{87}\text{Sr}/^{86}\text{Sr}$ where the abundance of ^{86}Sr is constant as it is a stable isotope. The present day $^{87}\text{Sr}/^{86}\text{Sr}$ ratio in a rock is related to the original ratio $(^{87}\text{Sr}/^{86}\text{Sr})_0$ when the rock was formed at time $t = 0$, the Rb content and the decay constant λ by the equation:

$$^{87}\text{Sr}/^{86}\text{Sr} = (^{87}\text{Sr}/^{86}\text{Sr})_0 + (^{87}\text{Rb}/^{86}\text{Sr})(e^{\lambda t} - 1).$$

$(^{87}\text{Sr}/^{86}\text{Sr})_0$ is an important petrogenetic indicator because magma derived by partial melting of source rocks with a high Rb/Sr ratio or contaminated by such material, such as old continental crustal material will inherit this signature in a high initial ratio. Low Rb/Sr sources, such as peridotitic mantle correspondingly yield magmas with low initial ratios (BEST, 1982).

Rearranging the above equation for the original $^{87}\text{Sr}/^{86}\text{Sr}$ ratio yields:

$$(^{87}\text{Sr}/^{86}\text{Sr})_0 = (^{87}\text{Sr}/^{86}\text{Sr})_t - (^{87}\text{Rb}/^{86}\text{Sr})(e^{\lambda t} - 1)$$

where the decay constant λ is $= 1.42 \times 10^{-11} \text{ a}^{-1}$ and $^{87}\text{Rb}/^{86}\text{Sr}$ is approximately $2.9 \times \text{Rb/Sr (ppm)}$.

The above equation can then be approximated by:

$$(^{87}\text{Sr}/^{86}\text{Sr})_t = (^{87}\text{Sr}/^{86}\text{Sr})_0 + 2.9(\text{Rb/Sr})\lambda$$

because ^{87}Rb is a known portion of total Rb, ^{86}Sr is nearly a constant portion of total Sr and because the half life of ^{87}Rb is so long (50×10^9 yrs) that the exponential in the decay can be ignored. Using the value of 85 M.a. for the age t , of the Troodos ophiolite (VINE ET AL., 1973 ; GASS, 1980) the original $^{87}\text{Sr}/^{86}\text{Sr}$ values are calculated and the results presented in table 5.4:

Table 5.4. Present day and initial $^{87}\text{Sr}/^{86}\text{Sr}$ values for analysed Troodos rocks.

Sample #	Rb/Sr	$(^{86}\text{Sr}/^{87}\text{Sr})_t$	$(^{86}\text{Sr}/^{87}\text{Sr})_o$
CY292	0.02	0.70526	0.7053
CY251	0.05	0.70492	0.7049
CY118	0.11	0.70444	0.7044
CY109	0.17	0.70530	0.7053
CY012	0.17	0.70560	0.7056
CY030	0.05	0.70510	0.7051
CY039	0.02	0.70583	0.7058
CY042	0.06	0.70513	0.7051
CY057	0.05	0.7082	0.7082
CY059	0.16	0.70594	0.7059
CY064	0.05	0.70530	0.7053
CY066	0.25	0.70536	0.7054
CYB61	0.03	0.70560	0.7056
CY073	0.06	0.70590	0.7059
CY084	0.10	0.70545	0.7055
CY089	0.05	0.71490	0.7149
CY099	0.06	0.70439	0.7044
CYB70	0.10	0.70620	0.7062
CYB80	0.13	0.70540	0.7054

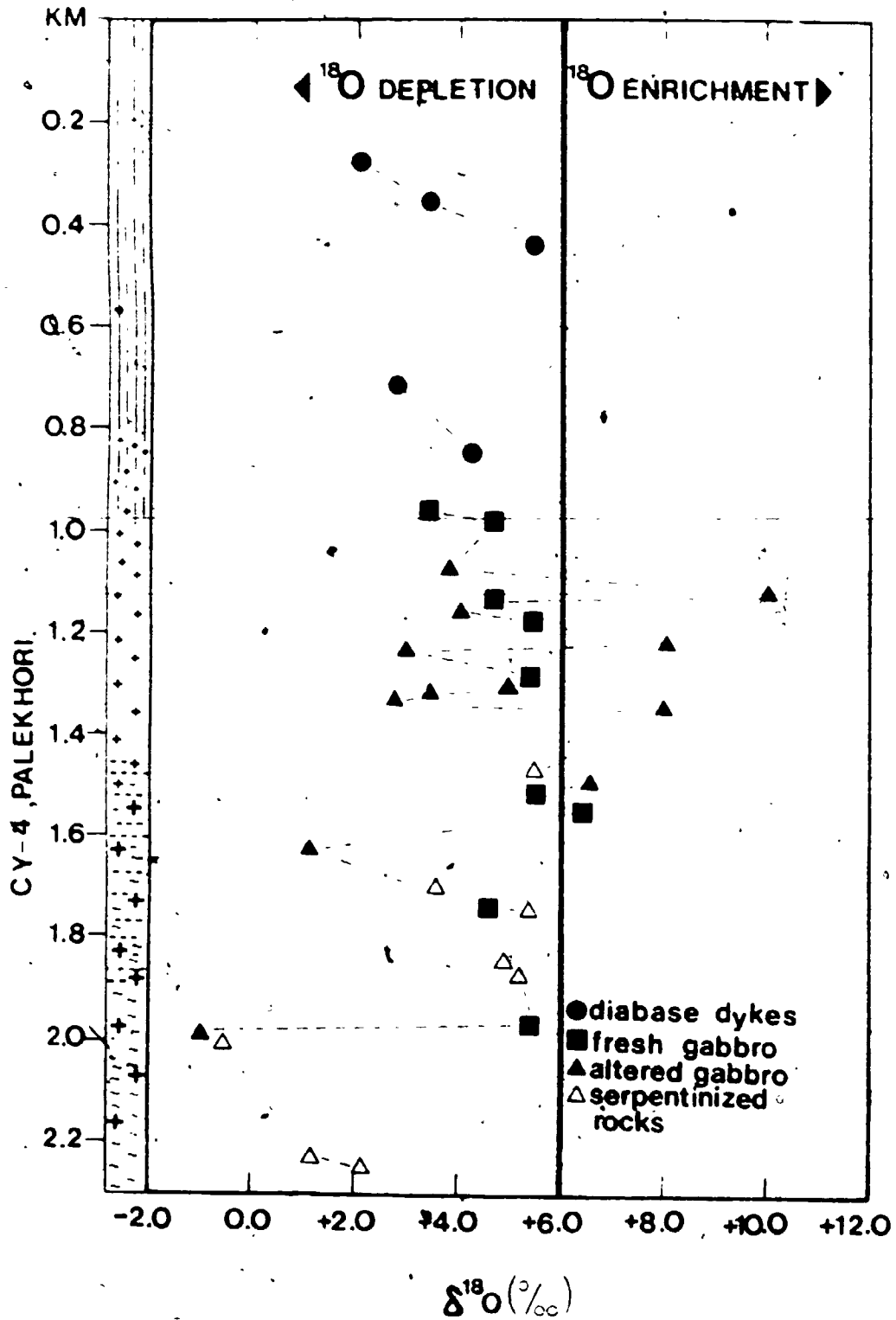
The freshest rocks have values in the range 0.7030 - 0.7049. These are the lowest values although one altered sample, an epidote-hornblende bearing metagabbro has a ratio of 0.7044. Sr isotope values for the altered rocks range from 0.7043 to 0.7149. The serpentinized samples possess the highest initial ratios. These values compare with the following:

Table 5.5. $^{86}\text{Sr}/^{87}\text{Sr}$ values of crust and oceanwater.

Reservoir	Present	85Ma B.P.
Continental crust	0.702-0.730	--
Oceanic crust*	0.7028	0.7029
Seawater**	0.7091	0.7074

* After MORRIS and HART, 1984 ; ** after BURKE ET AL., 1982.

Fig. 5.7. $^{18}\text{O}/^{16}\text{O}$ whole rock profile for the Troodos ophiolite as observed in drillhole CY-4.



The current study produces an average fresh rock value of $0.7049 \pm 0.0003(1\sigma)$ and an average altered rock value of $0.7056 \pm 0.0005(1\sigma)$.

The altered samples on average represent an increase of 0.0007 over the fresh samples. However, the values for the fresh samples are noticeably higher than estimated for Troodos age oceanic crust (PETERMAN, HEDGE and TOURTELOT, 1970) suggesting that the samples may in fact be altered on a submicroscopic scale.

The present study thus indicates that Troodos ophiolite mafic rocks have been contaminated with Sr deep into the gabbroic sequence. The contamination may be due to seawater/rock interaction because seawater is the only plausible source of more radiogenic $^{87}\text{Sr}/^{86}\text{Sr}$ ratio material present in the suboceanic environment. This observation is in accord with previous Sr isotope work done on Cyprus (e.g. SPOONER, 1976, 1977) which report the same phenomenon of $^{87}\text{Sr}/^{86}\text{Sr}$ enriched mafic rocks. However, the presence of two sample points, CY057, taken from a laumontite bearing shear zone in the isotropic gabbro $^{87}\text{Sr}/^{86}\text{Sr} = 0.7082$ and CY089 from serpentized pyroxenite with $^{87}\text{Sr}/^{86}\text{Sr} = 0.7149$ with ratios higher than that of postulated Campanian-Maestrichtian seawater is unusual and may indicate that Tethyan seawater may have had a slightly higher $^{87}/^{86}\text{Sr}$ ratio than average. Extensive limestone and anhydrite deposits (BEAR, 1960) at Troodos also suggest this.

5.5. OXYGEN ISOTOPE GEOCHEMISTRY

Recent oxygen isotope analyses carried out on rocks from ophiolite suites have generally shown that hydrothermal alteration in ancient oceanic crust is extensive, and can be considered to be the direct result of seawater convecting through oceanic crust in response to cooling (SPOONER and FYFE, 1973; HEATON and SHEPPARD, 1977; GREGORY and TAYLOR, 1981; SCHIFFMAN

ET.AL.,1984 ;STAKES and VANKO,1986). At Troodos the present study reveals broad hydrothermal alteration in the mafic rocks to be of the same nature as shown by previous studies, but with significant variations that add to produce a more complicated oxygen isotope profile than has previously been suggested by other workers (e.g. GREGORY and TAYLOR, 1981). The oxygen isotope composition of fresh and altered oceanic rocks, specifically of ophiolites has been employed to deduce the conditions of basalt-seawater interaction and to constrain the isotopic budget of the hydrosphere (MUEHLENBACHS and CLAYTON,1972 a; GREGORY and TAYLOR,1981 ; HOLLAND,1984). This study reports the results of an oxygen isotope investigation into Troodos ophiolite mafic rocks sampled from ICRDG drillhole CY-4, for both whole rocks and mineral separates. Isotope analyses were also performed on calcite bearing rocks coming mostly from the upper region of diabase dykes encountered by the drillhole.

Oxygen has three naturally occurring stable isotopes, ^{16}O , ^{17}O , and ^{18}O . The isotopes do not suffer from radioactive decay and have the following abundances in ocean water: ^{16}O 99.758‰ ; ^{17}O 0.039‰ ; ^{18}O 0.205‰. Substantial variation of the abundances of the three isotopes occur in nature and the conventional manner used to express the isotopic composition of a substance is by referring its $^{18}\text{O}/^{16}\text{O}$ ratio to Standard Mean Ocean Water ($^{18}\text{O}/^{16}\text{O}$ SMOW) which by definition is zero per mil.

$$\delta^{18}\text{O} = \left[\left(\frac{^{18}\text{O}/^{16}\text{O}_{\text{sample}}}{^{18}\text{O}/^{16}\text{O}_{\text{SMOW}}} \right) - 1 \right] \times 1000$$

the value is in parts per thousand (‰). Variations in oxygen isotope abundances are caused by kinetic and equilibrium fractionation mechanisms which are temperature dependent but insensitive to pressure. In a system at equilibrium, the isotopic composition of two coexisting phases is a function of temperature alone; i.e. a pair of minerals formed in nature at equilibrium thus can be used as a geothermometer (BEST,1982).

Fractionations or differences in δ among minerals are termed Δ which is defined as:

$$\Delta_{A-B} = 1000 \ln \alpha_{A-B} \text{ approximately } = \delta_A - \delta_B$$

where δ is the fractionation factor for the coexisting minerals A and B.

TAYLOR and EPSTEIN(1962) and JAVOY(1977) discuss in detail the background and theory of oxygen isotope fractionations. Troodos ophiolite diabase dykes analysed for $^{18}\text{O}/^{16}\text{O}$ ratios gave a range of values of $\delta^{18}\text{O}$ of 2.2-6.4 per mil. The freshest samples among them (CY227, CY145) yield the highest $\delta^{18}\text{O}$ values of the study, however these values barely lie at the low end of fresh tholeiitic oceanic rocks whose $\delta^{18}\text{O}$ is 5.7 ± 0.3 (GREGORY and TAYLOR, 1981). The other samples analysed, though fresh in appearance, megascopically have experienced oxygen exchange with an extraneous media. Electron microprobe investigation reveals minor and patchwork type alteration of diopsidic augite to actinolite, this in co-existence with fresh calcic plagioclase. Isotropic and layered gabbros with fresh ophitic to subophitic textures in thin section gave a range of $\delta^{18}\text{O}$ of 4.6 to 6.4 per mil (CY117, 017, 023, 036, 064, A2) thus also indicating that oxygen exchange with an external reservoir had occurred despite petrographic appearances of being fresh. Various altered gabbros (table 5.4) give a much wider range of values of $\delta^{18}\text{O}$ of 1.1-10.4 per mil. The whole rock $\delta^{18}\text{O}$ compositions of 34 selected samples from Troodos (CY-4) are presented in table 5.7. The metamorphic mineral assemblages of the analysed samples together with known mineral stability fields have been used to estimate isotope re-equilibration temperatures.

Table 5.6

Whole rock $^{18}\text{O}/^{16}\text{O}$ profile for CY-4.

S.#	D. (m)	Description	$\delta^{18}\text{O}$ Rock
253	266.5	sheared d.	2.2
239	356.8	sheared d.	3.3
227	443.9	sheared d.	5.3
212	515.7	sheared d.	2.8
145	836.2	sheared d.	4.1
119	980.0	HL gabbro	3.4
117	994.1	HL gabbro	4.6
006	1073.2	met.d.	3.7
012	1115.5	chl.gabbro	10.4
017	1147.7	ign.gabbro	4.6
021	1175.4	met.gabbro	4.1
023	1486.3	iso.gabbro	5.4
B81	1236.7	And.gabbro	7.9
030	1245.3	metagabbro	3.1
036	1283.0	ign.gabbro	5.4
B80	1310.2	lch.gabbro	5.1
039	1313.8	chl.gabbro	3.5
R4	1323.0	metagabbro	2.7
040	1329.7	qtz-ep v.	8.1
059	1478.6	serp.int.	5.5
063	1496.0	metagabbro	6.6
064	1503.1	ign.gabbro	5.5
068	1536.7	ign.gabbro	6.3
073	1618.4	lch.gabbro	1.1
084	1708.3	serp.vein	3.6
087	1730.6	qtz-plag v.	4.6
089	1742.7	serp.int.	5.4
WX	1977.0	serp.u/m.	4.6
A1	1850.4	serp.u/m.	5.0
A2	1860.3	gabbro	5.2
B2	1996.3	ep.u/m.	-0.5
WX0	1981.0	serp.u/m	-0.9
B15	2228.2	serp.u/m	1.2
B17	2235.3	serp.u/m	2.2

ign., igneous. met., metasomatized. serp., serpentized. lch., leached.u/m.
 ultramafic rock. d., diabase. ep., epidote. chl., chlorite. qtz., quartz. iso., isotropic.
 And., andradite. v., vein. Int., intrusion. HL., high level.

stratigraphic position. The sample with the lowest $\delta^{18}\text{O}$ value, CY073, is a metagabbro bearing hydrothermal diopside and hydrothermal anorthite (An96) from a bleached zone in CY-4 occurring at a depth of 1618.4m (plate 2) which has been left porous on the cm scale by heated hydrothermal fluids, and yields the highest water/rock ratio. Sample CY012, a gabbro from 1115.5m, has a $\delta^{18}\text{O}$ value of 10.4 per mil which is the highest whole rock value determined in this study. The sample is derived from a medium grained gabbro exhibiting a slight mineral orientation of plagioclase and whose only evidence of alteration is the presence of minor chlorite replacing clinopyroxene visible only in thin section.

Serpentinized ultramafic rocks composed mainly of relict olivine, enstatite and lizardite with minor antigorite yield $\delta^{18}\text{O}$ values in the range 3.8-5.5 per mil. These low values indicate that all the analysed serpentinized rocks have experienced open system oxygen isotopic exchange at low to high temperature. The values lie at the lower end of the range of values obtained by MARGARITZ and TAYLOR, (1974) who report an oxygen isotope range of serpentinites of 2.0 - 9.3 per mil.

Table 5.7. Oxygen data for mineral separates from altered Troodos rocks.

S. #	$\delta^{18}\text{O}_{\text{Qtz}}$	$\delta^{18}\text{O}_{\text{An}}$	$\delta^{18}\text{O}_{\text{Act}}$	$^{18}\text{O}_{\text{H}_2\text{O}}$
008	4.3	4.6	-	+3.4
021	2.3	5.3	-	+4.1
B77	4.2	8.9	-	+7.7
121	5.9	-	1.2	-2.5
004	7.6	-	5.3	-9.6
024	7.7	-	6.8	-4.6

* $\delta^{18}\text{O}$ of H_2O equation calculated as being in equilibrium with the rocks using feldspar geothermometry as defined by O'NEIL and TAYLOR (1967).

During open system exchange the $\delta^{18}\text{O}$ value of hydrothermal fluids and the temperature of interaction of the fluids with rock are the major controls of the oxygen isotope ratios of silicates in equilibrium with fluids. Both theoretical and experimental work show that silicate - water fractionations are large and positive at low temperatures and that they decrease rapidly with increase in temperature (TAYLOR, 1968; MUEHLENBACHS and CLAYTON, 1972 a, b, 1978). Over the geologically important temperature range from approximately 100°C to 700°C , this decrease in the isotopic difference between coexisting silicates and water is related to the reciprocal of the square of the absolute temperature. TAYLOR (1967) shows that the fractionations steadily decrease to being small and even negative by 400°C .

The $\delta^{18}\text{O}$ values of the analysed samples from Troodos in this study (tables 5.3, 5.4, fig 5.8) with few exceptions show ^{18}O negative shifts or depletions relative to $\delta^{18}\text{O}$ values for fresh tholeiitic basalts of $+5.7 \pm 0.3$ per mil. The maximum observed negative isotopic shift is by 6.6 per mil. The maximum positive isotopic shift is by 4.7 per mil, to whole rock values of -0.9 and +10.4 per mil respectively (samples CY-WXO and CY-012, respectively). The overall trend is that the $\delta^{18}\text{O}$ whole rock values decrease downwards producing larger depletions in the gabbros and ultramafics. At temperatures of about 300°C and under open system conditions of high water/rock ratios, the fractionation between rock and water with $\delta^{18}\text{O} = 0$ and basalt with $\delta^{18}\text{O} = 5.7 \pm 0.3$ per mil is such that no isotopic shift occurs. At temperatures less than this, basalts are enriched in the heavier isotope of oxygen. At temperatures higher than this, the rocks will be leached in ^{18}O due to the temperature effects of water rock

fractionation. Since a temperature for hydrothermal metamorphism of 300°C to approximately 370°C is suggested by the secondary mineral paragenesis albite + chlorite + actinolite in the diabase dykes and greater than 500°C in the high level gabbro by the critical assemblage anorthite + magnesio - hornblende the data are interpreted as primarily indicative of high temperature hydrothermal alteration of the ophiolite by seawater fluids at variable water/rock ratios. Isotope data for mineral separates (table 5.5) for a number of alteration zones confirm the influence of isotopically negative fluids. This is to be expected as these fluids have presumably reacted or exchanged oxygen with higher level oceanic crust such as pillow lavas and massive flows initially during their descent path at fairly low temperatures, enriching the $^{18}\text{O}/^{16}\text{O}$ ratios of the volcanic rocks. At temperatures above 400°C (TAYLOR, 1967) the $\delta^{18}\text{O}$ of the fluids increases to above $\delta^{18}\text{O} = 0$ while the plutonic rocks under going exchange become depleted in ^{18}O . The occurrence of ^{18}O - enriched rocks in the plutonic sequence where the metamorphic mineral assemblages suggest temperatures of recrystallization above 350°C indicates the influx of isotopically unreacted seawater. The samples whose $\delta^{18}\text{O}$ whole rock values are enriched ($>5.7 \pm 0.3$ per mil) are accordingly interpreted as being the products of low temperature hydrothermal fluid and rock interaction. The maximum observed positive shift yields a whole rock $\delta^{18}\text{O}$ value of +10.4 per mil.

Previous studies (e.g. SPOONER ET AL., 1974 ; HEATON and SHEPPARD, 1977 ; GREGORY and TAYLOR, 1981 ; SCHIFFMAN ET AL., 1984 ; STAKES and VANKO, 1986) of isotopic variation in ophiolites have shown both ^{18}O enrichment and depletion, with the enriched rocks primarily confined to the top level pillow lavas and flows, and with successive units showing progressively smaller fractionations. The present study indicates a much more complicated

oxygen isotope picture of the effects of ocean crust/basalt interaction and reveals fluctuations from overall ^{18}O depleted values to ^{18}O enriched values deep within the gabbroic sequence. In this suboceanic environment where geothermal gradients are very high, the observed shifts to positive values at deep levels must reflect massive influxes of seawater into deeper parts of the pile via pathways several orders of magnitude greater than the dominant infiltration pathways. Such conditions would enable huge quantities of seawater at lower than ambient temperatures and oxygen isotope composition of about $\delta^{18}\text{O} = 0$ per mil. access to deeper level rocks where oxygen exchange would produce the observed ^{18}O enrichments in the gabbros at depth.

5.6. CARBON ISOTOPE SYSTEMATICS

Analyses of $^{13}\text{C}/^{12}\text{C}$ and $^{18}\text{O}/^{16}\text{O}$ ratios were performed on secondary calcite bearing assemblages from late laumontite + stilbite + calcite veins, vugs, and shearzones encountered in CY-4 (table 5.8):

Table 5.8

Isotopic composition of CY-4 calcites.

S.#	D.(m)	$\delta^{13}\text{C}$	$\delta^{18}\text{O}$
225	462.1	-14.7	+21.2
218	494.0	-14.0	+20.8
207	535.8	-12.8	+21.1
175	705.4	-12.4	+20.4
155	794.5	-9.7	+19.7
126	941.1	-14.5	+21.8
125	948.9	-15.1	+20.5
019	1165.2	-15.7	+20.4

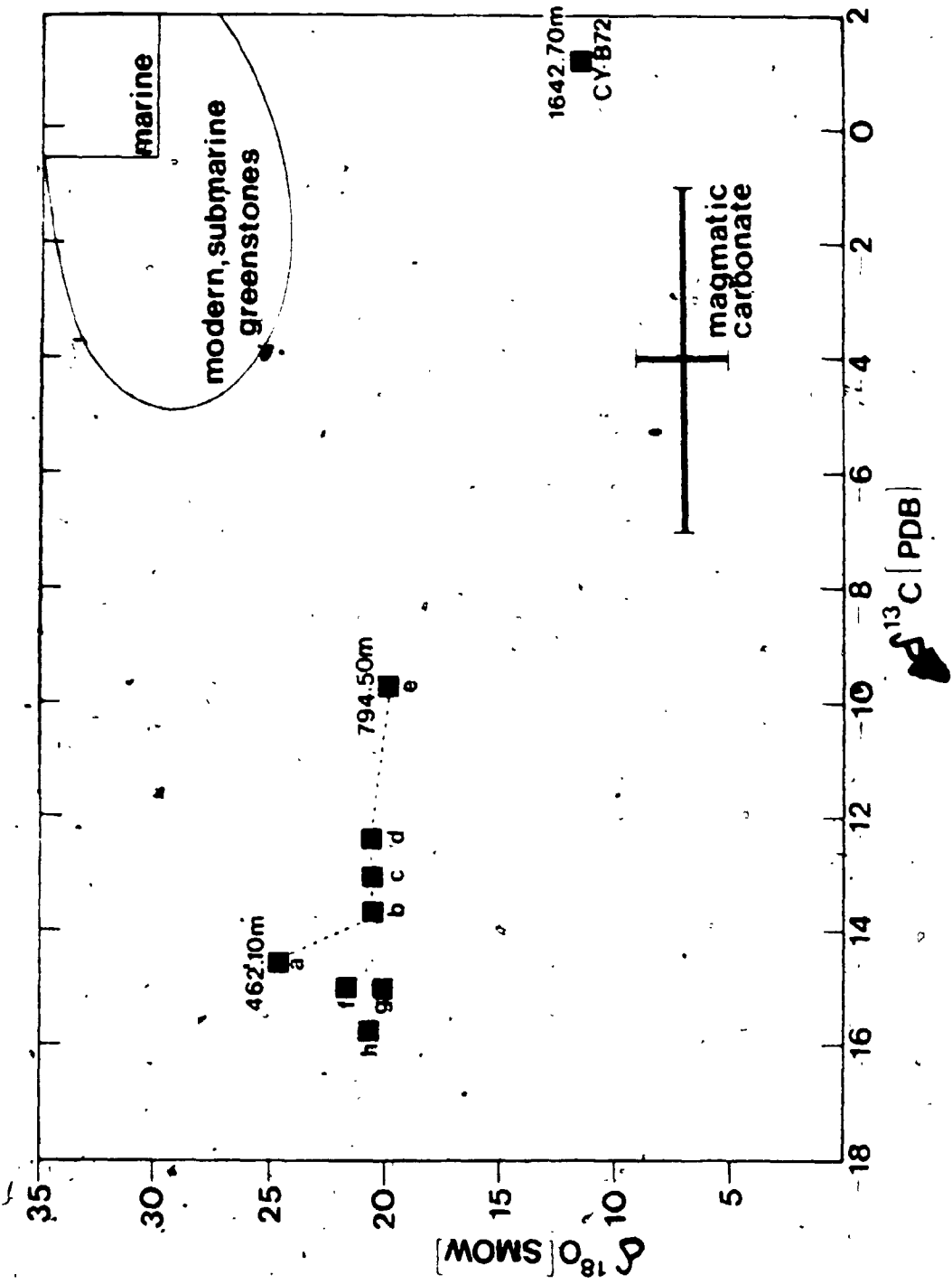
B72	1642.7	+1.2	+11.5
-----	--------	------	-------

Most of the samples are from the depth range 450-1200m in the sheeted dykes and high level gabbros. The $\delta^{13}\text{C}$ values obtained range from -15.7 to +1.2 per mil and the $\delta^{18}\text{O}$ values for the same samples range from +11.2 to +24.0 per mil. The $\delta^{13}\text{C}$ values cluster between +9 and -16 per mil with one isolated sample, which occurs far deeper in the ophiolite sequence than any other, having a value of +1.2 per mil. The first five calcite bearing samples, which all occur in the diabase, show a constant increase of $\delta^{13}\text{C}$ from -15 to -10 per mil with increasing depth. The samples occurring in the high level gabbros have negative $\delta^{13}\text{C}$ values clustered at -15 per mil (fig.5.7).

The carbon and oxygen isotopic compositions of naturally occurring carbonates are unique to the extent that they are routinely used as reservoir tracers and in conjunction with detailed geologic and geochemical studies are used to obtain information on the physicochemical conditions at the time of deposition and where applicable, ore formation (HOEFS, 1976). The average value of $\delta^{13}\text{C}$ for sedimentary marine carbonates is close to 0 per mil while that for igneous carbon is close to -5 per mil. Carbon derived from biogenic processes is isotopically more negative than igneous carbon, up to -35 per mil (OHMOTO and RYE, 1979).

Secondary carbonates formed by the low temperature alteration of fresh basalts by seawater have carbon and oxygen isotope compositions that range from -5 to +2 per mil (PDB) and from 25 to 30 per mil (SMOW), respectively (MUEHLENBACHS and CLAYTON, 1972; MUEHLENBACHS, 1977). High temperature (>300°C) seawater/rock interaction produces carbonates with oxygen and carbon isotopic compositions ranging from -1 to -16 per mil (SMOW) and from -7 to -4 per mil (PDB), respectively (MUEHLENBACHS and CLAYTON,

Fig. 5.8. Plot of $^{18}\text{O}(\text{SMOW})$ vs. $^{13}\text{C}(\text{PDB})$ for Proterozoic oriolite late calcites occurring in veins and fissures of CY-4.



1972b). However, while these possible carbon reservoirs appear to be distinctive, large ranges of $\delta^{13}\text{C}$, up to 50 per mil in a single deposit, are known to result from fluctuations in temperature, Eh and pH during carbonate precipitation from solution (OHMOTO, 1972).

The carbonates from Troodos reported in this study appear to be too negative to be consistent with an origin attributable to seawater/rock interaction alone. In other words it is difficult to interpret the results as the products of carbonates inorganically precipitated out of seawater at elevated temperatures. This leaves the suggestion open that the analysed carbonates owe their C content in part to a low $^{13}\text{C}/^{12}\text{C}$ biogenic reservoir. The presence of sulphur based chemotropic biological communities around discharge vents on the ocean floor (see RISE Project Group, 1979) provides a ready source of such biogenic carbon.

5.7. SUMMARY

The alteration sensitive element geochemistry of the Troodos ophiolite mafic rocks indicates that they were originally tholeiites with mafic to intermediate contents of silica. The alteration sensitive elements also show that the rocks have undergone hydrothermal alteration which has profoundly affected the distribution of most of the mobile major and trace elements.

The main effect of the alteration has been the fixation of H_2O and Na_2O in the upper diabase dykes that has converted parts of them into spilites. Calcium metasomatism in the lower gabbroic rocks has led to the development of rodingitized gabbros in places. Ferrous/ferric iron ratios for select rocks indicate that alteration has primarily been an oxidation process. Trace element analysis shows that Sr has been mobile but is equivocal as to whether it has been deposited or stripped from the lower ophiolite rocks. High Rb abundance is not consistent with the low K content of the rocks and appears to be seawater

derived. Zr/Y relations when plotted against Zr fall into the field of island arc basalts and MORB while U abundances, which are low, suggest that the ophiolite was obducted or exposed in a region close to its environment of formation. B and Cl contents are enriched up to 5 fold above average basaltic values. High $^{87}\text{Sr}/^{86}\text{Sr}$ values indicate strontium contamination approaching seawater values and $^{18}\text{O}/^{16}\text{O}$ isotope ratios show that locally alteration proceeded at high temperatures exceeding 400°C and was caused by seawater evolved fluids which produced $\delta^{18}\text{O}$ - depleted plutonic rocks. The presence of large positive $^{18}\text{O}/^{16}\text{O}$ ratios at depth in the gabbros greater than 6.0 per mil is attributed to giant influxes of seawater at lower than ambient temperatures through major deep going faults. Late carbonate bearing veins yield negative $\delta^{13}\text{C}$ values suggestive of the contribution of organic carbon.

Chapter Six FLUID INCLUSION ANALYSIS.

6.1. INTRODUCTION

A study of fluid inclusions was undertaken in an attempt to trace part of the chemical evolution of fluids convecting through oceanic crust. Although particulate laden 350°C fluids have been observed venting from oceanic crust near spreading centres (e.g. RISE Project Group, 1980) little is actually known about how seawater evolves chemically into this type of a fluid. Indirect evidence is available from metamorphic minerals and alteration assemblages.

At Troodos, apart from the metamorphosed rocks, various alteration zones and vein assemblages encountered reveal a definite mineralogic sequence with increasing depth indicative of an increasing temperature of alteration. However, a large number of late, retrograde assemblages are also present. Broadly, the major mineralogic trends in the alteration zones are as follows:

Low temperature zeolite facies minerals in pillow lavas and flows (GILLIS and ROBINSON, 1985). Laumontite + stilbite + calcite + gypsum (+albite + chlorite) in the diabase dykes. Epidote + quartz (+albite + actinolite) in the isotropic gabbros. Diopside + prehnite + andradite + quartz (+anorthite + hornblende) in lower isotropic and cumulate gabbros. Serpentine + magnetite + chlorite + quartz in layered gabbros.

Individual alteration zones range in aperture from a few cm to over 2m. Most veins encountered are in the aperture range 1mm to 2cm wide. The vein infill is varied, though most commonly retrograde laumontite in the diabase and gabbros. Shear zones are common. Many fractures appear to have been used more than once (see ICRDG, 1984; 1985).

Though practically insignificant, minute remnants of the actual fluids responsible for this alteration are preserved in the rock as fluid inclusions in minerals. Optical considerations render quartz as the only mineral in the rocks studied with readily observable inclusions. However quartz is not a common mineral in this environment as silica tends to be leached rather than deposited with increasing temperature (FYFE, 1974).

Fluid inclusion studies are based on the fact that when crystals grow or recrystallize in a fluid medium, growth irregularities trap small portions of the fluid in the solid crystal. The sealing off of such irregularities may occur during the growth of the surrounding crystal, yielding primary fluid inclusions, or by recrystallization along fractures at a later time yielding secondary inclusions (ROEDDER, 1979).

SORBY (1858) was one of the first workers to recognize that the gas bubbles present in most inclusions are the result of differential shrinkage of the liquid relative to the enclosing mineral during cooling from the higher temperature of trapping to that of observation. He correctly deduced that the temperature of trapping can be estimated by heating the sample to the point at which the bubble disappears i.e. the temperature of homogenization (T_h). Other parameters which can be obtained by merely observing phase transitions upon heating and cooling (i.e. non-destructive determinations) include the eutectic melting temperature (T_e) which gives an indication of the solute chemistry, the melting temperature (T_m) congruent or incongruent of salt-hydrate phases, the melting point of H_2O (T_m -ice) which is an indication of the salinity of the fluid, and the temperature of melting of mineral solids (T_m -solid) which persist after the melting of hydrates and ice.

6.2. EXPERIMENTAL TECHNIQUE

The current study employed nondestructive techniques on small (5 - 30 μm) inclusions in vein quartz. The inclusions were examined in doubly polished thin sections of thickness 60-70 μm .

Microthermometric measurements were carried out on a Linkam TH600 heating and freezing stage operational across the temperature range -180.0°C to $+600^{\circ}\text{C}$ (SHEPARD, 1981) mounted upon the stage of a Lertz Periplan microscope. The results are presented in tables 6.1 and 6.2. Liquid nitrogen was used to cool pure nitrogen gas which acted as a coolant for the stage and sample down to approximately -100°C to ensure freezing of the inclusions since metastable persistence of water at low temperatures inhibits nucleation of ice crystals. Samples were allowed to warm up slowly and phase changes were observed and recorded. Measurements were repeated until the fluid inclusion under observation gave consistent readings. The precision of melting temperatures obtained is $\pm 0.2^{\circ}\text{C}$ for the range under which the measurements were carried out.

Homogenization and melting measurements were carried out on the same inclusion. Controlled heating of the fluid inclusion to the temperature at which the gas bubble homogenized with the fluid gave the homogenization temperature (T_h). The reproducibility for this value is considered to be $\pm 0.2^{\circ}\text{C}$ below 200°C and $\pm 1^{\circ}\text{C}$ above this for the Linkam TH600 apparatus.

6.3. RESULTS

Two populations (plates 11,12)^o of primary fluid inclusions were identified by size, shape, and distribution with respect to the other observed inclusions in the various sample sections.

Table 6.1. Microthermometric data for two-phase primary fluid inclusions present in vein quartz from the Troodos Ophiolite.

Sample#	M.* Te	M. Tm	M. Th	No.	D.(m)
CY121	-20.5	-3.5	230	8	970.0
CY120	-20.4	-3.8	180	17	973.0
CY118	-52.4	-19.8	280	21	983.6
CY118b	-20.8	-4.5	381	10	983.6
CY004	-19.7	-4.7	300	15	1058.0
CY006	-21.8	-4.7	275	20	1073.2
CY024	-19.8	-5.3	295	15	1195.9

M.* = median.No. = number of inclusions.

ROEDDER(1979) gives a comprehensive list of criteria for discriminating the origin of fluid inclusions.

A minimum of two secondary populations were also found to be present. The secondary inclusions tended to be smaller (5 - 15 μ m) irregular shape, greater in number and often located on fracture planes. In contrast, the primary inclusions are generally larger(15 - 30 μ m), fewer in number, they tend to be isolated or to occur in small clusters. For all fluid inclusions observed and measurements performed, the gas bubble volume to fluid volume ratios are consistent and suggest that boiling has not occurred in these fluids (see ROEDDER,1984).

PAGE 52 Overleaf: Plate 11

Overleaf: Plate 11 All bar scales 0.06mm.

N. 2 and 3 phase primary fluid inclusions in vein quartz. Note relative volumes of daughter crystals compared to fluid inclusion volume.

O. Same as N.

P. Q. Primary 3 phase fluid inclusions in vein quartz.

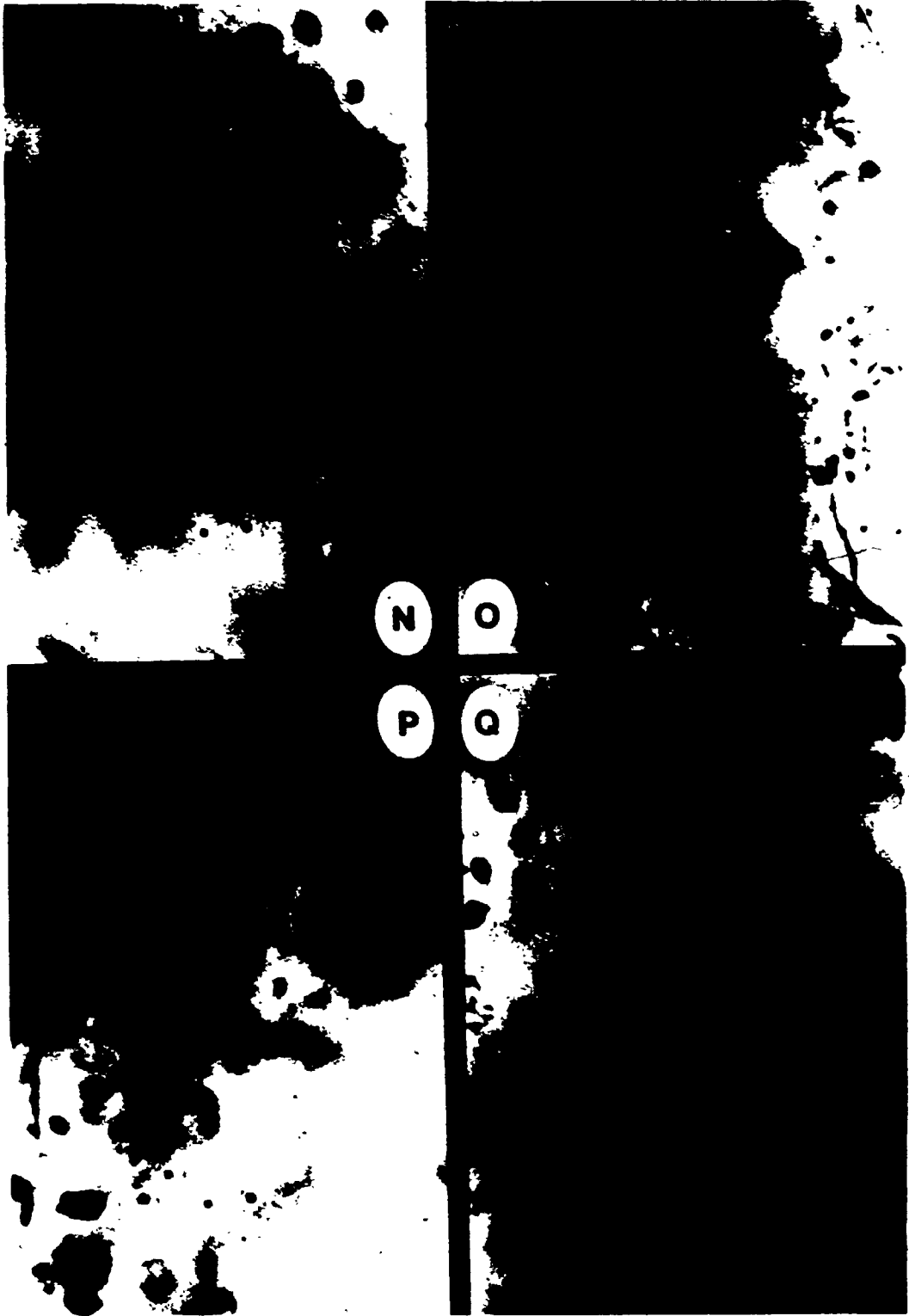
The first population of primary fluid inclusions occur in samples from lower sheeted dykes and are two phase (liquid + vapour) inclusions characterized by eutectic temperatures in the range -31.0° to -19.0° C; final melting temperatures -5.0° to -0.3° C (ice) and minimum homogenization temperatures of 140° to 365° C (table 6.1). The second population of primary inclusions occurs in the lower part of the observed depth range and consists of two, three, and four phase (liquid + vapour + daughter crystal[s]) inclusions.

Table 6. 2. Thermometric data for three phase fluid inclusions in quartz.

Sample#	M.Te	M.Tm-s.	M.Tm-l.	M.Th.	SAL.	No.
CY121	-27.7	-	-4.8	264	31.0	5
CY120	-22.1	-	-4.7	211	31.0	10
CY004a	-20.1	-	-3.0	235	28.1	7
CY004b	-45.8	-31.8	-17.0	135	21.0	6
CY024a	-49.7	-31.4	-17.8	172.1	22.1	8
CY024b	-30.0	-21.9	-17.5	301	23.4	3

M.= median ; s=solid ; l=ice ; No.=number of inclusions, SAL.= salinity in wt.% NaCl equiv. calculated according to the data of YANATIEVA (1946)

PLATE 11



The daughter crystals observed are composed of NaCl and apparently CaCl₂ according to their crystal form, (NaCl) eutectic temperatures and phase transition behaviour (see HOLLISTER and CRAWFORD, 1981 ; ROEDDER, 1984). This second population is characterized by very low eutectic temperatures in the range -55° to -43°C, hydrate melting temperatures -34° to -20.3°C ice melting temperatures -18° to -3.0°C and homogenization temperatures 130° to 310°C (table 6.2).

The two secondary populations were identified on the basis of their differing homogenization temperatures (table 6.3). The first secondary population occurs in all the samples studied. The second population was isolated only in one sample, but occurs in a significant number of inclusions to suggest that it was a separate population. The secondary inclusions were all simple two phase, and tend to be associated with fracture planes in all orientations.

Table 6.3. Thermometric determinations for secondary inclusions from the Troodos ophiolite:

Sample #	M.Th	M.Te	M.Tm	No.	Depth(m)
CY121	180	-21.0	-4.5	18	970.0
CY118	215	-24.3	-5.5	18	983.6
CY008	178	-19.1	-4.8	10	1073.2
CY024	305	-18.6	-3.0	21	1195.9

The overall high homogenization temperatures of the primary and secondary fluids and the varied degree of freezing point depressions indicate clearly that these are hydrothermal fluids that have evolved to various extents from seawater, and that the general trend of evolution has followed a path of increasing temperature and increasing salinity to the extent of saturation of several species.

Overleaf: Plate 12. All bar scales = 0.08mm.

W. Fluid Inclusion in vein quartz with large daughter crystal.

X. Cluster of 3 phase primary fluid inclusions (near bottom).

Y. Primary inclusion with 2 daughter crystals, but without vapour phase.

Z. Same as V.

Fluid salinities are conventionally expressed in weight percent NaCl equivalent (POTTER ET.AL.,1978), a self explanatory term. In most geologic situations, such salinity may indeed be caused by NaCl, but other ions in solution may have a similar effect on the freezing point of pure water (i.e. to depress it). Conversion of the melting points of the first primary population and the secondary population to equivalent salinity using the data of POTTER ET.AL.(1978) yields the following salinities:

Table 6.4. Salinities of two phase fluid inclusions.

Sample#	Median Tm-ice	SAL.
CY121	-3.5	29.0
* CY120	-3.8	29.4
* CY118	-19.6	21.9
CY118b	-4.5	7.4
CY004	-4.7	30.9
* CY006	-4.7	7.7
CY024	-5.3	31.9

* Indicates melting point of the ice phase observed at eutectic.

PLATE 12



Overleaf: Plate 13. All bar scales 0.08mm.

U. 3 phase primary fluid inclusions with halite daughter crystal in vein quartz.

V. Primary fluid inclusions with several daughter crystal phases in vein quartz.

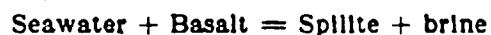
W. Enhanced reproduction of U.

X. Enhanced reproduction of V.

Y. Primary fluid inclusion with daughter crystal in vein quartz.

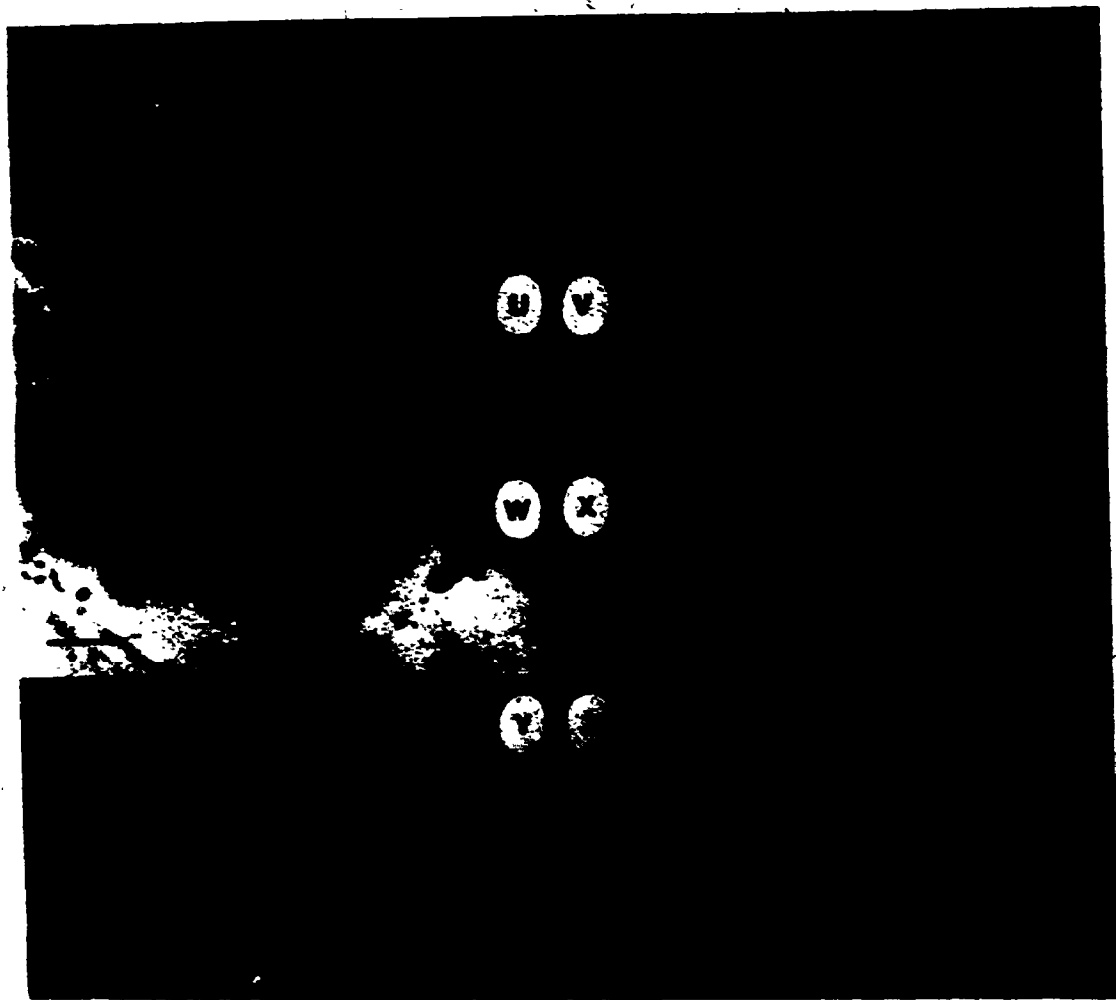
Z. Enhanced reproduction of Y.

The salinity of seawater ranges from 3.2 wt.% to 3.75 wt.% NaCl equiv. and may rise to 4.1 wt.% NaCl equiv. in small ocean basins such as the Red Sea and Mediterranean (RILEY and CHESTER, 1971). The calculated salinities (table 6.3; 6.4) are above that of seawater by almost ten times. Based on the premise that ordinary seawater was the starting fluid, then it has in the course of interaction with basalt become more saline. The premise is a reasonable one for rocks generated in an oceanic environment and is borne out by oxygen and sulphur isotope data as well as trace element abundances of Cl and B (see preceding chapters). Increases in seawater salinity of the magnitude observed may be generated by oceanic crust hydration via processes such as:



(HUTCHINSON ET AL., 1980). This correlates well with the alteration mineralogy of the rocks in which the quartz veins occur which exhibit greenschist

PLATE 13



facies metamorphism. The low eutectic temperatures and the presence of daughter crystals encountered in the fluid inclusions indicate that the fluids of the second primary population are saturated with respect to both NaCl and CaCl₂. Because of this it was found more appropriate to calculate salinities of the second group of inclusions using the phase relations of the NaCl - CaCl₂ - H₂O system based on the phase diagram of YANATIEVA(1946).

6.4. DISCUSSION

The system NaCl-CaCl₂-H₂O has a eutectic temperature of -52.0°C while the systems FeCl₃-H₂O and AlCl₃-H₂O both have eutectic temperatures of -55.0°C (ROEDDER ET.AL.,1984). CRAWFORD ET.AL.(1979) note that the presence of MgCl₂, FeCl₂ or FeCl₃ is difficult to determine from freezing and heating measurements alone, and hence the possibility of the presence of K⁺, Ca²⁺, Mg²⁺, Fe²⁺ and Fe³⁺ ions in solution can not be precluded. A major constraint however to the actual fluid composition[s] is afforded by the alteration mineralogy of which the quartz is a part. In general, two sets of alteration assemblages stand out. The first set can be said to be spilitic, while the second set appears to be the result of Ca metasomatism. The trend can be stated as follows:

CALCIC - PLAGIOCLASE = ALBITE = ANORTHITE

igneous = spilitized ⇒ Ca-metasomatized.

AUGITE = ACTINOLITE = DIOPSIDE

Quartz is locally associated with both alteration assemblages, with the hypersaline fluid inclusions in quartz generally occurring in the most calcic alteration assemblages. In other words, the high salinities encountered may partially be due to a "salting out" effect caused by the presence of Ca²⁺, Mg²⁺

and Fe^{2+} addition, any of which is known to drastically decrease NaCl solubility. LINKE (1958) shows that at 25°C in the system $\text{CaCl}_2\text{-NaCl-H}_2\text{O}$, NaCl has a solubility of only 1.02%. At higher temperatures, the solubility is even less (HARRIS, 1979). An important process which is capable of generating both high salinity fluids and releasing cations into solution in the oceanic environment is the process of serpentinization which proceeds exothermally via reactions such as



Continued reactions of this kind have been shown by MACDONALD AND FYFE (1985) to depend on the penetration of water through serpentine minerals to the peridotites as the reaction is quite rapid geologically. Their experiments indicate that the serpentine layers act as semipermeable membranes which allow H_2O to diffuse through to the unreacted anhydrous assemblages up to 300 times faster than the influx of NaCl and other dissolved salts thus increasing salinity by membrane separation. Such processes must be important in situations as observed at Troodos where the scale of serpentinization is extensive and Ca-metasomatism and serpentinization widespread. (WILSON, 1959 ; BEAR, 1963 ; GASS, 1968 ; MOORES and VINE, 1971 ; BARRIGA ET AL., 1985). The residual hypersaline fluids are probably injected into overlying rocks as a result of the large bulk expansion and fracturing accompanying serpentinization. The occurrence of an unusual epidote/clinozoisite + chlorite + calcite + sphene alteration zone in olivine websterites at a depth of 1992.32m to 1996.72m in drillhole CY-4 at Troodos may be a product of such brines. It is of note that the alteration zone is cut by serpentine coated fracture planes.

VANKO and BATIZA (1982); STAKES and VANKO (1986), also report daughter-crystal bearing fluid inclusions in vein quartz present in oceanic crust

gabbros dredged from the failed Mathematician Ridge, thus hypersaline fluids may be volumetrically significant in the oceanic environment, and may explain the Cl-rich amphiboles present in some oceanic metagabbros as reported by VANKO(1986). STAKES and VANKO(1986) report the presence of fluid inclusions in gabbroic rocks with salinities that vary from near seawater to over 50 wt. % NaCl and homogenization temperatures that vary from greater than 550°C to about 150°C.

The quartz in which the fluid inclusions are observed is most simply explained if the veins represent local discharge (cooling) pathways. However, if highly evolved brines rich in CaCl_2 cause replacement of albite by anorthite and other calcic phases, then silica will also be produced in such reactions. Some features then of the alteration might be best explained by rising fluids derived from rodignitization in the ultramafic portions of the sequence as serpentized and epidotized olivine websterites suggest. The present study presents clear evidence for the presence of two types of fluid; shallow level seawater and deep level hypersaline brines, and in the overall convective system, the potential for mixing must be large.

In a previous fluid inclusion study involving Troodos rocks, SPOONER and BRAY(1977) examined material from three relatively deep stockwork zones which occur beneath now exhausted massive sulphide deposits and observed fluid inclusions in which...

"the freezing point is statistically indistinguishable from that of seawater..."

and thus concluded that ...

"a hydrothermal fluid identical to seawater in its salinity formed the ophiolitic sulphide deposits of Cyprus."

The current observations do not support this point of view and lead to the suggestion that around the discharge sites of convection systems in oceanic crust, massive mixing with seawater must occur as this environment is characterized by a high fracture permeability (hence stockwork) and that because of the relative volumes involved, seawater may mask the composition of the venting hydrothermal fluids which are primarily responsible for ore formation.

6.5. SUMMARY

Hypersaline fluids have been observed in the gabbroic rocks of the Troodos ophiolite in fluid inclusions occurring together with other fluids of seawater salinity. It is suggested that these hypersaline fluids are a product of serpentinization and other hydration reactions occurring at depth and that mixing of these fluids with seawater has occurred.

Chapter Seven

SUMMARY AND CONCLUSIONS

The current petrological and geochemical study has sought to investigate the nature of postmagmatic alteration in the plutonic sequence of the Troodos ophiolite.

It is the finding of this study that such alteration is present on an extensive scale in the lower portion of the ophiolite, and that the characteristic features about it are as follows:

The alteration is related to discontinuities in the rock mass in that the intensity of alteration decreases with distance away from such discontinuities:

Apart from regions where movement has occurred, igneous textures have been preserved; i.e. there is an absence of an overall deformation fabric in the rocks.

Where the alteration has affected all the igneous minerals to the extent of complete recrystallization, metamorphic mineral assemblages are discernable to the extent that the altered rocks have been assigned a metamorphic facies. The metamorphic facies are observed to increase in grade downwards corresponding to the original geothermal gradient which is inferred to have mostly been temperature dependent.

The major observed petrologic effects of what appears to be fluid dominated alteration across a very high geothermal gradient may be summarized as follows:

- 1) The development of the characteristic greenschist metamorphic mineral assemblage of mafic rocks comprised of albite + actinolite + chlorite + sphene in the lower sheeted dykes and upper isotropic gabbros.

ii) The development of a restricted transitional metamorphic zone characterized by the mineral assemblage epidote + albite + magnesio - hornblende + sphene + chlorite in the lower isotropic gabbros.

iii) The development of hydrothermal anorthite + magnesio - hornblende in the lower isotropic gabbros and layered gabbros.

iv) The development of rodingitized gabbros in the vicinity of serpentinite intrusions into gabbroic parts of the ophiolite. The rodingitized gabbros are characterized by calc - silicate alteration assemblages of anorthite + diopside + tremolite + andradite + prehnite + calcite.

The whole rock geochemistry of the altered rocks indicates that the alteration observed may have been caused by:

a) Near pervasive but heterogeneous hydration reactions involving the mafic minerals of the sheeted dykes and gabbros and the transformation of calcic - plagioclase feldspars to albite; a process involving the fixation of Na^+ from the hydrothermal fluid and the release of Ca^{2+} from the rock mass into the fluid. The fixation of Mg via the formation of chlorite and the overall loss of Si, K, Fe, Mn from the rocks to the alteration fluids.

b) Restricted hydration alteration of the lower isotropic gabbros and underlying rocks. The decrease is a direct function of the decrease in fracture/vein density in the underlying rocks.

c) Oxidation reactions that have resulted in the increase in the ferrous/ferric iron ratios of most altered rocks.

d) Ca - metasomatism in the lower gabbroic rocks resulting in the formation of rodingitized rocks.

e) The increase of B and Cl abundances up to five fold above average basaltic values.

f) The increase of $^{87}\text{Sr}/^{86}\text{Sr}$ ratios of the altered rocks.

g) The complex $^{18}\text{O}/^{16}\text{O}$ whole rock isotope profile which in addition to the low values for sheeted dykes, also has high values for the gabbros.

h) The presence of very negative $^{13}\text{C}/^{12}\text{C}$ values for late stage vein and fissure filling carbonates.

i) The presence of low and high salinity fluid inclusions of varying homogenization temperature.

A general model for the postmagmatic alteration of the Troodos ophiolite that takes into account the above noted features is proposed as follows:

The Troodos ophiolite formed at a spreading centre 85 M.a. B.P. in a supra subduction zone environment. The extrusion of lava at a temperature of about 1200°C into a cold aqueous environment with an average temperature of about 1°C caused rapid cooling and contraction of the lava which in turn caused an increase in the bulk permeability of the rock. The greatly increased permeability of the upper part of the newly formed oceanic crust then made further cooling possible by the convective mass transfer of seawater through the rock.

The convective heat loss caused seawater to circulate vigorously in the upper part of the crust, down to near the base of the sheeted dykes. This caused the near pervasive alteration of the pillow lavas and flows as well as the sheeted dykes. Fluid flow in this upper part of oceanic crust was immediate and vigorous, and where the return flow was focussed upwards through major aqueducts, appears to have led to the massive sulphide and oxide base metal

deposits of the ophiolite. The major feature of this upper crustal initial postmagmatic activity was the significant hydration of the crust which appears to have led to a slight increase in fluid salinity.

Fracture propagation into the plutonic part of the ophiolite was concomittant with deep fluid penetration which led to the hydrothermal alteration of parts of the rock mass. As in the upper part of the ophiolite sequence, the process was mainly dependent on fracture permeability and hence not pervasive. The continued propagation of fractures into the ultramafic cumulates caused extensive serpentinization.

The process of serpentinization released Ca^{2+} into the circulating hydrothermal fluids of the lower part of the sequence and significantly altered the fluid chemistry. This process, together with the osmotic effects of the serpentinization process on the residual fluids led to the development, in the lower oceanic crust, of a fluid that was hypersaline and that caused the formation of rodingites.

The presence of spilittized basalts in the upper ophiolite sequence and rodingites in the lower sequence indicates the operation of at least two chemically distinct postmagmatic alteration processes at the Troodos ophiolite. This in turn indicates the development of at least two distinct fluid regimes, and in an environment whose permeability was dominantly fracture controlled, the possibility of mixing of the fluids must have been large.

Appendix A

ANALYTICAL METHODS AND RESULTS

A.1. MAJOR AND TRACE ELEMENT ANALYSIS

Whole rock samples were cut by diamond saw into sections about 1cm thick and the sections were then reduced to chips using a jaw crusher. The sample chips were cleared of Fe and Cu contamination from the jawcrusher and saw by use of Al_2O_3 abrasives. After washing and blow drying the sample chips they were then pulverized in a tungsten-carbide coated Bleuler mill.

Utilizing the method of HARVEY ET. AL. (1973), the resulting powders were then made into circular glass discs by taking 2.000g of commercially available Spectroflux-105 composed of lithium tetraborate 47.03%, lithium carbonate 38.83%, and lanthanum oxide 16.34%, 0.0287g of sodium nitrate and 0.3733g of sample. The mixture was then fused in a platinum crucible until it was homogeneous and bubble-free at $1000^{\circ}C$ and the melt poured onto an aluminium plate at a temperature of $250^{\circ}C$ and pressed into a glass disc. The glass discs were analysed using the heavy absorber fusion technique of NORRISH and HUTTON(1969) for the major elements with the exception of sodium by X-ray fluorescence spectrometry using a Phillips PW-1450 automatic sequential spectrometer fitted with a Cr tube. Sodium determinations were made on pressed powder pellets which consist of 2.00g of finely powdered sample mixed thoroughly with 0.20g of somar binding agent and backed by boric acid, all pressed hydraulically at $8,000\text{ kg/cm}^2$. The pressed pellets were run on the XRF spectrometer with a Cr tube at 60KV and 45MA as was also the case for all the other major elements. The trace elements Nb , Zr , Y , Sr , Rb , Pb , Zn , Cu , Ni , Cr , Ba , V , S and Ga were also determined by XRF on the aforementioned

pressed powder pellets. Accuracy checks were made using international standards and unknown duplicate samples. Results showed that major element determinations were accurate within 3% of the amount present and trace elements accurate within 10%. The data was reduced using a computer program developed at UWO by WU(1984).

Au, U, Th and B were determined by Neutron Activation Analysis at X-Ray Assay Laboratories in Don Mills, Ontario. Duplicate analyses showed a precision of 5%.

Volatile content or loss on ignition(LOI) was determined by the weight loss of sample powder upon heating for two hours at 1100°C.

Ferrous iron was determined using the cold titration method of WILSON(1955). This involved taking 0.25g of sample and 0.05g of ammonium metavanadate(AMV) and dissolving both in 5 ml cold 40% HF acid. The ferrous iron present in the sample was oxidized quantitatively by the AMV, and the excess amount was then titrated against standardized ferrous ammonium sulphate solution(FAS). The amount of FeO in the sample was this equal to the initial AMV minus the AMV titrated.

The reproducibility and accuracy of analysis was found to be dependent on the procedure of the standardization of the FAS. Repeated use of international standards BCR-1 and SY-3 (with each 4 sample run) indicated an accuracy of 5%.

A.2. MINERAL CHEMISTRY

Polished thin sections 25mm in diameter were carbon-coated and probed using a Materials Analysis Company(MAC) electron microprobe model 400 linked to 3 spectrometers and a Krissel control automation system which converted

counts received by the spectrometers into element percentages after correcting for machine conditions using the program MAGIC.

Operating conditions were 15 to 20 kV excitation voltage and 0.20 to 0.40 μ A beam current for 30 seconds or 20000 counts per analysis. Standards employed were well analysed known minerals. Precision was determined by repeated analyses per mineral grain and under stable working conditions was within 3%.

A.3. RARE EARTH ELEMENTS

Rare Earth element concentrations were determined by Spark Source spectroscopy using a JEOL mass spectrometer JMS-OIBM-2 and collected on Ilford Q2 spectrographic plates. Sample preparation followed the method of TAYLOR(1965), and the spectrographic plates were analysed semiquantitatively. The concentrations of the elements were estimated to within a factor of 3.

All analytical work i.e. major and trace element whole rock analysis by X-Ray Fluorescence, mineral chemistry analysis by Electron Microprobe, rare earth element analysis by Spark Source Spectroscopy were performed in house at UWO by the present writer. Additional analyses were performed by X-Ray assay Laboratories, Don Mills, Ontario, for the elements Au, Th, U, and B by neutron activation analysis.

A.4. OXYGEN AND CARBON ISOTOPE ANALYSIS

Whole rock powders were obtained by crushing chips approximately 2cm by 2cm to -200 mesh in tungsten carbide mills. Mineral separations were performed by means of standard techniques employing heavy liquids in conjunction with a Franz isodynamic electromagnetic separator. Conventional methods were employed for the liberation of silicate minerals with bromine pentafluoride, followed by quantitative conversion to CO_2 (see CLAYTON and MAYEDA, 1963).

Carbonate minerals were reacted with 100% H_3PO_4 at 25°C (see McCRAE, 1950). The isotopic abundance ratios were measured on a VG Micromass Sira 9cm triple collecting automated mass spectrometer, and are reported as δ values in per mil. The oxygen standard is NBS-28 quartz, which gives a value of 9.8 per mil (see COPLEN ET. AL., 1983). The carbonate standard is the Cretaceous age PeeDee Belemnite (PDB) where:

$$\delta^{18}O(SNOW) = 1.03086 \times (\delta^{18}O_{PDB}) + 30.86$$

The reproducibility of $\delta^{18}O$ values averages +/- 0.18 per mil (2σ).

A.5. MAJOR AND TRACE ELEMENT ANALYSES

UNALTERED DIABASE

S.#	253	234	220	212	145
D. (m)	266.5	356.8	482.7	515.7	836.2
SiO ₂	53.7	63.1	54.7	56.0	48.4
TiO ₂	1.3	1.0	0.8	0.9	1.1
Al ₂ O ₃	15.2	15.4	16.8	15.1	17.2
Fe ₂ O ₃	12.4	8.9	8.7	12.1	12.9
MnO	0.1	0.1	0.1	0.2	0.2
MgO	4.6	2.3	5.9	4.2	7.0
CaO	9.5	6.8	9.8	8.8	12.3
K ₂ O	0.1	nd	nd	0.1	nd
P ₂ O ₅	0.1	0.1	0.0	0.1	0.1
Na ₂ O	2.5	2.8	3.4	2.4	0.8
LOI	0.8	0.7	0.1	0.6	0.5
Total	100.3	101.2	100.1	100.5	100.7
Sppm	-	56	44	-	260
V	-	800	600	-	557
Cr	10	30	30	10	90
Co	-	90	85	-	60
Ni	-	20	20	-	40
Cu	-	30	30	-	60
Zn	-	30	25	-	50
Ga	-	5	10	-	10
Rb	10	1	5	10	2
Sr	110	120	105	90	130
Y	20	10	20	30	20
Zr	50	40	50	20	30
Nb	10	6	10	10	15
Ba	-	30	20	-	15
Pb	-	-	5	-	5
U	-	-	<1	-	<0.1
Th	-	-	<1	-	<1
Au (ppb)	-	-	<15	-	<10
Pb	-	-	5	-	5

ALTERED DIABASE

S#	A1	292	291	286	285	280
D. (m)	0.5	20.8	23.8	74.0	82.6	117.7
SiO ₂	58.2	44.8	53.8	50.1	53.5	54.6
TiO ₂	1.0	0.4	1.1	1.0	0.7	4.4
Al ₂ O ₃	14.4	16.7	14.8	15.9	13.9	15.5
Fe ₂ O ₃	10.8	14.1	11.8	10.5	8.6	12.4
MnO	0.1	0.2	0.1	0.1	0.2	0.2
MgO	4.3	8.7	4.0	3.6	8.3	5.0
CaO	7.3	11.4	7.6	8.6	6.7	7.2
K ₂ O	nd	nd	0.1	0.2	nd	nd
P ₂ O ₅	0.1	0.0	0.1	0.1	0.0	0.1
Na ₂ O	3.8	0.6	3.5	2.9	3.0	3.1
LOI	1.9	1.3	3.5	7.3	5.8	2.0
Total	101.9	98.2	100.5	100.3	100.7	101.5
Sppm	60	130	-	-	160	200
V	510	400	-	-	350	530
Cr	40	50	10	10	135	36
Co	88	40	-	10	55	60
Ni	25	20	-	-	65	25
Cu	30	60	-	-	60	40
Zn	30	120	-	-	60	60
Ga	10	70	-	-	10	15
Rb	15	2	10	10	10	10
Sr	160	100	100	20	100	140
Y	20	20	20	20	20	20
Zr	60	190	30	30	40	75
Nb	20	40	20	30	10	15
Ba	30	-	-	-	6	20
U	-	0.1	-	-	<0.1	<0.1
Th	-	<1	-	-	<1	<1
Au (ppb)	-	<15	-	-	<10	<15
Pb	10	-	-	-	10	10

ALTERED DIABASE

S#	275	271	267	257	254	251
D. (m)	160.9	180.4	196.0	242.5	255.3	279.8
SiO ₂	53.0	53.2	53.9	57.3	55.8	55.7
TiO ₂	0.8	1.2	1.2	1.3	1.0	1.3
Al ₂ O ₃	15.7	15.3	15.9	15.3	15.1	15.3
Fe ₂ O ₃	9.5	10.7	11.0	5.7	7.4	5.7
MnO	0.2	0.2	0.2	0.1	0.1	0.1
MgO	6.8	5.5	5.6	5.2	4.5	6.2
CaO	8.7	8.6	6.8	6.7	8.6	6.8
K ₂ O	nd	nd	nd	nd	0.2	nd
P ₂ O ₅	0.1	0.0	0.1	0.0	0.1	0.1
Na ₂ O	3.1	2.3	3.6	4.3	4.3	4.3
LOI	2.0	4.4	1.4	3.6	3.5	2.7
Total	101.7	99.4	99.6	99.5	100.4	99.9
Sppm	50	1310	40	35	-	-
V	460	3990	500	690	-	180
Cr	65	50	45	35	20	30
Co	70	130	60	80	-	70
Ni	40	50	30	30	-	10
Cu	30	60	40	30	-	30
Zn	30	120	30	20	-	20
Ga	15	70	15	15	-	10
Rb	10	2	20	15	20	6
Sr	150	330	165	75	100	120
Y	20	130	30	30	10	20
Zr	60	570	60	80	20	10
Nb	20	20	20	20	20	10
Ba	30	20	20	10	nd	-
U	<0.1	0.2	0.1	0.2	-	<0.1
Th	<1	<1	<1	<1	<-	1
Au (ppb)	-	<10	<20	<20	-	36
Pb	10	-	10	10	-	-

ALTERED DIABASE

S#	246	236	232	229	227	225
D. (m)	307.6	369.7	406.9	430.0	443.9	462.1
SiO ₂	57.1	53.5	52.9	53.6	50.7	48.4
TiO ₂	1.3	0.9	1.0	1.1	0.6	0.1
Al ₂ O ₃	15.1	14.3	15.2	15.2	15.4	18.1
Fe ₂ O ₃	11.2	9.7	10.9	10.8	8.7	2.9
MnO	0.1	0.2	0.2	0.2	0.2	0.0
MgO	3.4	5.3	5.6	6.4	8.2	2.5
CaO	6.0	8.1	8.7	8.8	12.1	14.7
K ₂ O	0.0	0.1	0.0	0.0	0.1	0.1
P ₂ O ₅	0.2	0.1	0.1	0.1	0.1	0.0
Na ₂ O	2.9	3.6	2.0	3.8	1.7	0.7
LOI	1.1	3.9	3.8	1.8	1.9	13.0
Total	98.2	99.6	100.4	101.7	99.7	100.7

Sppm	40	-	100	70	-	-
V	90	-	510	360	-	-
Cr	30	50	90	nd	260	10
Co	20	-	70	60	60	-
Ni	20	-	40	50	-	-
Cu	40	-	50	30	-	-
Zn	40	-	60	40	-	-
Ga	30	-	10	20	-	-
Rb	20	10	10	20	10	10
Sr	180	100	130	150	60	40
Y	30	20	20	20	10	10
Zr	100	10	70	60	10	10
Nb	30	20	15	25	10	10
Ba	nd	-	10	nd	-	-
U	<0.1	0.2	0.1	0.2	-	<0.1
Th	1	<1	<1	<1	-	-
Au(ppb)	47	<10	<10	<15	-	-
Pb	20	-	3	10	-	-

ALTERED DIABASE

S#	211	207	205	168	167	166
D. (m)	519.8	535.8	556.6	742.5	745.8	750.7
SiO ₂	54.0	51.1	51.9	54.6	55.2	51.2
TiO ₂	0.9	0.8	0.2	0.3	1.0	0.2
Al ₂ O ₃	15.7	13.0	18.5	18.9	15.2	15.2
Fe ₂ O ₃	10.7	9.2	5.4	5.4	3.8	6.2
MnO	0.1	0.1	0.1	0.1	0.0	0.1
MgO	5.2	4.5	7.9	7.3	5.9	9.3
CaO	7.8	10.5	13.1	10.2	12.1	10.0
K ₂ O	nd	0.1	nd	0.1	0.2	0.2
P ₂ O ₅	0.0	0.1	0.0	0.0	0.1	0.0
Na ₂ O	4.0	3.5	1.9	3.8	4.2	2.6
LOI	2.4	7.5	1.8	2.2	2.5	4.9
Total	100.6	100.3	100.7	100.7	100.4	100.2
Sppm	40	-	40	-	-	-
V	520	-	-	-	-	-
Cr	-	10	50	120	30	230
Co	50	-	-	-	-	-
Ni	-	-	40	-	-	-
Cu	30	-	-	-	-	-
Zn	30	-	-	-	-	-
Ga	10	-	-	-	-	-
Rb	20	10	-	10	10	10
Sr	-	30	160	80	150	60
Y	20	20	20	30	20	10
Zr	50	10	40	10	40	10
Nb	20	10	20	10	40	10
Ba	30	10	30	10	20	10
U	0.1	-	<0.1	-	-	-
Th	<1	-	<1	-	-	-
Au(ppb)	<10	-	<10	-	-	-
Pb	10	-	-	-	-	-

ALTERED DIABASE

S#	195	190	184	180	164	154
D. (m)	603.3	638.8	662.0	683.8	758.5	799.3
SiO ₂	52.1	52.0	52.2	52.0	51.2	51.9
TiO ₂	0.6	1.1	0.8	1.1	1.6	1.6
Al ₂ O ₃	16.8	15.9	16.0	15.8	16.4	16.5
Fe ₂ O ₃	8.4	11.4	10.0	11.3	12.1	12.1
MnO	0.1	0.2	0.2	0.2	0.1	0.1
MgO	7.8	5.5	6.6	6.0	4.1	4.7
CaO	10.6	8.4	10.7	8.5	7.5	7.6
K ₂ O	0.0	0.0	0.0	0.0	0.0	0.0
P ₂ O ₅	0.0	0.1	0.1	0.0	0.0	0.0
Na ₂ O	3.0	3.8	2.2	3.9	2.4	3.3
LOI	2.4	1.8	1.6	3.9	2.4	1.7
Total	101.9	100.2	100.5	99.9	100.7	99.4

Sppm	60	650	-	40	50	80
V	360	500	-	270	870	500
Cr	220	100	50	410	40	40
Co	60	60	-	70	70	50
Ni	70	40	-	120	40	40
Cu	40	70	-	30	40	40
Zn	50	100	-	50	50	30
Ga	10	10	-	10	20	20
Rb	5	10	10	20	10	-
Sr	110	150	100	50	160	150
Y	10	20	20	20	20	30
Zr	40	70	10	40	40	80
Nb	10	20	20	20	20	30
Ba	20	10	-	-	1	-
U	0.1	<0.1	-	0.1	0.1	<0.1
Th	<1	<1	-	<1	<1	<1
Au(ppb)	<10	<10	-	<5	<15	<15
Pb	10	5	-	3	5	6

FRESH GABBRO

S#	119	117	001	007	017	018
D. (m)	980.0	994.1	1045.7	1077.5	1123.2	1155.0
SiO ₂	47.1	53.5	53.8	58.1	48.3	50.2
TiO ₂	1.3	0.3	0.3	0.8	0.2	0.2
Al ₂ O ₃	15.9	12.0	15.1	13.7	17.4	23.2
Fe ₂ O ₃	13.2	9.2	6.4	5.1	8.2	5.6
MnO	0.2	0.2	0.1	0.1	0.1	0.1
MgO	6.8	10.1	7.2	4.3	10.4	5.5
CaO	11.8	10.2	12.1	12.0	13.1	11.9
K ₂ O	0.0	0.0	0.0	0.1	0.1	0.0
P ₂ O ₅	0.1	0.0	0.0	0.1	0.0	0.0
Na ₂ O	1.8	1.8	2.6	6.3	0.7	2.2
LOI	0.2	0.2	0.7	0.6	1.0	0.8
Total	98.2	98.1	98.3	101.0	99.5	99.7

Sppm	-	50	60	60	-	50
V	400	370	180	170	-	100
Cr	50	180	150	150	190	100
Co	130	90	80	60	-	60
Ni	20	85	60	40	-	50
Cu	180	30	30	30	-	30
Zn	120	40	30	20	-	20
Ga	20	10	10	20	-	10
Rb	5	5	5	15	20	nd
Sr	100	80	90	100	40	120
Y	40	15	25	30	10	5
Zr	70	30	30	60	10	10
Nb	40	10	15	20	40	5
Ba	10	25	30	nd	-	nd
U	<0.1	0.1	<0.1	0.3	<0.1	<0.1
Th	-	<1	<1	-	<1	<1
Au (ppb)	<20	<15	<15	<15	<10	<20
Pb	-	-	1	3	-	1

FRESH GABBRO

S#	023	036	044	048	068	086
D. (m)	1186.3	1245.3	1367.7	1405.9	1564.2	1724.3
SiO ₂	48.3	46.5	50.8	49.7	50.4	50.3
TiO ₂	0.3	0.2	0.1	0.1	0.1	0.1
Al ₂ O ₃	17.5	15.5	16.6	13.4	17.8	16.2
Fe ₂ O ₃	9.0	3.4	6.4	6.3	5.5	5.3
MnO	0.2	0.1	0.1	0.1	0.1	0.1
MgO	9.6	7.4	10.8	12.6	9.2	11.6
CaO	14.2	22.7	15.1	16.1	17.4	15.3
K ₂ O	0.0	nd	nd	0.0	nd	nd
P ₂ O ₅	0.0	0.0	0.0	0.0	0.0	0.0
Na ₂ O	0.7	1.5	0.5	0.3	0.5	0.3
LOI	0.2	2.7	0.9	1.0	0.5	0.6
Total	100.1	99.9	101.2	99.7	101.6	99.7

Sppm	-	-	180	-	170	70
V	-	400	270	-	250	215
Cr	80	500	250	310	570	380
Co	-	45	70	-	90	90
Ni	-	70	100	-	90	90
Cu	-	30	100	-	50	30
Zn	-	10	30	-	30	30
Ga	-	10	20	-	15	5
Rb	10	5	20	20	10	nd
Sr	40	160	80	10	70	45
Y	10	10	20	10	10	10
Zr	5	20	40	5	25	15
Nb	10	10	25	10	15	5
Ba	-	2	5	-	10	15
U	-	0.1	<0.1	-	0.1	<0.1
Th	-	<1	<1	-	<1	<1
Au (ppb)	-	<10	<10	-	<20	<15
Pb	-	1	5	-	1	1

FRESH PYROXENITE

S#	101	107
D. (m)	1819.8	1847.1
SiO ₂	49.8	52.2
TiO ₂	0.1	0.1
Al ₂ O ₃	2.8	13.1
Fe ₂ O ₃	7.8	5.3
MnO	0.1	0.1
MgO	20.5	13.7
CaO	16.5	15.1
K ₂ O	0.0	0.0
P ₂ O ₅	0.0	0.0
Na ₂ O	0.2	0.1
LOI	1.0	0.6
Total	99.2	100.3
Sppm	-	60
V	-	215
Cr	1910	1685
Co	-	70
Ni	-	215
Cu	-	30
Zn	-	30
Ga	5	-
Rb	10	10
Sr	5	40
Y	20	15
Zr	5	30
Nb	10	20
Ba	-	20
U	-	<0.1
Th	-	<1
Au(ppb)	-	<15
Pb	-	-

ALTERED GABBRO

S#	149	139	130	126	122	054
D. (m)	821.5	863.3	919.1	941.1	960.8	1438.0
SiO ₂	52.8	60.0	53.5	49.8	52.8	48.4
TiO ₂	0.4	0.2	0.3	0.3	0.6	0.0
Al ₂ O ₃	13.7	14.8	4.5	3.9	16.5	23.3
Fe ₂ O ₃	5.3	2.3	8.1	8.6	9.8	3.7
MnO	0.1	0.0	0.2	0.1	0.2	0.1
MgO	9.1	5.3	15.4	16.7	6.4	7.1
CaO	10.8	11.4	13.7	16.6	7.7	16.6
K ₂ O	0.2	0.2	nd	0.0	nd	0.0
P ₂ O ₅	0.1	0.0	0.0	0.0	0.0	0.1
Na ₂ O	3.3	4.6	0.7	0.5	2.7	0.5
LOI	4.7	1.5	2.8	3.3	2.0	1.3
Total	100.5	100.5	99.1	100.2	98.7	101.0

Sppm	-	-	70	-	550	60
V	-	-	380	-	120	150
Cr	170	130	1055	1450	320	210
Co	-	-	80	-	20	60
Ni	-	-	160	-	90	70
Cu	-	-	40	-	440	60
Zn	-	-	40	-	30	20
Ga	-	-	10	-	15	12
Rb	10	10	15	10	20	20
Sr	380	240	40	10	120	90
Y	30	10	20	10	20	20
Zr	60	60	40	5	60	30
Nb	20	30	20	20	30	20
Ba	-	-	5	-	-	10
U	-	-	<0.1	-	<0.1	0.1
Th	-	-	<1	-	<1	<1
Au (ppb)	-	-	<10	-	<20	<15
Pb	-	-	-	-	10	5

ALTERED GABBRO

S#	118	114	109	012	013	015
D. (m)	983.6	995.8	1036.0	1115.5	1122.8	1156.9
SiO ₂	76.3	54.4	56.9	55.3	45.3	55.2
TiO ₂	0.3	0.6	0.3	1.2	1.6	0.8
Al ₂ O ₃	12.0	16.6	17.3	18.2	15.6	9.0
Fe ₂ O ₃	0.6	2.6	1.7	3.6	14.7	9.5
MnO	0.0	0.0	0.1	0.1	0.2	0.2
MgO	1.0	4.5	2.2	3.6	6.3	9.8
CaO	3.9	13.5	18.2	8.4	11.4	12.6
K ₂ O	0.0	0.0	0.0	0.0	0.0	0.1
P ₂ O ₅	0.0	0.1	0.1	0.2	0.1	0.0
Na ₂ O	5.2	4.6	2.1	7.9	2.1	1.5
LOI	1.1	3.5	1.2	4.3	1.5	1.2
Total	100.2	100.5	100.1	100.6	98.7	99.9

Sppm	60	-	40	150	180	-
V	40	-	80	250	1150	-
Cr	20	40	40	40	30	260
Co	80	-	60	65	15	-
Ni	5	-	20	45	30	-
Cu	20	-	30	40	50	-
Zn	10	-	10	50	40	-
Ga	2	-	10	15	10	-
Rb	10	10	5	15	10	5
Sr	90	150	30	90	130	40
Y	10	20	10	30	20	30
Zr	40	30	40	50	30	20
Nb	10	10	5	20	10	-
Ba	-	-	-	20	-	-
Pb	2	-	-	-	5	5

ALTERED GABBRO

S#	057	059	060	063	064	065
D. (m)	1470.6	1478.5	1480.8	1496.0	1503.1	1520.2
SiO ₂	56.1	50.2	47.7	46.8	50.7	48.4
TiO ₂	0.0	0.1	0.1	0.1	0.3	0.1
Al ₂ O ₃	13.7	7.0	17.1	14.1	12.0	20.2
Fe ₂ O ₃	5.6	6.7	7.8	8.9	7.8	5.8
MnO	0.1	0.2	0.1	0.2	0.2	0.1
MgO	5.1	18.7	11.1	11.6	10.5	7.7
CaO	16.8	13.7	13.2	12.8	15.8	14.2
K ₂ O	nd	nd	nd	nd	nd	nd
P ₂ O ₅	0.1	0.1	nd	0.0	0.1	0.0
Na ₂ O	nd	nd	1.0	0.1	0.2	1.0
LOI	2.9	4.5	3.0	5.2	2.6	2.8
Total	100.3	101.4	101.1	100.0	100.2	100.3

Sppm	110	70	570	150	300	330
V	100	340	300	340	430	230
Cr	260	700	160	210	160	175
Co	50	65	75	90	65	60
Ni	50	120	90	100	75	85
Cu	50	40	65	60	40	105
Zn	25	40	40	50	40	40
Ga	20	10	10	15	10	10
Rb	10	5	10	10	-	15
Sr	180	30	90	65	20	100
Y	10	10	10	15	10	15
Zr	20	15	30	25	25	30
Nb	10	10	20	20	5	20
Ba	40	40	20	25	30	15
Pb	5	5	5	15	5	5

ALTERED GABBRO

S#	066	071	073	076	081	084
D. (m)	1536.7	1604.3	1618.4	1635.1	1676.0	1708.3
SiO ₂	54.9	50.2	52.1	51.6	49.4	49.0
TiO ₂	0.1	0.2	0.1	0.4	0.1	0.2
Al ₂ O ₃	2.8	20.6	7.3	16.2	10.4	16.0
Fe ₂ O ₃	5.8	1.4	4.1	6.4	6.3	5.2
MnO	0.1	0.0	0.1	0.1	0.1	0.1
MgO	17.5	6.3	12.7	8.5	13.9	7.8
CaO	18.8	18.8	21.7	14.7	13.3	15.0
K ₂ O	nd	nd	nd	nd	nd	nd
P ₂ O ₅	nd	0.1	0.1	0.1	nd	0.1
Na ₂ O	nd	1.4	nd	1.4	0.6	nd
LOI	1.7	1.4	2.1	1.0	4.6	6.8
Total	101.8	100.3	100.2	100.5	98.9	100.2

Sppm	240	950	175	70	130	1240
V	370	160	350	400	270	230
Cr	1610	110	950	210	510	280
Co	65	50	50	65	70	65
Ni	150	55	110	90	125	75
Cu	65	30	50	30	60	45
Zn	30	10	20	20	20	30
Ga	10	10	10	20	10	10
Rb	5	10	-	15	10	10
Sr	20	130	120	120	60	100
Y	10	10	5	15	10	10
Zr	20	30	10	35	25	20
Nb	10	15	5	20	10	5
Ba	30	-	25	20	10	25
Pb	1	2	5	5	-	5

ALTERED GABBRO

S#	087	089	093	098	099	104
D. (m)	1730.6	1742.7	1764.0	1803.0	1808.9	1816.7
SiO ₂	53.4	49.7	50.1	54.9	44.5	51.5
TiO ₂	0.0	0.2	0.1	0.1	0.1	0.1
Al ₂ O ₃	1.1	16.6	11.4	2.5	20.3	2.2
Fe ₂ O ₃	4.1	4.6	4.7	5.5	3.3	5.2
MnO	0.1	0.1	0.2	0.1	0.1	0.1
MgO	17.7	10.0	8.8	18.5	10.8	18.3
CaO	18.8	14.7	22.3	18.5	11.5	19.4
K ₂ O	nd	nd	nd	nd	nd	nd
P ₂ O ₅	0.1	0.1	0.1	0.0	0.1	0.0
Na ₂ O	1.0	0.7	0.1	-	1.1	0.2
LOI	4.0	3.6	2.3	1.2	8.7	1.8
Total	100.3	100.1	100.0	101.4	101.4	99.2

Sppm	70	130	-	120	65	7
V	230	250	240	300	100	-
Cr	350	230	600	3600	300	3130
Co	120	70	55	120	54	-
Ni	80	100	75	180	60	-
Cu	30	30	30	30	40	-
Zn	30	20	20	30	20	-
Ga	15	10	10	10	5	-
Rb	10	5	10	-	5	10
Sr	110	100	30	10	100	5
Y	10	5	10	5	10	5
Zr	20	10	20	5	20	5
Nb	10	5	15	5	10	30
Ba	50	15	2	2	5	-
Pb	5	5	1	2	3	-

ALTERED GABBRO

S#	105	053	106
D. (m)	1834.8	1437.7	1843.1
SiO ₂	55.5	47.4	51.5
TiO ₂	0.0	0.0	0.0
Al ₂ O ₃	1.2	18.6	6.1
Fe ₂ O ₃	4.0	3.6	5.4
MnO	0.1	0.1	0.1
MgO	19.2	6.4	16.5
CaO	19.0	22.3	18.2
K ₂ O	0.0	0.0	0.0
P ₂ O ₅	0.0	0.1	0.0
Na ₂ O	0.0	0.0	0.0
LOI	1.1	3.5	2.6
Total	100.1	101.9	100.6
Sppm	100	6650	80
V	230	220	250
Cr	3960	160	3560
Co	80	70	60
Ni	160	90	200
Cu	25	40	40
Zn	20	40	30
Ga	10	20	10
Rb	-	20	10
Sr	5	175	20
Y	5	15	10
Zr	5	20	20
Nb	-	10	10
Ba	10	35	20
Pb	-	5	5

Table 5.1

ANALYSES OF RODINGITIZED GABBRO FROM CY-4.

S#	006	B81	B80	R4	B77	B62
D. (m)	1073.2	1236.7	1310.2	1322.0	1428.7	1537.0
SiO ₂	35.7	47.8	46.5	32.9	30.1	51.5
TiO ₂	0.0	0.8	0.5	0.4	0.8	0.8
Al ₂ O ₃	21.5	13.6	22.1	19.8	20.7	14.1
Fe ₂ O ₃	4.3	6.6	2.0	4.4	3.6	1.5
MnO	0.0	0.1	0.0	0.0	0.0	0.0
MgO	10.0	7.2	1.5	12.8	12.9	0.0
CaO	24.1	15.5	22.0	24.4	26.6	18.8
K ₂ O	0.0	0.1	0.1	0.1	0.1	0.1
P ₂ O ₅	0.0	0.0	0.1	0.1	0.0	0.0
Na ₂ O	0.5	0.9	1.3	0.9	2.9	2.0
LOI	2.9	7.1	4.2	3.2	1.8	4.3
Total	99.2	99.6	100.3	98.8	99.6	100.1
Rb ppm	10	20	5	10	20	10
Sr	260	40	30	290	190	70
Y	10	10	5	10	30	10
Zr	5	5	10	10	5	5
Nb	5	20	20	10	20	10
Ba	5	30	20	5	20	20

A.6. FERRIC/FERROUS IRON RATIOS

S. #	Fe(Wt.%)*	Fe(II)	Fe(II)/Fe
FRESH DIABASE			
253	12.4	7.2	0.6
234	8.9	7.7	0.9
220	8.7	5.4	0.6
212	12.1	6.5	0.5
145	12.9	7.9	0.6
FRESH GABBRO			
119	13.2	8.5	0.6
117	9.2	7.1	0.8
017	8.2	6.8	0.8
023	9.0	6.9	0.8
036	7.8	6.4	0.8
068	5.4	4.3	0.8

*Fe= Total iron in sample.

S.#	Fe*	* Fe(II)	Fe(II)/Fe
ALTERED DIABASE			
286	10.5	5.6	0.5
254	7.4	3.5	0.5
236	9.7	3.6	0.4
229	9.2	3.8	0.4
227	8.7	5.6	0.6
211	9.3	5.3	0.6
209	3.1	1.5	0.5
207	9.2	4.8	0.5
184	10.0	5.8	0.6
168	5.4	2.6	0.5
167	3.8	2.1	0.6
166	6.2	3.5	0.6
149	5.3	2.9	0.6

*=Total iron.

S.#	Fe*	Fe(II)	Fe(II)/Fe
ALTERED GABBRO			
128	8.6	4.3	0.5
006	5.53	0.03	0.01
012	3.61	2.54	0.70
030	3.4	2.2	0.6
039	2.6	1.8	0.8
059	7.0	5.5	0.8
063	8.1	6.0	0.7
064	7.8	6.1	0.8
068	5.8	3.0	0.5
073	4.1	2.9	0.7
084	6.0	2.3	0.5
089	5.7	4.2	0.7

*=Total iron.

ALTERED GABBRO

S#	024	036	039	040	042	047
D. (m)	1195.9	1283.0	1313.8	1330.0	1347.3	1395.2
SiO ₂	49.2	51.1	50.3	47.0	53.6	48.7
TiO ₂	1.2	0.2	0.9	1.6	0.4	0.1
Al ₂ O ₃	15.4	13.3	15.6	17.5	13.8	24.1
Fe ₂ O ₃	10.1	7.8	2.4	1.0	4.8	5.3
MnO	0.1	0.1	0.0	0.0	0.1	0.1
MgO	4.7	11.3	8.0	5.5	8.4	0.2
CaO	14.4	15.0	18.9	16.7	15.0	16.0
K ₂ O	0.0	0.0	0.0	0.0	0.0	0.0
P ₂ O ₅	0.1	0.0	0.0	0.1	0.0	0.1
Na ₂ O	2.0	0.8	1.7	2.6	0.9	4.0
LOI	1.3	2.7	1.1	3.3	7.8	3.0
Total	98.6	100.9	101.2	99.8	100.1	101.4

Sppm	188	90	40	-	130	90
V	1330	330	400	-	400	260
Cr	30	400	110	-	20	150
Co	60	70	50	-	40	60
Ni	30	90	70	-	20	10
Cu	50	50	30	-	20	30
Zn	30	50	20	-	40	10
Ga	10	10	20	-	70	20
Rb	10	10	20	5	2	15
Sr	120	70	205	90	35	300
Y	20	15	30	10	130	20
Zr	30	30	55	40	190	40
Nb	20	20	20	10	20	20
Ba	3	20	-	80	-	20
U	0.1	-	0.2	-	0.1	0.1
Th	<1	-	<1	-	<1	<1
Au (ppb)	<10	-	<5	-	69	<20
Pb	4	4	4	-	-	2

A.7. RARE EARTH ELEMENT DATA

Sample #	292	271	119	039	042
Depth(m)	21	180	980	1314	1347
La	12	25	10	-	5
Ce	25	15	12	-	5
Pr	ND	3	1	-	ND
Nd	20	10	10	-	5
Sm	10	7	5	-	2
Eu	5	2	1	-	1
Gd	5	7	5	-	1
Tb	ND	1	ND	-	ND
Dy	5	7	2	-	1
Ho	ND	2	ND	-	1
Er	ND	4	ND	-	ND
Tm	ND	1	ND	-	ND
Yb	3	2	2	-	1
Lu	ND	ND	ND	-	ND

SELECT TRACE ELEMENTS

B	0.2	0.5	0.2	0.2	0.2
F	470	160	160	50	20
Cl	500	500	500	500	150
Sc	10	30	10	30	10
Ge	2	2	2	2	2
As	7	2	1	2	1
Se	0.1	0.3	0.1	0.03	0.1
Br	2	0.5	0.2	0.15	0.2

RARE EARTH ELEMENT DATA

S.	#	044	071	076	093	107
D.	(m)	1368	1604	1635	1764	1847
La	1		1	0.4	0.9	4
Ce	0.5		0.5	0.4	0.5	15
Pr	2		1	0.3	ND	ND
Nd	3		ND	0.8	ND	10
Sm	3		ND	0.7	ND	5
Eu	0.7		0.1	0.3	ND	0.6
Gd	1		ND	ND	ND	ND
Tb	0.1		ND	ND	ND	ND
Dy	2		0.8	ND	ND	0.8
Ho	1.2		ND	ND	ND	ND
Er	3		ND	ND	ND	ND
Tm	0.05		0.7	1.1	ND	ND
Yb	0.05		ND	ND	ND	0.7
Lu	0.05		ND	0.6	ND	ND

SELECT TRACE ELEMENTS

B	1	1	1	1	1
F	500	160	160	500	480
Cl	500	500	500	500	500
Sc	30	30	30	30	10
Ge	5	2	2	2	2
As	2	1	2	2	2
Se	0.1	0.03	0.03	0.1	0.1
Br	0.2	0.2	0.2	0.2	0.2

A.8. SELECT TRACE ELEMENT DATA

Sample#	Au(ppb)	Th(ppm)	U(ppm)
DIABASE			
293	23	<1	0.2
251	36	<1	<0.1
GABBRO			
018	<20	<1	<0.1
019	<10	<1	0.1
030	-	<1	0.1
060	<20	<1	0.2
065	<20	<1	<0.1
068	<20	<1	0.1
071	<10	<1	<0.1
076	<5	<1	<0.1
081	<15	<1	0.1
093	<10	<1	<0.1
098	<10	<1	0.1
106	<15	<1	<0.1

A.9. BORON ANALYSIS DATA

Sample#		B(ppm)
	DIABASE	
130		30
	GABBRO	
024		30
030		20
039		20
068		20
076		20
093		20
098		20
	ULTRAMAFICS	
106		20
107		20

Table 6.5: Select phase data for aqueous solutions of chloride species commonly found in fluid inclusions.

Dissolved species	Eutectic temperature °C	Eutectic composition	Solid phases	Solid melting relations
-	-	-	H ₂ O(ice)	0.C.
NaCl	-20.8	23.3%NaCl	NaCl.2H ₂ O	+0.1.IC.
-	-	-	NaCl	-
KCl	-10.6	19.7%KCl	KCl	-
CaCl ₂	-49.8	30.2%CaCl ₂	CaCl ₂ .6H ₂ O	+30.IC.
MgCl ₂	-33.6	21.0%MgCl ₂	MgCl ₂ .12H ₂ O	-16.C.
NaCl-KCl	-22.9	20.17%NaCl	-	-
-	-	5.81%KCl	-	-
NaCl-CaCl ₂	-52.0	1.8%NaCl	-	-
-	-	29.4%CaCl ₂	-	-
NaCl-MgCl ₂	-35.0	1.56%NaCl	-	-
-	-	22.75%MgCl ₂	-	-

All temperatures in °C. Composition in Wt.%. C=congruent, IC= incongruent.
After CRAWFORD(1981).

A.10. TROODOS PLAGIOCLASE ANALYSES

S. #	006	006	006	006	006	006
D. (m)	1073.2	1073.2	1073.2	1073.2	1073.2	1073.2
SiO ₂	51.16	47.88	48.00	48.83	47.50	45.20
Al ₂ O ₃	31.07	32.89	32.89	33.20	32.74	34.96
FeO*	0.00	0.00	0.00	0.00	0.00	0.00
MgO	0.00	0.00	0.00	0.00	0.00	0.00
CaO	14.67	15.72	15.84	15.74	14.67	18.02
Na ₂ O	2.76	2.46	2.30	1.92	4.20	1.46
K ₂ O	0.04	0.08	0.03	0.03	0.03	0.01
Total	99.70	99.03	98.86	99.72	99.14	99.65

NO. OF IONS ON THE BASIS OF 32(O)

Si	9.319	8.847	8.870	8.923	8.801	8.363
Al	6.669	7.161	7.162	7.149	7.149	7.623
Fe(II)	0.000	0.000	0.000	0.000	0.000	0.000
Fe(III)	0.000	0.000	0.000	0.000	0.000	0.000
Mg	0.000	0.000	0.000	0.000	0.000	0.000
Na	0.975	0.881	0.824	0.680	1.509	0.524
Ca	2.863	3.112	3.097	3.082	2.912	3.572
K	0.009	0.019	0.007	0.007	0.007	0.002
AB	25.34	21.96	20.98	18.05	34.07	10.58
AN	74.42	77.57	78.84	81.77	65.77	89.42
OR	0.24	0.47	0.18	0.19	0.16	0.00

TROODOS PLAGIOCLASE ANALYSES

S.#	B40	021	021	046	013	013
D. (m)	1999.8	1175.4	1175.4	1386.90	1122.8	1122.8
SiO ₂	49.66	55.61	52.03	55.30	51.02	51.53
Al ₂ O ₃	31.13	28.69	31.23	23.00	30.19	30.41
FeO	0.07	0.00	0.06	0.05	0.52	0.30
MgO	0.02	0.00	0.00	0.04	0.00	0.01
CaO	11.10	10.58	11.25	17.35	14.75	14.77
Na ₂ O	5.77	3.53	4.66	5.05	4.19	3.31
K ₂ O	0.43	0.07	0.02	0.00	0.00	0.00
Total	98.18	98.48	99.25	100.79	100.67	100.33

NO OF IONS ON THE BASIS OF 32(O)

Si	9.228	10.068	9.465	10.120	9.291	9.362
Al	6.818	6.121	6.694	4.960	6.478	6.511
Fe(II)	0.000	0.000	0.000	0.008	0.079	0.046
Fe(III)	0.011	0.000	0.009	0.000	0.000	0.00
Mg	0.006	0.000	0.000	0.011	0.000	0.003
Na	2.079	1.239	1.644	1.792	1.479	1.166
Ca	2.210	2.052	2.193	3.402	2.878	2.875
K	0.102	0.016	0.005	0.000	0.000	0.000
AB.	47.35	37.46	42.79	34.50	33.95	28.85
AN	50.33	62.05	57.09	65.50	66.05	71.15
OR.	2.32	0.49	0.12	0.00	0.00	0.00

TROODOS PLAGIOCLASE ANALYSES

S.#	024	024	245	013	013	013
D. (m)	1195.9	1195.9	321.4	1122.8	1122.8	1122.8
SiO ₂	56.10	55.87	57.15	54.71	50.95	50.70
Al ₂ O ₃	26.96	26.81	25.66	29.26	30.72	30.68
FeO	0.00	0.00	0.40	0.00	0.00	0.00
MgO	0.00	0.00	0.02	0.00	0.00	0.00
CaO	10.15	10.23	9.47	13.18	14.48	13.99
Na ₂ O	5.16	5.20	6.43	3.65	3.30	3.46
K ₂ O	0.04	0.03	0.05	0.02	0.05	0.04
Total	98.41	98.14	99.18	100.82	99.50	98.87

NO OF IONS ON THE BASIS OF 32(O)

Si	10.213	10.207	10.365	9.790	9.319	9.323
Al	5.784	5.771	5.484	6.170	6.621	6.648
Fe(II)	0.000	0.000	0.061	0.000	0.000	0.000
Fe(III)	0.000	0.000	0.000	0.000	0.000	0.000
Mg	0.000	0.000	0.005	0.000	0.000	0.000
Na	1.821	1.842	2.261	1.266	1.170	1.234
Ca	1.980	2.002	1.840	2.527	2.837	2.756
K	0.009	0.007	0.012	0.005	0.012	0.009
AB	47.80	47.83	54.98	33.34	29.11	30.85
AN	51.96	51.99	44.74	66.54	70.60	68.92
OR	0.24	0.18	0.28	0.12	0.29	0.23

A.11. TROODOS HYDROTHERMAL PLAGIOCLASE ANALYSES

S. #	245	245	220	220	220	220
D. (m)	321.4	321.4	482.7	482.7	482.7	482.7
SiO ₂	68.19	67.52	71.82	74.02	73.04	74.04
Al ₂ O ₃	20.71	19.17	20.63	19.84	19.75	20.51
FeO	0.12	1.10	0.24	0.02	0.00	0.22
MgO	0.03	1.56	0.20	0.00	0.11	0.02
CaO	1.59	1.63	0.23	6.89	0.04	0.31
Na ₂ O	9.74	9.75	7.61	0.01	5.55	5.42
K ₂ O	0.04	0.07	0.01	0.00	0.09	0.13
Total	100.42	100.74	100.74	100.78	98.58	100.65

NO OF IONS ON THE BASIS OF 32(O)

Si	11.839	11.785	12.209	12.432	12.523	12.455
Al	4.237	3.943	4.132	3.927	3.990	4.066
Fe(II)	0.000	0.161	0.000	0.000	0.000	0.000
Fe(III)	0.017	0.000	0.034	0.003	0.000	0.031
Mg	0.008	0.390	0.051	0.000	0.028	0.005
Na	3.279	3.300	2.508	0.003	1.845	1.768
Ca	0.296	0.305	0.042	1.240	0.007	0.056
K	0.009	0.016	0.002	0.000	0.020	0.028
AB	91.50	91.15	98.27	0.26	98.56	95.48
AN	8.25	8.42	1.64	99.74	0.39	3.02
OR	0.25	0.43	0.08	0.00	1.05	1.51

TROODOS HYDROTHERMAL PLAGIOCLASE ANALYSES

S. #	245	245	245	024	024	024
D. (m)	321.4	321.4	321.4	1195.9	1195.9	1195.9
SiO ₂	68.06	63.41	63.70	65.71	65.01	67.95
Al ₂ O ₃	21.27	20.27	21.84	19.54	20.39	18.36
FeO	0.06	2.44	0.34	0.39	0.13	0.12
MgO	0.00	2.95	0.50	0.12	0.05	0.0
CaO	2.93	2.13	4.25	1.44	1.82	0.23
Na ₂ O	8.30	8.21	8.40	10.73	11.05	11.63
K ₂ O	0.04	0.18	0.50	0.00	0.00	0.02
Total	100.66	99.59	99.53	97.93	98.45	98.31

NO OF IONS ON THE BASIS OF 32(O)

Si	11.773	11.307	11.321	11.785	11.627	12.080
Al	4.336	4.259	4.574	4.130	4.297	3.846
Fe(II)	0.000	0.364	0.051	0.058	0.019	0.018
Fe(III)	0.009	0.000	0.000	0.000	0.000	0.000
Mg	0.000	0.784	0.132	0.032	0.013	0.000
Na	2.784	2.838	2.894	3.731	3.832	4.009
Ca	0.543	0.407	0.809	0.277	0.349	0.044
K	0.009	0.041	0.113	0.000	0.000	0.005
AB	83.46	86.37	75.83	93.10	91.66	98.81
AN	16.28	12.38	21.20	6.90	8.34	1.08
OR	0.26	1.25	2.97	0.00	0.00	0.11

TROODQS HYDROTHERMAL PLAGIOCLASE ANALYSES

S. #	024	024	024	024	024	024
------	-----	-----	-----	-----	-----	-----

Meta-gabbro at 1195.90m in CY-4.

SiO ₂	64.33	65.00	66.05	67.52	43.60	44.00
Al ₂ O ₃	20.56	20.55	20.03	20.32	35.64	35.20
FeO	0.08	0.00	0.01	0.00	0.00	0.00
MgO	0.00	0.02	0.00	0.00	0.00	0.00
CaO	3.01	2.28	1.96	0.40	19.45	19.88
Na ₂ O	10.24	10.12	10.97	10.41	0.11	0.39
K ₂ O	0.00	0.18	0.00	0.02	0.01	
Total	98.22	98.15	99.02	98.65	98.82	99.48

NO. OF IONS ON THE BASIS OF 32(Q)

Si	11.550	11.637	11.725	12.022	8.151	8.190
Al	4.350	4.335	4.190	4.054	7.851	7.720
Fe(II)	0.012	0.000	0.001	0.000	0.000	0.000
Fe(III)	0.000	0.000	0.000	0.000	0.000	0.000
Mg	0.000	0.005	0.000	0.000	0.000	0.000
Na	3.565	3.513	3.776	3.594	0.040	0.141
Ca	0.579	0.437	0.373	0.076	3.896	3.964
K	0.000	0.041	0.000	0.000	0.005	0.002
AB	86.03	88.01	91.01	97.92	1.01	3.43
AN	13.97	10.96	8.99	2.08	98.87	96.52
OR	0.00	1.03	0.00	0.00	0.12	0.06

TROODOS HYDROTHERMAL PLAGIOCLASE ANALYSES

S.#	046	046	046	046	B40	B40
D. (m)	1386.9	1386.9	1386.9	1386.9	1999.8	1999.8
SiO ₂	43.54	44.04	44.24	43.82	44.60	43.57
Al ₂ O ₃	34.46	34.68	34.25	34.26	36.39	36.84
FeO	0.12	0.45	0.45	0.54	0.08	0.00
MgO	0.04	0.31	0.09	0.09	0.00	0.00
CaO	20.16	19.20	19.71	19.64	20.11	20.27
Na ₂ O	0.35	0.66	0.59	0.47	0.51	0.30
K ₂ O	0.00	0.00	0.00	0.02	0.00	0.00
Total	98.67	99.34	99.42	98.76	101.69	100.98

NO. OF IONS ON THE BASIS OF 32(O)

Si	8.190	8.220	8.264	8.236	8.125	8.000
Al	7.639	7.627	7.539	7.588	7.612	7.970
Fe(II)	0.019	0.070	0.084	0.072	0.012	0.000
Fe(III)	0.000	0.000	0.000	0.000	0.000	0.000
Mg	0.011	0.086	0.025	0.025	0.000	0.000
Na	0.128	0.239	0.214	0.171	0.180	0.107
Ca	4.063	3.839	3.945	3.955	3.925	3.987
K	0.000	0.000	0.000	0.005	0.000	0.000
AB	3.05	5.86	5.14	4.15	4.39	2.61
AN	96.95	94.14	94.86	95.74	95.61	97.39
OR	0.00	0.00	0.00	0.12	0.00	0.00

TROODOS HYDROTHERMAL PLAGIOCLASE ANALYSES

S.#	061V	061	061	061	061V	061V
-----	------	-----	-----	-----	------	------

VEIN AT 1483.70m

SiO ₂	67.10	66.95	67.64	67.09	66.21	66.72
Al ₂ O ₃	19.69	20.34	20.02	20.10	19.54	19.52
FeO	0.00	0.00	0.00	0.00	0.04	0.00
MgO	0.00	0.00	0.00	0.00	0.00	0.00
CaO	0.56	0.97	0.59	0.88	0.44	0.28
Na ₂ O	11.30	10.13	11.13	10.59	12.13	11.76
K ₂ O	0.03	0.04	0.04	0.05	0.00	0.02
Total	98.68	98.46	99.42	98.71	98.38	98.30

NO. OF IONS ON THE BASIS OF 32(O)

Si	11.890	11.854	11.885	11.864	11.819	11.883
Al	4.111	4.242	4.145	4.188	4.110	4.097
Fe(II)	0.000	0.000	0.000	0.000	0.006	0.000
Fe(III)	0.000	0.000	0.000	0.000	0.000	0.000
Mg	0.000	0.000	0.000	0.000	0.005	0.000
Na	3.882	3.476	3.792	3.631	4.198	4.061
Ca	0.106	0.184	0.111	0.167	0.084	0.053
K	0.007	0.009	0.009	0.11	0.000	0.005
AB	97.17	94.74	96.93	95.33	98.03	98.59
AN	2.66	5.01	2.84	4.38	1.97	1.30
OR	0.17	0.25	0.23	0.30	0.00	0.11

PLAGIOCLASE FROM RODINGITIZED GABBRO*

SiO ₂	44.31	58.34	45.08	66.32	44.85	46.68
Al ₂ O ₃	34.76	20.77	34.77	20.23	34.24	34.66
FeO	0.00	0.00	0.00	0.04	0.07	0.00
MgO	0.00	0.00	0.00	0.00	0.00	0.00
CaO	18.81	1.45	17.39	1.32	19.95	18.00
Na ₂ O	0.95	10.35	2.67	11.39	1.09	0.68
K ₂ O	0.07	0.05	0.04	0.00	0.00	0.00
Total	98.90	98.96	99.95	99.30	100.20	100.02

NO. OF IONS ON THE BASIS OF 32(O)

Si	8.282	11.727	8.344	11.732	8.309	8.556
Al	7.656	4.326	7.584	4.217	7.475	7.486
Fe(II)	0.000	0.000	0.000	0.008	0.011	0.000
Fe(III)	0.000	0.000	0.000	0.000	0.000	0.000
Mg	0.000	0.000	0.000	0.000	0.000	0.000
Na	0.344	3.547	0.958	3.906	0.392	0.242
Ca	3.767	0.275	3.449	0.250	3.960	3.535
K	0.017	0.011	0.009	0.000	0.000	0.000
AB	8.34	92.54	21.70	93.98	9.00	6.40
AN	91.26	7.16	78.09	6.02	91.00	93.60
OR	0.40	0.29	0.21	0.00	0.00	0.00

* Rodingitized gabbro at 1175.35m, CY-4.

TROODOS HYDROTHERMAL PLAGIOCLASE

S.#	006	006	006	006	006	006
-----	-----	-----	-----	-----	-----	-----

PLAG.FROM LEACHED ZONE IN GABBRO*

SiO ₂	68.71	68.16	46.11	69.32	68.75	47.07
Al ₂ O ₃	19.84	19.35	34.06	20.29	20.11	34.08
FeO	0.00	0.00	0.00	0.00	0.02	0.00
MgO	0.00	0.00	0.00	0.02	0.01	0.00
CaO	0.27	0.20	18.05	0.24	0.21	16.11
Na ₂ O	10.61	10.83	1.18	10.97	11.33	2.37
K ₂ O	0.02	0.03	0.00	0.00	0.00	0.05
Total	99.45	98.57	99.40	100.84	100.43	99.68

NO.OF IONS ON THE BASIS OF 32(O)

Si	12.009	12.033	8.533	11.962	11.937	8.657
Al	4.086	4.025	7.427	4.126	4.115	7.386
Fe(II)	0.000	0.000	0.000	0.000	0.000	0.000
Fe(III)	0.000	0.000	0.000	0.000	0.000	0.000
Mg	0.000	0.000	0.000	0.005	0.003	0.000
Na	3.595	3.707	0.423	3.670	3.814	0.845
Ca	0.051	0.038	3.579	0.044	0.039	3.175
K	0.004	0.007	0.000	0.000	0.000	0.000
AB	98.49	98.81	10.58	98.81	98.99	20.96
AN	1.39	1.01	89.42	1.19	1.01	78.75
OR	0.12	0.18	0.00	0.00	0.00	0.29

* ZONE AT 1073.15M,CY-4.

TROODOS CLINOPYROXENE ANALYSES

S.#	013	013	013	013	013
CPX. FROM MICROGABBRO AT 1122.80M					
SiO ₂	52.35	52.21	54.84	54.28	51.16
TiO ₂	0.28	0.28	0.00	0.15	0.23
Al ₂ O ₃	1.25	1.07	0.29	1.41	1.91
FeO	10.59	10.64	4.17	5.23	7.77
MnO	0.27	0.28	0.07	0.02	0.08
MgO	14.16	14.13	15.60	15.92	14.67
CaO	22.29	22.02	26.50	21.89	24.54
Na ₂ O	0.20	0.13	0.16	0.32	0.37
K ₂ O	0.00	0.00	0.01	0.00	0.00
Total	101.39	100.74	101.64	99.22	100.73

NO.OF IONS ON THE BASIS OF 6 OXYGENS

Si	1.944	1.950	1.988	1.996	1.905
Al	0.055	0.047	0.012	0.004	0.084
Al	0.000	0.000	0.000	0.057	0.000
Ti	0.008	0.007	0.000	0.004	0.006
Fe	0.329	0.332	0.126	0.161	0.242
Mg	0.784	0.787	0.843	0.873	0.814
Mn	0.008	0.009	0.002	0.001	0.003
Ca	0.887	0.881	1.029	0.862	0.979
Na	0.014	0.009	0.011	0.023	0.027
K	0.000	0.000	0.000	0.000	0.000
FS	16.45	16.62	6.33	8.48	11.89
WO	44.35	44.06	51.50	45.49	48.11
EN	39.20	39.33	42.18	46.03	40.01

A.12. TROODOS CLINOPYROXENE ANALYSES

S.#	021	021	021	021	021	021
CLINOPYROXENE FROM META-GABBRO AT 1175.35m ,CY-4.						
SiO ₂	52.00	51.14	52.14	52.38	52.04	51.69
TiO ₂	0.00	0.02	0.02	0.02	0.01	0.02
Al ₂ O ₃	0.18	0.31	0.26	0.36	0.23	0.32
FeO	8.34	9.29	8.68	7.66	8.79	8.36
MnO	0.03	0.11	0.17	0.20	0.18	0.21
MgO	12.62	12.36	12.95	13.88	13.18	13.19
CaO	25.63	25.01	26.59	26.03	26.29	26.34
Na ₂ O	0.11	0.13	0.14	0.08	0.11	0.07
K ₂ O	0.00	0.00	0.00	0.01	0.00	0.01
Total	98.91	98.37	100.95	100.62	100.83	100.21

NO.OF IONS ON THE BASIS OF 6 OXYGENS.

Si	1.978	1.966	1.954	1.969	1.952	1.949
Al	0.008	0.014	0.011	0.016	0.010	0.014
Al	0.000	0.000	0.000	0.000	0.000	0.000
Ti	0.000	0.001	0.001	0.001	0.000	0.001
Fe	0.265	0.299	0.272	0.236	0.276	0.264
Mg	0.716	0.708	0.723	0.763	0.737	0.741
Mn	0.001	0.004	0.005	0.006	0.006	0.007
Ca	1.045	1.030	1.068	1.029	1.057	1.064
Na	0.008	0.010	0.010	0.006	0.008	0.005
K	0.000	0.000	0.000	0.000	0.000	0.000
FS	13.10	14.66	13.19	11.65	13.33	12.74
WO	51.57	50.57	51.75	50.72	51.06	51.43
EN	35.33	34.77	35.06	37.63	35.61	35.83

TROODOS CLINOPYROXENE ANALYSES

S.#	024	024	024	024	024	024
-----	-----	-----	-----	-----	-----	-----

CPX.IN META-GABBRO AT 1195.90M.

SiO ₂	52.77	51.84	52.22	51.66	51.98	50.96
TiO ₂	0.02	0.00	0.04	0.04	0.04	0.01
Al ₂ O ₃	0.38	0.32	0.52	0.34	0.15	0.33
FeO	8.29	8.94	10.41	13.91	8.35	10.38
MnO	0.09	0.07	0.07	0.14	0.35	0.00
MgO	12.55	12.54	11.95	9.68	13.32	11.47
CaO	24.73	24.60	24.32	23.95	24.15	24.86
Na ₂ O	0.11	0.26	0.10	0.36	0.22	0.21
K ₂ O	0.00	0.00	0.00	0.00	0.00	0.00
Total	98.94	98.57	99.63	100.08	98.56	98.22

NO.OF IONS ON THE BASIS OF 8 OXYGENS.

Si	1.984	1.980	1.981	1.985	1.980	1.971
Al	0.016	0.014	0.019	0.015	0.007	0.015
Al	0.001	0.000	0.004	0.000	0.000	0.000
Fe	0.266	0.286	0.330	0.447	0.266	0.336
Mg	0.717	0.714	0.676	0.554	0.756	0.661
Mn	0.003	0.002	0.002	0.005	0.011	0.000
Ca	1.015	1.007	0.989	0.986	0.986	1.030
Na	0.008	0.019	0.007	0.027	0.016	0.016
K	0.000	0.000	0.000	0.000	0.000	0.000
FS	13.30	14.23	16.56	22.49	13.25	16.56
WO	50.82	50.18	49.56	49.61	49.09	50.82
EN	35.88	35.59	33.88	27.90	37.66	32.62

TROODOS CLINOPYROXENE ANALYSES

S. #	035	035	035	035	035	035
------	-----	-----	-----	-----	-----	-----

CPX.FROM MICROGABBRO AT 1271.20M.

SiO ₂	52.82	53.73	53.29	52.71	52.89	52.25
TiO ₂	0.06	0.05	0.12	0.08	0.11	0.01
Al ₂ O ₃	0.25	0.26	0.39	0.25	0.40	0.38
FeO	7.39	7.42	7.35	8.86	8.16	10.48
MnO	0.32	0.38	0.24	0.20	0.46	0.02
MgO	14.29	13.45	13.40	13.36	13.77	11.03
CaO	23.58	24.38	24.52	24.23	24.29	25.63
Na ₂ O	0.22	0.48	0.36	0.62	0.19	0.15
K ₂ O	0.00	0.02	0.00	0.00	0.00	0.02
Total	98.93	100.17	99.67	100.31	100.27	99.97

NO.OF IONS ON THE BASIS OF 6 OXYGENS.

Si	1.975	2.000	1.993	1.976	1.976	1.984
Al	0.011	0.000	0.007	0.011	0.018	0.016
Al	0.000	0.011	0.011	0.000	0.000	0.001
Ti	0.002	0.001	0.003	0.002	0.003	0.000
Fe	0.236	0.231	0.230	0.278	0.255	0.333
Mg	0.812	0.746	0.747	0.747	0.767	0.624
Mn	0.010	0.012	0.008	0.008	0.015	0.001
Ca	0.963	0.972	0.983	0.973	0.972	1.043
Na	0.016	0.035	0.026	0.045	0.014	0.011
K	0.000	0.001	0.000	0.000	0.000	0.001
FS	11.72	11.85	11.73	13.91	12.79	16.64
WO	47.90	49.87	50.14	49.72	48.76	52.14
EN	40.38	38.28	38.12	37.37	38.45	31.22

TROBOS CLINOPYROXENE ANALYSES

S.#	054	054	054	054	054	054
-----	-----	-----	-----	-----	-----	-----

CPX.FROM GABBRO AT 1438.00M IN CY-4.

SiO ₂	50.13	52.64	53.27	52.98	53.27	53.27
TiO ₂	0.12	0.18	0.09	0.09	0.18	0.09
Al ₂ O ₃	1.46	1.08	0.37	0.34	0.36	0.37
FeO	8.81	6.88	5.57	6.38	5.07	5.57
MnO	0.21	0.18	0.07	0.14	0.09	0.07
MgO	14.84	15.37	15.52	14.83	16.00	15.52
CaO	25.68	23.08	25.54	25.16	25.42	25.54
Na ₂ O	0.17	0.28	0.00	0.05	0.38	0.00
K ₂ O	0.00	0.00	0.00	0.01	0.02	0.00
Total	101.42	99.69	100.43	99.98	100.79	100.43

NO.OF IONS ON THE BASIS OF 6 OXYGENS.

Si	1.876	1.958	1.966	1.971	1.958	1.966
Al	0.064	0.042	0.016	0.015	0.016	0.016
Al	0.000	0.000	0.000	0.000	0.000	0.000
Ti	0.003	0.005	0.002	0.003	0.005	0.002
Fe	0.276	0.214	0.172	0.199	0.156	0.172
Mg	0.828	0.852	0.854	0.822	0.877	0.854
Mn	0.007	0.006	0.002	0.004	0.003	0.002
Ca	1.029	0.920	1.010	1.003	1.001	1.010
Na	0.012	0.020	0.000	0.004	0.027	0.000
K	0.000	0.000	0.000	0.000	0.001	0.000
FS	12.93	10.78	8.45	9.81	7.66	8.45
WO	48.27	46.32	49.61	49.56	49.23	49.61
EN	38.80	42.91	41.94	40.64	43.11	41.94

TROODOS CLINOPYROXENES ANALYSES

S.#	075	075	075	075	075	075
-----	-----	-----	-----	-----	-----	-----

CPX.FROM GABBRO AT 1633.90M IN CY-4.

SiO ₂	53.34	53.12	54.17	53.93	52.75	53.54
TiO ₂	0.14	0.05	0.21	0.01	0.21	0.21
Al ₂ O ₃	0.95	0.81	1.22	1.00	1.81	1.98
FeO	6.04	5.64	6.37	5.44	6.38	6.80
MnO	0.05	0.11	0.09	0.06	0.11	0.21
MgO	16.18	16.14	15.88	16.28	15.60	16.61
CaO	23.73	24.68	22.58	24.76	23.13	21.21
Na ₂ O	0.09	0.26	0.06	0.17	0.18	0.18
K ₂ O	0.00	0.00	0.00	0.00	0.00	0.00
Total	100.52	100.61	100.58	101.65	100.17	100.74

NO.OF IONS ON THE BASIS OF 6 OXYGENS

Si	1.960	1.956	1.980	1.959	1.946	1.954
Al	0.040	0.026	0.020	0.041	0.054	0.046
Al	0.001	0.000	0.033	0.001	0.025	0.039
Ti	0.004	0.001	0.006	0.000	0.006	0.006
Fe	0.186	0.174	0.195	0.165	0.197	0.208
Mg	0.886	0.886	0.865	0.881	0.858	0.903
Mn	0.002	0.003	0.003	0.002	0.003	0.006
Ca	0.934	0.974	0.884	0.963	0.914	0.829
Na	0.006	0.019	0.004	0.012	0.013	0.013
K	0.000	0.000	0.000	0.000	0.000	0.000
FS	9.25	8.54	10.02	8.22	10.00	10.70
WO	46.57	47.89	45.48	47.93	46.43	42.74
EN	44.18	43.57	44.50	43.85	43.57	46.56

TROODOS CLINOPYROXENES ANALYSES

S. #	075	047	047	013
D. (m)	1633.9	1395.2	1395.2	1122.8
SiO_2	52.52	54.19	52.78	54.24
TiO_2	0.05	0.00	0.00	0.01
Al_2O_3	2.15	0.86	0.91	0.91
FeO	6.57	1.04	0.98	1.18
MnO	0.18	0.00	0.00	0.00
MgO	15.89	17.22	17.13	17.18
CaO	23.59	26.89	25.93	26.00
Na_2O	0.10	0.07	0.98	0.13
K_2O	0.00	0.00	0.00	0.00
Total	101.05	100.27	98.71	99.65

NO. OF IONS ON THE BASIS OF 6 OXYGENS.

Si	1.926	1.967	1.952	1.976
Al	0.074	0.033	0.040	0.024
Al	0.019	0.004	0.000	0.015
Ti	0.001	0.000	0.000	0.000
Fe	0.201	0.032	0.030	0.036
Mg	0.869	0.932	0.944	0.933
Mn	0.006	0.000	0.000	0.000
Ca	0.927	1.046	1.027	1.015
Na	0.007	0.005	0.070	0.009
K	0.000	0.000	0.000	0.000
FS	10.09	1.57	1.51	1.81
WO	46.42	52.05	51.32	51.16
EN	43.49	46.37	47.17	47.03

TROODOS CLINOPYROXENE ANALYSES

S. #	077	077	044	044	044	044
D. (m)	1644.8	1644.8	1367.7	1367.7	1367.7	1367.7
SiO ₂	55.63	52.56	53.19	53.01	51.95	52.54
TiO ₂	0.18	0.11	0.00	0.00	0.29	0.24
Al ₂ O ₃	2.66	0.57	0.37	0.20	1.66	1.45
FeO	10.38	6.25	7.06	5.35	7.96	7.38
MnO	0.16	0.24	0.15	0.15	0.19	0.09
MgO	18.42	14.98	14.33	15.69	15.51	15.77
CaO	13.09	25.24	24.59	24.83	21.59	21.89
Na ₂ O	1.37	0.09	0.05	0.02	0.19	0.09
K ₂ O	0.00	0.00	0.00	0.01	0.41	0.09
Total	101.89	100.04	99.74	99.26	99.75	99.45

NO. OF IONS ON THE BASIS OF 6 OXYGENS.

Si	1.988	1.957	1.984	1.976	1.939	1.954
Al	0.012	0.025	0.016	0.009	0.061	0.046
Al	0.101	0.000	0.001	0.000	0.012	0.018
Ti	0.005	0.003	0.000	0.000	0.008	0.007
Fe	0.310	0.195	0.220	0.167	0.248	0.230
Mg	0.981	0.831	0.797	0.872	0.863	0.874
Mn	0.005	0.008	0.005	0.005	0.006	0.003
Ca	0.501	1.007	0.983	0.991	0.863	0.872
Na	0.095	0.006	0.004	0.001	0.014	0.006
K	0.000	0.000	0.000	0.000	0.020	0.000
FS	17.31	9.57	11.01	8.21	12.58	11.62
WO	27.96	49.53	49.14	48.85	43.72	44.14
EN	54.73	40.90	39.84	42.94	43.70	44.24

TROODOS CLINOPYROXENE ANALYSES

S. #	030	030	030	030	030
------	-----	-----	-----	-----	-----

CPX. IN META-GABBRO AT 1245.30M.

SiO ₂	52.82	68.03	51.90	52.48	52.83
TiO ₂	0.09	0.30	0.09	0.16	0.34
Al ₂ O ₃	1.18	1.23	1.48	1.69	1.58
FeO	2.17	4.36	2.32	6.78	2.37
MnO	0.00	0.13	0.00	0.00	0.00
MgO	16.11	10.59	16.22	15.91	15.48
CaO	25.50	17.77	25.71	23.19	26.49
Na ₂ O	0.00	0.28	0.12	0.08	0.07
K ₂ O	0.00	0.00	0.00	0.00	0.00
Total	97.87	100.67	97.82	100.25	99.12

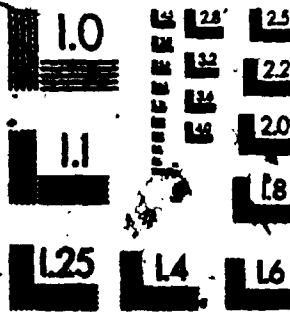
NO. OF IONS ON THE BASIS OF 6 OXYGENS.

Si	1.968	2.283	1.943	1.938	1.952
Al	0.032	0.000	0.057	0.062	0.048
Al	0.020	0.050	0.007	0.011	0.020
Ti	0.003	0.008	0.003	0.004	0.009
Fe	0.068	0.128	0.073	0.209	0.073
Mg	0.995	0.548	0.905	0.878	0.851
Mn	0.000	0.004	0.000	0.000	0.000
Ca	1.018	0.658	1.031	0.918	1.049
Na	0.000	0.017	0.009	0.006	0.005
K	0.000	0.000	0.000	0.000	0.000
FS	3.41	9.46	3.62	10.43	3.71
WO	51.41	49.49	51.33	45.83	53.14
EN	45.18	41.03	45.05	43.74	43.15

3

3

MICROCOPY RESOLUTION TEST CHART
NBS 1010a
(ANSI and ISO TEST CHART No. 2)



TROODOS CLINOPYROXENE ANALYSES

S.#.	046	046	046	046	046
CPX.FROM METAGABBRO AT 1386.90M.					
SiO ₂	53.58	54.05	53.88	54.31	54.14
TiO ₂	0.07	0.04	0.02	0.17	0.02
Al ₂ O ₃	1.56	0.34	2.15	0.98	0.22
FeO	1.80	0.83	0.55	2.12	2.61
MnO	0.00	0.02	0.06	0.02	0.03
MgO	16.35	17.44	17.05	16.67	16.76
CaO	25.65	26.44	26.33	26.46	27.30
Na ₂ O	0.13	0.05	0.09	0.25	0.00
K ₂ O	0.00	0.00	0.00	0.00	0.00
Total	99.14	99.21	100.13	100.98	101.08

NO.OF IONS ON THE BASIS OF 6 OXYGENS.

SiO	1.966	1.979	1.950	1.965	1.967
Al	0.034	0.015	0.050	0.035	0.009
Al	0.034	0.000	0.041	0.007	0.000
Ti	0.002	0.001	0.001	0.005	0.001
Fe	0.055	0.025	0.017	0.064	0.079
Mg	0.894	0.952	0.920	0.899	0.908
Mn	0.000	0.001	0.002	0.001	0.001
Ca	1.008	1.037	1.021	1.006	1.063
Na	0.009	0.004	0.006	0.018	0.000
K	0.000	0.000	0.000	0.000	0.000
FS	2.82	1.26	0.85	3.23	3.87
WO	51.51	51.49	52.16	51.53	51.85
EN	45.67	47.25	46.99	45.20	44.28

TROODOS CLINOPYROXENE ANALYSES

S. #	039	006	006	006	006	B65
D. (m)	1313.8	1073.2	1073.2	1073.2	1073.2	1046.5
SiO ₂	55.21	52.96	52.36	52.63	53.50	51.30
TiO ₂	0.00	0.29	0.35	0.36	0.30	0.28
Al ₂ O ₃	0.45	1.02	1.18	1.14	0.96	1.05
FeO	1.44	10.43	10.66	10.25	9.20	11.55
MnO	0.00	0.34	0.30	0.63	0.36	0.37
MgO	15.94	14.70	14.44	14.58	14.39	13.36
CaO	26.26	21.29	21.30	20.55	21.95	21.08
Na ₂ O	0.07	0.28	0.21	0.20	0.19	0.31
K ₂ O	0.02	0.04	0.01	0.17	0.02	0.02
Total	99.39	101.35	100.81	100.51	100.87	99.32

NO. OF IONS ON THE BASIS OF 6 OXYGENS.

Si	2.015	1.959	1.951	1.962	1.978	1.952
Al	0.000	0.041	0.049	0.038	0.022	0.047
Al	0.019	0.004	0.002	0.012	0.020	0.000
Ti	0.000	0.008	0.010	0.010	0.008	0.008
Fe	0.044	0.323	0.332	0.320	0.284	0.368
Mg	0.867	0.811	0.802	0.810	0.793	0.758
Mn	0.000	0.011	0.009	0.020	0.011	0.012
Ca	1.027	0.844	0.850	0.821	0.869	0.860
Na	0.005	0.020	0.015	0.014	0.014	0.023
K	0.001	0.002	0.000	0.008	0.001	0.001
FS	2.27	16.32	16.74	16.38	14.61	18.52
WO	52.99	42.68	42.85	42.08	44.66	43.30
EN	44.74	41.00	40.41	41.54	40.73	38.18

TROODOS CLINOPYROXENE ANALYSES

S. #.	R4	R4	R4	R4	R4	R4
CPX.FROM METAGABBRO AT 1322.0M						
SiO ₂	54.35	52.91	54.66	53.97	54.11	53.32
TiO ₂	0.05	0.09	0.05	0.00	0.02	0.03
Al ₂ O ₃	0.34	0.34	0.34	0.20	0.38	0.23
FeO	1.44	6.75	1.63	3.30	3.88	4.23
MnO	0.07	0.00	0.00	0.00	0.15	0.03
MgO	17.21	14.32	17.15	16.45	15.48	15.90
CaO	26.79	25.68	26.79	26.35	26.63	26.41
Na ₂ O	0.17	0.13	0.03	0.01	0.31	0.39
K ₂ O	0.02	0.00	0.00	0.02	0.02	0.00
Total	100.44	100.22	100.65	100.30	100.96	100.54

NO.OF IONS ON THE BASIS OF 6 OXYGENS.

Si	1.974	1.970	1.980	1.977	1.977	1.962
Al	0.015	0.015	0.015	0.009	0.016	0.010
Al	0.000	0.000	0.000	0.000	0.000	0.000
Ti	0.001	0.003	0.001	0.000	0.001	0.001
Fe	0.044	0.210	0.049	0.101	0.119	0.130
Mg	0.932	0.795	0.928	0.898	0.842	0.872
Mn	0.002	0.000	0.000	0.000	0.005	0.001
Ca	1.043	1.024	1.040	1.034	1.043	1.041
Na	0.012	0.009	0.002	0.001	0.022	0.028
K	0.001	0.000	0.000	0.001	0.001	0.000
FS	2.17	10.36	2.45	4.97	5.92	6.37
WO	51.66	50.48	51.60	50.86	52.05	50.95
EN	46.17	39.18	45.95	44.17	42.03	42.68

TROODOS CLINOPYROXENE ANALYSES

S.#	098	098	098	098	098	098
CPX.FROM PYROXENITE AT 1803.02M.						
SiO ₂	53.20	53.60	53.92	54.02	53.34	53.28
TiO ₂	0.07	0.07	0.03	0.03	0.03	0.05
Al ₂ O ₃	1.75	1.94	1.71	1.83	1.87	1.76
FeO	3.48	3.27	3.53	3.48	3.30	3.35
MnO	0.16	0.18	0.14	0.11	0.08	0.16
MgO	17.56	17.17	17.60	18.01	17.43	17.46
CaO	22.44	23.38	23.05	22.50	23.14	23.07
Na ₂ O	0.07	0.06	0.06	0.16	0.17	0.12
K ₂ O	0.04	0.01	0.02	0.01	0.02	0.01
Total	98.77	99.68	100.06	100.13	99.38	99.26

NO.OF IONS ON THE BASIS OF 6(O)

Si	1.959	1.957	1.961	1.959	1.954	1.955
Al	0.041	0.043	0.039	0.041	0.046	0.045
Al	0.035	0.041	0.034	0.038	0.034	0.031
Ti	0.002	0.002	0.001	0.001	0.001	0.001
Fe	0.107	0.100	0.107	0.105	0.101	0.103
Mg	0.964	0.934	0.954	0.974	0.952	0.955
Mn	0.005	0.006	0.004	0.003	0.002	0.005
Ca	0.885	0.915	0.893	0.874	0.908	0.907
Na	0.005	0.004	0.004	0.011	0.012	0.009
K	0.002	0.000	0.001	0.000	0.001	0.000
FS	5.48	5.12	5.48	5.37	5.16	5.23
WO	45.26	46.93	45.83	44.77	46.31	46.16
EN	49.27	47.95	48.69	49.85	48.53	48.60

A.13. TROODOS ORTHOPYROXENES ANALYSES

SiO ₂	58.04	52.96	53.70	53.76	53.61	55.73
TiO ₂	0.09	0.14	0.09	0.13	0.13	0.02
Al ₂ O ₃	1.18	1.14	1.25	1.14	0.98	1.36
FeO	13.55	17.34	18.15	16.47	17.36	9.48
MnO	0.21	0.32	0.28	0.40	0.34	0.22
MgO	28.86	25.39	25.93	26.83	25.85	30.30
CaO	1.82	1.62	1.24	1.68	1.54	1.56
Na ₂ O	0.00	0.09	0.00	0.00	0.00	0.00
K ₂ O	0.00	0.00	0.00	0.00	0.00	0.01
Total	101.75	99.00	100.64	100.41	99.81	98.68

NO. OF IONS ON THE BASIS OF 6 OXYGENS.

Si	1.989	1.954	1.951	1.947	1.980	1.980
Al	0.031	0.046	0.049	0.049	0.040	0.020
Al	0.018	0.004	0.005	0.000	0.002	0.037
Ti	0.002	0.004	0.002	0.004	0.004	0.001
Fe	0.398	0.535	0.551	0.499	0.531	0.282
Mg	1.511	1.397	1.404	1.449	1.408	1.605
Mn	0.006	0.010	0.009	0.012	0.011	0.007
Ca	0.069	0.064	0.048	0.065	0.060	0.059
Na	0.000	0.008	0.000	0.000	0.000	0.000
K	0.000	0.000	0.000	0.000	0.000	0.000
FS	20.13	26.81	27.52	24.79	26.54	14.48
WO	3.46	3.21	2.41	3.24	3.02	3.05
EN	76.41	69.98	70.07	71.97	70.44	82.47

TROODOS ORTHOPYROXENE ANALYSES

S. #	054	054	054	054	054	054
OPX FROM GABBRO AT 1438.0M						
SiO ₂	54.90	55.18	55.55	55.48	54.66	55.45
TiO ₂	0.05	0.04	0.04	0.04	0.04	0.05
Al ₂ O ₃	1.39	1.42	1.58	1.39	1.41	1.37
FeO	11.24	11.29	10.88	10.95	11.71	12.61
MnO	0.44	0.34	0.29	0.28	0.33	0.29
MgO	29.27	29.54	29.87	29.63	29.39	28.80
CaO	1.62	1.79	1.54	1.74	1.65	1.73
Na ₂ O	0.01	0.05	0.00	0.00	0.00	0.00
K ₂ O	0.02	0.03	0.02	0.02	0.00	0.03
Total	98.94	99.78	99.77	99.53	99.19	100.33

NO. OF IONS ON THE BASIS OF 6 OXYGENS.

Si	1.967	1.961	1.967	1.971	1.958	1.969
Al	0.033	0.039	0.033	0.029	0.042	0.031
Al	0.025	0.021	0.032	0.029	0.017	0.026
Ti	0.001	0.001	0.001	0.001	0.001	0.001
Fe	0.337	0.336	0.322	0.325	0.351	0.374
Mg	1.563	1.570	1.576	1.569	1.569	1.524
Mn	0.031	0.010	0.009	0.008	0.010	0.009
Ca	0.062	0.068	0.058	0.066	0.063	0.066
Na	0.001	0.003	0.000	0.000	0.000	0.000
K	0.001	0.001	0.001	0.001	0.000	0.001
FS	17.16	17.00	16.46	16.59	17.69	19.06
WO	3.17	3.45	2.99	3.38	3.19	3.35
EN	79.67	79.55	80.55	80.03	79.12	77.59

TROODOS AMPHIBOLE ANALYSES

S. #	245	245	245	245	245	245
AMPHIBOLES	FROM DIABASE AT 321.4m, CY-4.					
SiO ₂	52.66	50.30	50.17	51.41	50.70	50.57
TiO ₂	0.29	0.23	0.20	0.20	0.32	0.24
Al ₂ O ₃	3.79	4.82	3.62	3.20	2.48	3.03
FeO	12.19	12.84	18.06	17.77	19.15	18.07
MnO	0.50	0.40	0.29	0.41	0.41	0.38
MgO	16.18	15.09	12.56	12.50	12.15	12.89
CaO	11.00	12.17	11.78	11.99	11.97	11.50
Na ₂ O	0.33	0.39	0.39	0.30	0.43	0.42
K ₂ O	0.05	0.02	0.06	0.06	0.04	0.09
Total	97.15	96.28	97.19	97.85	97.66	97.21

NO. OF IONS ON THE BASIS OF 23 (O,OH).

Si	7.593	7.393	7.482	7.589	7.571	7.537
Al	0.407	0.607	0.518	0.411	0.429	0.463
Al	0.237	0.228	0.118	0.146	0.008	0.069
Ti	0.031	0.025	0.022	0.022	0.036	0.027
Mg	3.477	3.306	2.792	2.750	2.704	2.864
Fe	1.470	1.578	2.252	2.194	2.392	2.252
Mn	0.061	0.050	0.037	0.051	0.052	0.048
Ca	1.699	1.916	1.882	1.896	1.915	1.836
Na	0.092	0.111	0.113	0.086	0.124	0.121
K	0.009	0.004	0.011	0.011	0.008	0.017
WQ	25.57	28.18	27.17	27.72	27.32	26.41
CUMM	52.32	48.61	40.31	40.21	38.57	41.19
RUN	22.12	23.21	32.52	32.07	34.11	32.40

A.14. TROODOS AMPHIBOLE ANALYSES

S. #	220	220	220	220	220
	AMPHIBOLES FROM DIABASE AT 482.70M, CY-4.				
SiO ₂	54.73	53.53	52.07	52.17	50.76
TiO ₂	0.23	0.24	0.42	0.28	0.80
Al ₂ O ₃	1.93	2.34	2.93	2.68	4.13
FeO	12.36	12.62	14.03	13.24	14.68
MnO	0.36	0.36	0.46	0.29	0.37
MgO	15.94	15.88	15.50	15.52	14.13
CaO	12.44	12.67	12.66	12.74	12.34
Na ₂ O	0.17	0.43	0.31	0.33	0.64
K ₂ O	0.04	0.04	0.06	0.04	0.25
Total	98.20	98.19	98.51	97.45	98.12

NO. OF IONS ON THE BASIS OF 23 (O,OH).

Si	7.812	7.685	7.524	7.588	7.403
Al	0.188	0.315	0.476	0.412	0.597
Al	0.137	0.081	0.023	0.047	0.113
Ti	0.025	0.026	0.046	0.031	0.002
Mg	3.391	3.398	3.338	3.365	0.088
Fe	1.475	1.515	1.695	1.610	3.072
Mn	0.044	0.044	0.056	0.036	1.790
Ca	1.902	1.949	1.960	1.985	0.046
Na	0.047	0.120	0.087	0.093	0.181
K	0.007	0.007	0.011	0.007	0.047
WO	28.10	28.40	28.02	28.52	28.40
CUMM	50.10	49.52	47.73	48.34	45.23
RUN	21.80	22.08	24.24	23.14	26.37

TROODOS AMPHIBOLE ANALYSES

S. #	149	149	149	006	006	006
D. (m)	821.5	821.5	821.5	1073.2	1073.2	1073.2
SiO ₂	51.70	49.95	51.77	51.91	51.70	49.30
TiO ₂	0.42	1.38	0.53	0.15	0.14	0.10
Al ₂ O ₃	3.95	5.57	4.03	3.74	3.84	5.50
FeO	10.59	10.49	10.11	14.20	14.66	15.67
MnO	0.03	0.02	0.09	0.31	0.50	0.25
MgO	16.64	15.50	17.54	14.75	15.64	15.46
CaO	12.00	11.82	11.73	12.05	11.20	9.99
Na ₂ O	0.73	1.21	0.66	0.32	0.28	0.28
K ₂ O	0.15	0.04	0.08	0.02	0.00	0.02
Total	96.22	96.00	96.54	97.45	97.96	96.62

NO. OF IONS ON THE BASIS OF 23 (O,OH).

Si	7.500	7.282	7.462	7.556	7.494	7.274
Al	0.500	0.718	0.538	0.444	0.506	0.726
Al	0.176	0.239	0.146	0.197	0.150	0.230
Ti	0.046	0.151	0.057	0.016	0.015	0.011
Mg	3.598	3.368	3.768	3.200	3.379	3.400
Fe	1.285	1.279	1.219	1.729	1.777	1.934
Mn	0.004	0.002	0.011	0.038	0.061	0.031
Ca	1.865	1.846	1.811	1.879	1.739	1.579
Na	0.205	0.342	0.184	0.090	0.079	0.080
K	0.028	0.007	0.015	0.004	0.000	0.004
WO ₄	27.64	28.43	26.65	27.60	25.22	22.85
CUMM	53.32	51.87	55.43	47.01	49.00	49.18
RUN	19.04	19.70	17.93	25.39	25.77	27.97

TROODOS AMPHIBOLE ANALYSES

S. #	035	035	035	044	044	044
D. (m)	1271.2	1271.2	1271.2	1367.7	1367.7	1367.7
SiO ₂	46.91	52.65	49.02	50.82	49.77	53.20
TiO ₂	1.09	0.85	1.25	0.78	0.30	0.07
Al ₂ O ₃	9.21	4.27	5.27	4.18	7.09	3.77
FeO	12.71	12.03	12.55	11.20	8.89	7.97
MnO	0.21	0.11	0.16	0.14	0.09	0.07
MgO	13.41	14.86	15.24	16.46	17.17	18.72
CaO	12.18	12.70	12.33	12.16	12.06	12.41
Na ₂ O	1.69	0.55	0.82	0.80	0.60	0.41
K ₂ O	0.05	0.02	0.05	0.03	0.01	0.00
Total	97.48	98.10	96.74	7.390	7.183	7.575

NO. OF IONS ON THE BASIS OF 23 (O, OH).

Si	6.860	7.538	7.234	7.390	7.183	7.575
Al	1.140	0.482	0.766	0.610	0.817	0.425
Al	0.447	0.258	0.151	0.106	0.389	0.208
Ti	0.120	0.092	0.139	0.085	0.033	0.007
Mg	2.923	3.171	3.352	3.567	3.694	3.973
Fe	1.554	1.440	1.426	1.362	1.073	0.949
Mn	0.026	0.013	0.020	0.017	0.011	0.008
Ca	1.908	1.948	1.950	1.894	1.865	1.893
Na	0.479	0.153	0.235	0.226	0.168	0.113
K	0.009	0.004	0.009	0.006	0.002	0.000
WO	29.89	29.70	28.98	27.76	28.12	27.78
CUMM	45.77	48.34	49.83	52.28	55.70	58.30
RUN	24.34	21.96	21.19	19.96	16.18	13.93

TROODOS AMPHIBOLE ANALYSES

S. #	021	047	047	054	054	054
D. (m)	1175.4	1395.2	1395.2	1438.0	1438.0	1438.0
SiO ₂	56.09	56.80	49.21	53.57	56.37	56.04
TiO ₂	0.00	0.00	1.11	0.28	0.08	0.07
Al ₂ O ₃	0.76	0.80	4.78	4.53	1.23	1.27
FeO	3.59	2.23	13.49	8.68	6.91	8.55
MnO	0.00	0.00	0.20	0.05	0.02	0.14
MgO	21.25	22.43	15.05	18.08	20.02	19.56
CaO	13.75	13.24	11.04	12.91	12.43	12.41
Na ₂ O	0.07	0.00	1.24	0.43	0.01	0.00
K ₂ O	0.00	0.00	0.06	0.14	0.02	0.02
Total	95.51	95.62	96.18	98.67	97.09	98.06

NO. OF IONS ON THE BASIS OF 23 (O, OH).

Si	7.915	7.935	7.279	7.498	7.901	7.847
Al	0.085	0.065	0.721	0.502	0.099	0.153
Al	0.041	0.067	0.112	0.245	0.104	0.056
Ti	0.000	0.000	0.023	0.029	0.008	0.007
Mg	4.469	4.670	3.318	3.772	4.182	4.082
Fe	0.424	0.261	1.669	1.016	0.810	1.001
Mn	0.000	0.000	0.025	0.006	0.002	0.017
Ca	2.079	1.982	1.750	1.936	1.867	1.862
Na	0.019	0.000	0.356	0.117	0.003	0.000
K	0.000	0.000	0.011	0.025	0.004	0.004
WO	29.82	28.67	25.97	28.79	27.21	26.81
CUMM	64.11	67.56	49.26	56.10	60.98	58.78
RUN	6.08	3.77	24.77	15.11	11.81	14.42

TROODOS AMPHIBOLES ANALYSES

S. #	024	076	075	075	077	077'
D. (m)	1195.9	1635.1	1633.9	1633.9	1644.8	1644.8
SiO ₂	49.21	52.92	54.00	51.69	51.53	54.20
TiO ₂	1.11	0.20	0.06	0.31	0.29	0.23
Al ₂ O ₃	4.78	2.27	3.62	3.82	2.67	2.28
FeO	13.49	13.75	8.97	11.45	16.04	11.05
MnO	0.20	0.19	0.10	0.09	0.33	0.24
MgO	15.05	16.12	18.89	16.68	14.32	16.75
CaO	11.04	12.61	11.32	12.46	12.65	12.79
Na ₂ O	1.24	0.12	0.45	0.45	0.25	0.19
K ₂ O	0.08	0.00	0.00	0.00	0.02	0.00
Total	96.18	98.18	97.41	96.95	98.10	97.73

NO. OF IONS ON THE BASIS OF 23 (O, OH)

Si	7.279	7.681	7.624	7.477	7.529	7.739
Al	0.721	0.319	0.376	0.523	0.460	0.261
Al	0.112	0.062	0.226	0.129	0.000	0.123
Ti	0.123	0.021	0.006	0.034	0.032	0.025
Mg	3.318	3.422	3.975	3.596	3.119	3.565
Fe	1.669	1.638	1.059	1.385	1.980	1.320
Mn	0.025	0.023	0.012	0.011	0.041	0.029
Ca	1.750	1.924	1.712	1.931	1.980	1.957
Na	0.356	0.033	0.123	0.126	0.071	0.053
K	0.011	0.000	0.000	0.000	0.004	0.000
WO	25.97	27.55	25.38	27.94	28.05	28.60
CUMM	49.26	49.00	58.92	52.03	44.18	52.11
RUN	24.77	23.45	15.70	20.04	27.77	19.29

A.15. TROODOS CHLORITES ANALYSES

S.#	290	290	245	245	245	245
D. (m)	30.9	30.9	321.4	321.4	321.4	321.4
SiO ₂	27.62	25.44	31.83	31.68	34.66	30.04
TiO ₂	0.10	0.13	0.00	0.00	0.05	0.00
Al ₂ O ₃	20.46	20.63	16.97	17.32	15.11	17.79
FeO	19.00	19.15	13.71	13.81	12.58	14.04
MnO	0.26	0.26	0.15	0.15	0.17	0.19
MgO	20.40	22.32	24.63	24.06	23.17	24.36
CaO	0.07	0.00	0.63	1.01	2.18	0.64
Na ₂ O	0.00	0.05	0.13	0.08	0.13	0.08
K ₂ O	0.06	0.04	0.02	0.01	0.03	0.01
Total	88.04	88.02	88.07	88.12	88.08	87.15

NO. OF IONS ON THE BASIS OF 28(O)EQUIV.

Si	5.593	5.194	6.242	6.217	6.749	5.986
Al	2.407	2.806	1.758	1.783	1.251	2.014
Al	2.476	2.158	2.163	2.222	2.216	2.163
Ti	0.015	0.020	0.000	0.000	0.007	0.000
Fe	3.218	3.270	2.248	2.266	2.049	2.340
Mn	0.045	0.045	0.025	0.025	0.028	0.032
Mg	6.158	6.793	7.199	7.037	6.725	7.235
Ca	0.015	0.000	0.132	0.212	0.455	0.137
Na	0.027	0.020	0.049	0.030	0.049	0.031
K	0.015	0.010	0.005	0.003	0.007	0.003

TROODOS CHLORITE ANALYSES

S. #	B65	B65	006	024	B40	B40
D. (m)	1046.5	1046.5	1073.2	1195.9	1999.8	1999.8
SiO ₂	27.25	27.32	31.23	34.68	32.12	30.11
TiO ₂	0.03	0.04	0.05	0.09	0.04	0.00
Al ₂ O ₃	19.17	17.48	17.81	12.04	21.90	21.36
FeO	25.96	25.55	20.66	21.95	8.97	9.54
MnO	0.36	0.32	0.15	0.20	0.11	0.05
MgO	15.93	16.17	19.60	14.39	24.92	26.01
CaO	0.00	0.00	0.40	5.08	0.20	0.00
Na ₂ O	0.00	0.07	0.00	0.20	0.00	0.00
K ₂ O	0.03	0.06	0.02	0.01	0.01	0.00
Total	88.73	87.01	89.92	88.64	88.27	87.07

NO. OF IONS ON THE BASIS OF 28(O) EQUIV.

Si	5.615	5.757	6.198	7.315	6.077	5.709
Al	2.385	2.233	1.802	0.685	1.923	2.291
Al	2.269	2.281	2.363	2.144	2.960	2.645
Ti	0.005	0.007	0.007	0.013	0.006	0.000
Fe	4.818	4.316	3.429	3.661	1.419	1.565
Mn	0.063	0.059	0.025	0.034	0.016	0.008
Mg	4.892	5.281	5.798	4.277	7.028	7.603
Ca	0.000	0.000	0.085	1.085	0.041	0.000
Na	0.000	0.030	0.000	0.077	0.000	0.000
K	0.008	0.017	0.005	0.003	0.002	0.000

TROODOS CHLORITE ANALYSES

S. #	B40	B40	075	075	B2	B2
D. (m)	1999.8	1999.8	1633.9	1633.9	1996.0	1996.0
SiO ₂	29.40	29.39	35.95	35.31	30.79	30.83
TiO ₂	0.00	0.00	0.00	0.00	0.00	0.00
Al ₂ O ₃	20.38	20.74	15.32	15.83	17.88	17.21
FeO	12.30	12.81	12.78	12.79	13.70	13.02
MnO	0.19	0.16	0.13	0.05	0.11	0.06
MgO	24.22	23.34	23.76	24.22	25.10	24.76
CaO	0.25	0.92	0.17	0.80	0.09	0.16
Na ₂ O	0.02	0.04	0.05	0.04	0.01	0.01
K ₂ O	0.00	0.00	0.08	0.08	0.01	0.02
Total	86.76	87.40	88.24	89.12	87.69	86.07

NO. OF IONS ON THE BASIS OF 28(O) EQUIV.

Si	5.811	5.791	6.919	6.753	6.060	6.160
Al	2.189	2.209	1.081	1.247	1.940	1.840
Al	2.557	2.606	2.394	2.321	2.206	2.213
Ti	0.000	0.000	0.000	0.000	0.000	0.000
Fe	2.033	2.111	2.057	2.046	2.255	2.176
Mn	0.032	0.027	0.021	0.008	0.018	0.010
Mg	7.135	6.854	6.816	6.905	7.363	7.374
Ca	0.053	0.194	0.035	0.164	0.019	0.034
Na	0.008	0.015	0.019	0.015	0.004	0.004
K	0.000	0.000	0.020	0.020	0.003	0.005

A.16. TROODOS EPIDOTE/CLINOZOISITE ANALYSES

S.#	006	006	024	024	B2	B2
D. (m)	1073.2	1073.2	1195.9	1195.9	1996.3	1996.3
SiO ₂	38.79	38.84	38.69	38.43	37.77	37.39
TiO ₂	0.08	0.07	0.68	0.16	0.03	0.13
Al ₂ O ₃	23.99	25.76	24.20	27.66	24.51	23.29
FeO	11.71	9.48	10.61	8.41	11.05	12.73
MnO	0.21	0.26	0.00	0.02	0.06	0.02
MgO	0.12	0.04	0.15	0.10	0.05	0.14
CaO	23.35	24.03	24.18	24.69	23.84	23.41
Na ₂ O	0.02	0.00	0.00	0.00	0.00	0.00
K ₂ O	0.03	0.01	0.00	0.00	0.04	0.00
Total	98.30	98.49	98.51	97.47	97.35	97.11

NO. OF IONS ON THE BASIS OF 13(O,OH)

Si	3.247	3.210	3.220	3.162	3.191	3.196
Al	0.000	0.000	0.000	0.000	0.000	0.000
Al	2.366	2.509	2.373	2.682	2.440	2.346
Ti	0.005	0.004	0.043	0.010	0.002	0.008
Fe	0.820	0.655	0.738	0.441	0.781	0.910
Mn	0.015	0.018	0.000	0.001	0.004	0.001
Mg	0.015	0.005	0.019	0.012	0.006	0.018
Ca	2.094	2.128	2.156	2.177	2.158	2.144
Na	0.003	0.000	0.000	0.000	0.000	0.000
K	0.003	0.001	0.000	0.000	0.004	0.000

TROODOS EPIDOTE/CLINOZOISITE ANALYSES

S.#	047	047	047	B2	B2	B2
D.(m)	1395.2	1395.2	1395.2	1996.3	1996.3	1996.3
SiO ₂	39.09	39.02	39.14	38.41	37.59	39.25
TiO ₂	0.05	0.00	0.00	0.07	0.04	0.12
Al ₂ O ₃	31.28	30.81	31.57	24.14	22.60	23.52
FeO	2.69	3.73	3.54	11.71	13.30	11.72
MnO	0.16	0.06	0.15	0.13	0.08	0.06
MgO	0.10	0.09	0.14	0.07	3.88	0.07
CaO	24.62	24.36	24.30	23.64	20.56	23.51
Total	97.99	98.07	98.84	98.18	98.07	98.26

NO.OF IONS ON THE BASIS OF 13(O,OH)

Si	3.128	3.133	3.113	3.222	3.169	3.283
Al	0.000	0.000	0.000	0.000	0.000	0.000
Al	2.949	2.915	2.959	2.387	2.245	2.318
Ti	0.003	0.000	0.000	0.004	0.003	0.008
Fe	0.180	0.250	0.235	0.822	0.938	0.820
Mn	0.011	0.004	0.010	0.009	0.006	0.004
Mg	0.012	0.011	0.017	0.009	0.488	0.009
Ca	2.111	2.095	2.071	2.125	1.857	2.107

A.17. TROODOS PREHNITE ANALYSES

S.#	006	006	006	006	006	006
FROM ALTERATION ZONE AT 1073.2m						
SiO ₂	43.29	43.86	43.93	44.81	44.77	43.81
TiO ₂	0.01	0.02	0.05	0.04	0.02	0.02
Al ₂ O ₃	22.89	22.06	22.75	22.86	22.60	23.27
FeO	2.54	2.03	1.30	0.88	0.94	0.91
MnO	0.02	0.07	0.06	0.13	0.08	0.09
MgO	0.02	0.04	0.02	0.04	0.01	0.01
CaO	26.64	27.31	26.94	27.41	26.40	27.61
Na ₂ O	0.06	0.05	0.08	0.05	0.19	0.00
K ₂ O	0.01	0.00	0.00	0.00	0.01	0.00
Total	95.48	95.44	95.13	96.22	95.02	95.72

NO.OF IONS ON THE BASIS OF 24(O,OH)

Si	6.733	6.667	6.661	6.704	6.763	6.603
Al	0.000	0.000	0.000	0.000	0.000	0.000
Al	3.829	3.952	4.065	4.030	4.023	4.133
Ti	0.001	0.002	0.006	0.005	0.002	0.002
Fe	0.330	0.258	0.165	0.110	0.119	0.115
Mg	0.005	0.009	0.005	0.009	0.002	0.002
Mn	0.003	0.009	0.008	0.016	0.010	0.010
Ca	4.439	4.448	4.377	4.394	4.273	4.459
Na	0.018	0.015	0.024	0.015	0.056	0.000
K	0.002	0.000	0.000	0.000	0.02	0.000

TROODOS PREHNITE ANALYSES

S.#	047	047	047	035	035	035
D. (m)	1395.2	1395.2	1395.2	1271.2	1271.2	1271.2
SiO ₂	43.54	42.80	43.37	43.78	45.02	45.25
TiO ₂	0.05	0.00	0.00	0.04	0.00	0.11
Al ₂ O ₃	23.63	23.55	22.73	22.89	23.29	22.95
FeO	0.19	0.19	0.12	1.30	0.37	0.78
MnO	0.00	0.00	0.00	0.04	0.04	0.01
MgO	0.03	0.00	0.00	0.04	0.01	0.00
CaO	28.07	27.77	26.25	28.02	27.79	27.56
Na ₂ O	0.00	0.00	0.12	0.30	0.00	0.02
K ₂ O	0.00	0.00	0.00	0.01	0.00	0.06
Total	95.51	94.31	92.59	96.42	96.52	96.74

NO. OF IONS ON THE BASIS OF 24(O,OH)

Si	6.563	6.536	6.704	6.584	6.696	6.725
Al	0.000	0.000	0.000	0.000	0.000	0.000
Al	4.197	4.238	4.140	4.056	4.082	4.019
Ti	0.006	0.000	0.000	0.005	0.000	0.012
Fe	0.024	0.024	0.016	0.163	0.046	0.097
Mg	0.007	0.000	0.000	0.009	0.002	0.000
Mn	0.000	0.000	0.000	0.005	0.005	0.001
Ca	4.533	4.544	4.347	4.515	4.429	4.388
Na	0.000	0.000	0.038	0.087	0.000	0.006
K	0.000	0.000	0.000	0.002	0.000	0.011

TROODOS PREHNITE ANALYSES

S. #	039	039	046	046	046	046
D. (m)	1313.8	1313.8	1386.9	1386.9	1386.9	1386.9
SiO ₂	43.89	43.83	42.95	42.16	43.28	42.90
TiO ₂	0.03	0.00	0.00	0.00	0.00	0.00
Al ₂ O ₃	23.75	23.70	22.04	22.67	23.13	23.08
FeO	0.05	0.01	1.64	1.16	0.90	0.32
MnO	0.01	0.00	0.00	0.07	0.00	0.03
MgO	0.02	0.01	0.04	0.01	0.04	0.04
CaO	27.45	27.71	27.08	27.84	27.18	26.56
Na ₂ O	0.05	0.05	0.04	0.00	0.00	0.00
K ₂ O	0.03	0.04	0.00	0.00	0.00	0.00
Total	95.28	95.35	93.79	93.91	94.53	92.93

NO. OF IONS ON THE BASIS OF 24(O,OH)

Si	6.609	6.601	6.635	6.516	6.600	6.625
Al	0.000	0.000	0.000	0.000	0.000	0.000
Al	4.214	4.208	4.012	4.129	4.156	4.200
Ti	0.003	0.000	0.000	0.000	0.000	0.000
Fe	0.006	0.001	0.212	0.150	0.115	0.041
Mg	0.004	0.002	0.009	0.002	0.009	0.009
Mn	0.001	0.000	0.000	0.009	0.000	0.004
Ca	4.429	4.471	4.482	4.610	4.441	4.394
Na	0.015	0.015	0.012	0.000	0.000	0.000
K	0.006	0.008	0.000	0.000	0.000	0.000

TROODOS PREHNITE ANALYSES

S. #	024	024	024	B40	B40	B40
D. (m)	1195.9	1195.9	1195.9	1999.8	1999.8	1999.8
SiO ₂	42.20	42.86	43.13	43.92	43.79	43.82
TiO ₂	0.00	0.02	0.00	0.00	0.00	0.00
Al ₂ O ₃	20.13	20.89	22.49	24.66	24.37	24.46
FeO	3.89	3.87	1.47	0.33	0.25	0.17
MnO	0.00	0.02	0.00	0.00	0.00	0.00
MgO	0.02	0.00	0.00	0.03	0.01	0.02
CaO	27.15	27.16	26.88	27.49	27.99	26.23
Na ₂ O	0.29	0.00	0.00	0.02	0.14	0.12
K ₂ O	0.00	0.00	0.00	0.02	0.00	0.00
Total	93.68	94.82	93.97	96.47	97.05	94.84

NO. OF IONS ON THE BASIS OF 24(O,OH)

Si	6.635	6.635	6.633	6.537	6.491	6.602
Al	0.000	0.000	0.000	0.000	0.000	0.000
Al	3.729	3.811	4.076	4.325	4.344	4.342
Ti	0.000	0.002	0.000	0.000	0.000	0.000
Fe	0.511	0.501	0.189	0.041	0.031	0.021
Mg	0.005	0.000	0.000	0.007	0.002	0.004
Mn	0.000	0.003	0.000	0.000	0.000	0.000
Ca	4.574	4.505	4.429	4.384	4.445	4.237
Na	0.088	0.000	0.000	0.008	0.040	0.035
K	0.000	0.000	0.000	0.004	0.000	0.000

A.18. TROODOS GARNET ANALYSES

S.#	006	006	021	021	024	024
D(m)	1073.2	1073.2	1175.4	1175.4	1195.9	1195.9
SiO ₂	36.13	36.70	35.98	34.98	36.37	36.41
TiO ₂	0.22	0.13	0.63	0.77	0.32	0.79
Al ₂ O ₃	4.19	4.83	1.33	1.18	3.39	2.23
FeO	24.85	23.83	28.71	28.81	25.00	25.26
MnO	0.30	0.29	0.25	0.26	0.22	0.29
MgO	0.02	0.07	0.05	0.05	0.08	0.09
CaO	34.59	33.57	33.90	33.98	34.59	34.11
Na ₂ O	0.00	0.00	0.00	0.13	0.00	0.00
K ₂ O	0.00	0.03	0.00	0.00	0.00	0.00
Total	100.30	99.45	100.85	100.16	99.97	99.18

NO.OF IONS ON THE BASIS OF 24 OXYGENS.

Si	6.278	6.364	6.355	6.210	6.399	6.476
Al	0.000	0.000	0.000	0.000	0.000	0.000
Al	0.858	0.987	0.277	0.247	0.703	0.467
Ti	0.029	0.017	0.084	0.103	0.042	0.106
Mg	0.005	0.018	0.013	0.013	0.021	0.024
Fe	3.611	3.456	4.241	4.277	3.678	3.757
Mn	0.044	0.043	0.037	0.039	0.033	0.044
Ca	6.439	6.237	6.415	6.653	6.332	6.310
	0.000	0.000	0.000	0.045	0.000	0.000
K	0.000	0.007	0.000	0.000	0.000	0.000
GROSS	63.76	63.95	59.92	60.58	62.92	62.26
ALM	35.75	35.43	39.51	38.94	36.55	37.07
PYRO	0.05	0.19	0.12	0.12	0.21	0.24
SPESS	0.44	0.44	0.35	0.36	0.33	0.43

A.19. TROODOS SPHENE ANALYSES

S.#	035	039	039	024	046	046
D.(m)	1271.2	1313.8	1313.8	1195.9	1386.9	1386.9
SiO ₂	31.20	30.66	30.43	31.22	30.99	30.23
TiO ₂	39.18	34.62	35.12	39.14	37.91	39.48
Al ₂ O ₃	0.50	0.81	0.95	1.11	0.80	0.12
FeO	0.46	1.55	1.58	0.98	0.66	0.80
MnO	0.00	0.03	0.02	0.00	0.00	0.03

MgO	0.00	0.00	0.02	0.05	0.06	0.01
CaO	29.02	29.41	29.36	28.36	29.24	28.84
Na ₂ O	0.03	0.06	0.08	0.00	0.00	0.03
K ₂ O	0.03	0.03	0.04	0.01	0.02	0.02
Total	100.42	97.17	97.60	100.87	99.68	99.56

NO. OF IONS ON THE BASIS OF 20(O,OH)

Si	4.059	4.151	4.104	4.040	4.067	3.985
Al	0.000	0.000	0.000	0.000	0.000	0.015
Al	0.077	0.129	0.151	0.169	0.124	0.004
Ti	3.833	3.525	3.562	3.809	3.741	3.914
Fe	0.050	0.175	0.178	0.106	0.072	0.088
Mg	0.000	0.000	0.004	0.010	0.012	0.002
Mn	0.000	0.003	0.002	0.000	0.000	0.003
Ca	4.045	4.266	4.243	3.932	4.111	4.074
Na	0.008	0.016	0.021	0.000	0.000	0.008
K	0.005	0.005	0.007	0.002	0.003	0.003

A.20. TROODOS ZEOLITE ANALYSES

S. #	245	245	245	245	220	220
D. (m)	321.4	321.4	321.4	321.4	482.7	482.7
SiO ₂	54.73	52.83	60.01	53.84	51.94	52.54
Al ₂ O ₃	20.79	21.07	18.71	21.03	21.14	21.36
CaO	10.93	11.67	8.57	10.63	11.76	11.61
Na ₂ O	0.19	0.08	0.24	0.36	0.00	0.10
K ₂ O	0.08	0.03	0.00	0.50	0.00	0.14
Total	86.72	85.68	85.53	86.36	84.84	85.75

NO. OF IONS ON THE BASIS OF 48 EQUIV.

Si	16.609	16.306	18.118	16.469	16.204	16.221
Al	0.000	0.000	0.000	0.000	0.000	0.000
Al	7.435	7.663	5.945	7.580	7.772	7.771
Ca	3.554	3.859	2.772	3.484	3.931	3.840
Na	0.112	0.048	0.140	0.213	0.000	0.060
K	0.031	0.012	0.000	0.195	0.000	0.055

REFERENCES.

Aldiss, D., (1978). Plagiogranites and associated plutonic rocks of various ophiolite complexes.

Unpubl. Ph.D. thesis, Open University, 243p.

Alt, J.C., Muehlenbachs, K., Honnorez, J., (1986).

An oxygen isotope profile through the upper kilometer of the oceanic crust, DSDP hole 504B.

Earth Planet. Sci. Lett., 80, p217-229.

Anderson, R.N., Skilbeck, J.N., (1981). Oceanic heat flow.

In: Emiliani, C., (Ed.) The Sea, vol. 7, The Oceanic Lithosphere: Wiley-Interscience, New York. p489-524.

Andrews, A.J., Fyfe, W.S., (1976). Metamorphism and massive sulphide generation in oceanic crust.

Geosci. Can. vol. 3 No. 2: 84-94.

Apted, M.J., Liou, J.G., (1983). Phase relations among greenschist, epidote-amphibolite, and amphibolite in a basaltic system. Am. Jour. Sci. Vol., 283-A p328-354.

Aumento, F., Loncaravic, B.D., Ross, D.I., (1971). Hudson

geotraverse: Geology of the Mid-Atlantic Ridge at 45°N.

Phil. Trans. Roy. Soc. London, A268, 623-650.

Aumento, F., (1979). Distribution and evolution of uranium in the oceanic lithosphere.

Phil. Trans. Roy. Soc. London, A291, p423-431.

Bailey, E. B., McCallien, W. J., (1960). Some aspects of the Steifmann trinity, mainly chemical.

Quart. J. Geol. Soc. London. 116, p365-395.

Barriga, F., Munha, J., Fyfe, W. S., Vibetti, N. J., (1985). Extreme hydrothermal alteration in the intrusive layers of the Troodos Ophiolite, Cyprus. (abs.).

EoS. Trans. Am. Geophys. Union., vol. 66 No. 46 p1128.

Bear, L. M., (1960). The geology and mineral resources of the Agros-Apsiou area.

Cyprus Geol. Surv. Dept. Mem. No. 7

Bear, L. M., (1963). The mineral resources and mining industry of Cyprus.

Cyprus Geol. Surv. Bull. 1.

Best, M. G., (1982). Igneous and Metamorphic Petrology.

W. H. Freeman and Company, San Francisco, 630p.

Bischoff, J. L., Dickson, F. W., (1975). Sea water-basalt interaction at 200°C and 500 bars: Implications for the origin of sea-floor heavy-metal deposits

and regulation of sea water chemistry.

Earth Planet. Sci. Lett., 25, 385-397.

Bischoff, J. L., Seyfried, W. E., (1978). Hydrothermal chemistry of seawater from 25° to 350°C. Am. Jour. Sci. 278 p838-860.

Bodvarsson, G., Lowell, R. P., (1972). Ocean-floor heat flow and the circulation of interstitial waters. J. Geophys. Res., 77, p4472-4475.

Bogdanov, N. A., (1980). On tectonic merging of the crust in oceans. In: A. Panayiotou. Ophiolites. Proc. Internat. Symp. Ophiolites. Nicosia, 1979. Cyprus Geol. Surv.

Bohlke, J. K., Alt, J. C., Muehlenbachs, K., (1984). Oxygen isotope - water relationships in altered deep sea-basalts: low temperature mineralogical controls. Can. J. Earth Sci. 21, p67-77.

Boles, J. R., Coombs, D. S., (1975). Mineral reactions in zeolitic Triassic tuff, Hokonui Hills, New Zealand. Geol. Soc. Amer. Bull., 86, 163-173.

Bonnatti, E., Honnorez, J., Kirst, P., Radicati, F.,
Metagabbros from the Mid-Atlantic Ridge at 06N:
contact - hydrothermal - dynamic

the axial valley. *J. Geol.*, 83, p61-778

Budge, E. A. W., (1926). The dwellers on the Nile: Chapter on the life, history, religion and literature of the Ancient Egyptians.

The Religious Tract Society, London.

Burke, W. H., Denison, R. E., Hetherington, E. A., Koepnick, R. B.,

Nelson, H. F., Otto, J. B., (1982). Variation of seawater $^{87}\text{Sr}/$

^{86}Sr throughout Phanerozoic time. *Geology* 10, p516-519.

Campbell, I. A., Nolan, J., (1974). Factors effecting the stability

field of Ca-poor pyroxene and the origin of the Ca-poor minimum in Ca-rich pyroxenes from tholeiitic intrusions.

Contrib. Mineral. Petrol., 48, 205-219.

Cann, J. R., (1969). Spilites from the Calsbury Ridge, Indian

Ocean. *J. Petrol.* 10, p1-19

Cann, J. R., (1970). Rb, Sr, Y, Zr and Nb in some ocean floor

basaltic rocks.

Earth Planet. Sci. Lett., 10, 7-11.

Carr, J. H., Bear, L. M., (1960). The geology and mineral resources

of the Peristerona-Lagoudhera area.

Cyprus Geol. Surv. Dept. Mem. No. 2, 1-79.

- Christensen, N. J., Salisbury, M. H., (1975). Structure and constitution of the lower oceanic crust. *Rev. Geophys. Space Phys.*, 13, 57-86.
- Clayton, R. N., Mayeda, T. K., (1963). The use of bromine pentafluoride in the extraction of oxygen from oxides and silicates for isotopic analysis. *Geochim. et Cosmochim. Acta*, 27, 43-52.
- Coleman, R. G., (1971). Plate tectonic emplacement of upper mantle peridotites along continental edges. *J. Geophys. Res.* 76, p1212-1222.
- Coleman, R. G., (1977). *Ophiolites. Ancient oceanic lithosphere?* Springer-Verlag. Berlin. 229p.
- Constantinou, G., (1973). The area of copper mineralization at Ayios Ioannis Pitsillia. *Cyprus Geol. Surv. Dept. Internal Memo.* 10p.
- Constantinou, G., Govett, G. J. S., (1973). Geology, geochemistry, and genesis of Cyprus sulphide deposits. *Econ. Geol.* 68, p843-858.
- Coombs, D. S., (1974). On the mineral facies of spilitic rocks and their genesis. In: G. C. Amstutz (ed), *Spilites and spilitic rocks. I. U. G. S. Series A, No. 4.* Springer-

Verlag, Berlin.

Coombs, D. S., Ellis, A. J., Fyfe, W. S., Taylor, A. M., (1959). The zeolite facies, with comments on the interpretation of hydrothermal syntheses.

Geochim. et Cosmochim. Acta. 17, p53-107.

Coplen, T. B., Kendall, C., Hopple, J., (1983). Comparison of stable isotope reference samples.

Nature. 360. p236-362.

Crawford, A. J., Beccaluva, L., Serrì, G., (1981). Tectono - magmatic evolution of the west Phillipine region and the origin of boninites. Earth Planet. Sci. Lett. v. 54, p346-356.

Crawford, M. L., Kraus, D. W., Hollister, L. S., (1979). Petrologic and fluid inclusion study of calc-silicate rocks, Prince Rupert, British Columbia:

Am. J. Sci. 279, p1135-1159.

Crawford, M. L., (1981). Phase equilibria in aqueous fluid inclusions. In: Hollister, L. S., Crawford, M. L., (Eds.). Mineral. Assoc. Canada Short Course Handbook 6, p75-100.

Daly, R. A., Manger, G. E., Clark, S. P., (1966). Handbook of

Physical constants.

Geol. Soc. Am. Mem. 97, p20-26. .

Davis, E. E., Lister, C. R. B., (1974). Fundamentals of ridge crest topography.

Earth Planet. Sci. Lett., 21, p405-413.

Davis, E. E., Lister, C. R. B., (1977). Heat flow measurements over the Juan de Fuca Ridge: Evidence for wide spread hydrothermal circulation in a highly heat transportive crust.

J. Geophys. Res., 82, p4845-4860.

De Rover, W. P., (1956). Sind die Alpinotypen Peridotitmassen vielleicht tektonisch verfrachtete Bruchstücke der Peridotitschale?

Geol. Rundschau., 46, p137-146.

Deer, W. A., Howie, R. A., Zussman, J., (1966). An introduction to the rock forming minerals.

Longman, Hong Kong. 528p.

Dewey, J. F., Bird, J. M., (1971). Origin and emplacement of the ophiolite suite: Appalachian ophiolites in Newfoundland.

Jour. Geophys. Res. 76, p3179-3206.

- Dietz, R.S., (1963). Alpine serpentinites as oceanic rind fragments.
Geol. Soc. Am. Bull. 74, p947-952.
- Elder, J., (1976). The bowels of the Earth.
Oxford University Press, Oxford. 222p
- Elthon, D., (1981). Metamorphism in oceanic spreading centers. In: C. Emiliani, (Ed): The Sea, Vol 7. The oceanic lithosphere. Wiley-Interscience, New York p285-304.
- Embley, R.W., (1986). Galapagos hydrothermal alteration zone found.
EoS. Trans. Am. Geophys. Union. vol. 67, No. 22 p497.
- Eugster, H.P., (1959). Reduction and oxidation in metamorphism.
In: P.H. Abelson (Ed.). Researches in geochemistry.
Wiley, New York, New York. p397-426.
- Fairbridge, R.W., (1972). (Ed.). The Encyclopedia of Geochemistry and Environmental Sciences. Encyclopedia of Earth Science series. vol. IV A. Van Nostrand Reinhold Co., New York.
- Fehn, U., Cathles, L., (1978). Hydrothermal convection through oceanic crust between 0 and 70 m.y. old.

EoS. 59. p384.

Fehn, U., Cathles, L., (1979). Hydrothermal convection at slow-spreading mid-ocean ridges.

Tectonophysics. 55. p239-250.

Fox, P. J., Stroup, J. B., (1981). The plutonic foundation of the oceanic crust. In: C. Emiliani, (Ed): The Sea, vol. 7. The Oceanic Lithosphere. Wiley-Interscience, New York.

Friedman, I., O'Neil, J. R., (1977). Compilation of stable isotope fractionation factors of geochemical interest. U.S. Geol. Surv. Prof. P. 440-kk.

Fyfe, W. S., (1960). Stability of epidote minerals. Nature, 187, p497-498.

Fyfe, W. S., (1974). Geochemistry. Clarendon Press. Oxford. 107p.

Fyfe, W. S., Price, N. J., Thompson, A. B., (1978). Fluids in the Earth's crust. Elsevier. Amsterdam, 383p.

Fyfe, W. S., Lonsdale, P., (1981). Ocean floor activity. In: C. Emiliani, (Ed.). The Sea vol. 7 The Oceanic

Lithosphere.

Wiley Interscience, New York. p589-638.

Gass, I.G., (1960). The geology and mineral resources of
the Dhal area.

Cyprus geol. Surv. Dept. Mem. No. 4, 116p.

Gass, I.G., Masson-Smith, D., (1963). The geology and gravity
anomalies of the Troodos massif, Cyprus.

Roy. Soc. London Phil. Trans., a255, p417-467.

Gass, I.G., (1968). Is the Troodos massif of Cyprus a fragment
of Mesozoic ocean floor?

Nature, 220, p39-42.

Gass, I.G., Smewing, J.D., (1973). Intrusion, extrusion and
metamorphism at constructive margins: Evidence
from the Troodos massif, Cyprus.

Nature, 242, p26-29.

Gass, I.G., (1976). Origin and emplacement of ophiolites.

In: Volcanic Processes in Ore Genesis.

Inst. Min. Metall., Lond., p72-76.

Gass, I.G., Smewing, J.D., (1979). Ophiolites: obducted oceanic
lithosphere.

In: Emiliani, C., The Sea. vol. 7 Oceanic Lithosphere.

Wiley Interscience, New York.

Gass, I.G. (1980). The Troodos Massif: Its role in the unravelling of the ophiolite problem and significance in the understanding of constructive plate margin processes.

In: A. Panayiotou, (Ed.). Ophiolites. Proc. Int. Ophiolite Symp Cyprus Geol. Surv. Publ.

George, R.P.J., (1975). The internal structure of the Troodos ultramafic complex, Cyprus.

Unpubl. Ph.D. thesis, State Univ. New York (Stony Brook). 196p.

Gillis, K.M., Robinson, P.T., (1985). Low temperature alteration of the extrusive sequence, Troodos Ophiolite, Cyprus. Canadian Mineralogist, vol. 23, p431-441.

Goldich, S.S., (1984). Determination of ferrous iron in silicate rocks.

Chem. Geol., 42, p343-347.

Greenbaum, D., (1972). Magmatic processes at ocean ridges:

Evidence from the Troodos Massif, Cyprus.

Nature, 238, p18-21.

Greenbaum, D., (1977). The chromitiferous rocks of the Troodos

Ophiolite Complex, Cyprus

Econ. Geol., 72, p1175-1194.

Gregory, R.T., Taylor, H.P., (1981). An oxygen isotope profile in a section of Cretaceous oceanic crust, Semail Ophiolite, Oman: Evidence for ^{18}O buffering of the oceans by deep (>5Km) seawater-hydrothermal circulation at mid-ocean ridges.

Jour. Geophys. Res. 86(B4): p2737-2755.

Guillemot, D., Nesteroff, W.D., (1980). Les depots metalliferes Cretaces de Chypre: Comparison avec leurs homologues actuels du Pacifique.

In: A. Panayiotou, (Ed.), Ophiolites. Proc. Int. Ophiolite Symp. Cyprus.

Cyprus Geol. Surv. Dept.

Hajash, A. (1975). Hydrothermal processes along mid-ocean ridges: An experimental investigation.

Contrib. Mineral. Petrol., 53, p205-228.

Harris, D.M., (1979). Pre-eruption variations of H_2O , S and Cl in a subduction zone basalt.

EoS. Trans. Am. Geophys. Union, 60, p968.

Harvey, P.K., Taylor, D.M., Hendry, R.D., Bancroft, F., (1973).

An accurate fusion method for the analysis of rocks and chemically related materials by X-ray fluorescence spectrometry.

X-Ray Spectrometry, 2. p33-44.

Hashimoto, M., (1972). Reactions producing actinolite in basic metamorphic rocks.

Lithos, v. 5, p19-31.

Hawkesworth, C. J., (1981). Trace element and isotope geochemistry.

In: Smith, D. G., (Ed.), The Cambridge Encyclopedia of Earth Sciences.

Cambridge University Press, Cambridge. p124-140.

Heaton, T. H. E., Sheppard, S. M. F., (1977). Hydrogen and oxygen isotope evidence for seawater-hydrothermal alteration and ore deposition, Troodos Complex, Cyprus.

In: Volcanic Processes in Ore Genesis.

Inst. Min. Metall. and Geol. Soc., p42-57.

Heirtzler, J. R., (1972). Understanding the mid-Atlantic Ridge.

Natl. Acad. Sciences. Washington, D. C., 131p.

Helgeson, H. C., Kirkham, D. H., (1976). Thermal

prediction of the thermodynamic behavior of aqueous electrolytes at high pressures and temperatures. III. Equation of state for aqueous species at infinite dilution.

Am. J. Sci., 276, p97-240.

Henley, R. W., Ellis, A. J., (1983). Geothermal systems, ancient and modern: A geochemical review.

Earth Sci. Rev. 19. 1-50.

Hess, H. H., (1965). Mid-ocean ridges and tectonics of the seafloor.

In: W. F. Whittard, R. Bradshaw (Eds.), Submarine geology and geophysics. 17th Colston Res. Symp. Bristol, England. Butterworths.

Hoefs, J., (1973). Stable isotope geochemistry.

Springer-Verlag, New York. 135p.

Holdaway, M. J., (1972). Thermal stability of Al-Fe epidote as a function of f_{O_2} and Fe content.

Contrib. Mineral. Petrol. vol. 37, p307-340.

Holdaway, M. J., (1988). Hydrothermal stability of clinozoisite plus quartz.

Am. J. Sci. 284, p643-667.

Holland, H.D., (1984). The chemical evolution of the atmosphere and oceans.

Princeton University Press, Princeton, N.J. 582p.

Hollister, L.S., Crawford, M.L., (eds.), (1981). Fluid inclusions: Applications to petrology.

Mineral. Assoc. Canada Short Course Handbook, 6, 304p.

Hutchinson, R.W., Fyfe, W.S., Kerrich, R., (1980). Deep fluid penetration and ore deposition.

Minerals Sci. Engng, vol. 12 No. 3.

Hyndman, D.W., (1985). Petrology of Igneous and Metamorphic Rocks.

McGraw-Hill, New York. 786p.

International Crustal Research Drilling Group, (1984).

CY-4 Drillcore descriptions. Vol. 1. Unpubl. report.

Dalhousie University, Canada.

International Crustal Research Drilling Group, (1985).

CY-4 Drillcore descriptions. Vols. 2, 3, 4. Unpubl. reports.

Dalhousie University, Canada.

Ito, E., Anderson, A.T., (1983). Submarine metamorphism

of gabbros from the mid-Cayman Rise: petrographic

and mineralogic constraints on hydrothermal processes at slow spreading ridges. *Contrib. Mineral. Petrol.*, 82, p371-388.

Javoy, M., (1977). Stable isotopes and geothermometry. *J. Geol. Soc. Lond.*, v. 135, p609-639.

Jenkins, W. J., Edmond, J. M., Corliss, J. B., (1978). Excess ^3He and ^4He in Galapagos submarine hydrothermal waters. *Nature*, 272, p156-158.

Kay, R. W., Senechal, R. G., (1976). The Rare Earth geochemistry of the Troodos Ophiolite Complex. *Jour. Geophys. Res.*, 81, p964-970.

Khan, M. A., Summers, C., Bamford, S. A. D., Chroston, P. N., Poster, C. K., Vine, F. J., (1972). Reversed seismic refraction line on the Troodos massif, Cyprus. *Nature*, 238, p134-136.

Kuniyoshi, S., Liou, J. G., (1973). Contact metamorphism of the Karmutsen Group, Vancouver Island, British Columbia, (abs.). *Geol. Soc. America Abs. with Programs*, v. 5, p703.

Kurshakova, L. D., (1971). Stability fields of hedenburgite on the $\log \text{PO}_2$ -T

diagram. *Geochem. Internat.* v. 8, p340-49.

Kushiro, I., (1960) Si-Al relations in clinopyroxenes from igneous rocks. *Am. J. Sci.*, 258, p548-554.

Lapwood, R.R., (1948) Convection of a fluid in a porous medium. *Proc. Cambridge Phil. Soc.*, 44, p508-521.

Leake, B.E., (1978) Nomenclature of amphiboles. *Am. Mineral.* 63, p1023-1052.

Le Bas, M.J., (1962) The role of aluminium in igneous clinopyroxenes with relation to their parentage. *Am. J. Sci.*, 260, p287-288.

Linke, N.F., (1958) Solubilities of inorganic and metal organic compounds (4th Ed.). I. Van Nostrand, Princeton, N. J. 1407p.

Liou, J.G., (1971) P-T stabilities of laumontite, wairakite, lawsonite, and related minerals in the system $CaAl_2Si_2O_8-SiO_2-H_2O$. *Jour. Petrol.*, vol. 12, part 2, p379-411.

Liou, J.G., (1973) Synthesis and stability relations

of epidote, $\text{Ca}_2\text{Al}_2\text{FeSi}_3\text{O}_{12}(\text{OH})$.

Jour. Petrol. v. 14, p381-413.

Liou, J.G., (1979). Zeolite facies metamorphism of basaltic rocks from the East Taiwan Ophiolite. Am. Mineral. v. 64, p1-14.

Liou, J.G., Ernst, W.G., (1979). Ocean ridge metamorphism of the East Taiwan ophiolite. Contrib. Mineral. Petrol., v. 68, p335-348.

Liou, J.G., Kuniyoshi, S., Ito, K., (1974). Experimental studies of the phase relations between greenschist and amphibolite in a basaltic system. Am. Jour. Sci. vol., 273 p613-632.

Lister, C.R.B., (1972). On the thermal balance of a mid-ocean ridge. Geophys. J. Roy. Ast. Soc., 26, p515-535.

Loomis, A.A., (1966). Contact metamorphic reactions and processes in the Mt. Tallac roof remnant, Sierra Nevada, California. J. Petrol. 7, p221-245.

Lowell, R.P., (1975). Circulation in fractures, hot springs, and convective heat transport on mid-ocean ridge crests.

Geophys. J. Roy. Ast. Soc., 40, p351-365.

Lubimova, E. A., (1977). Heat loss from the Earth.

IASPEI-IAVCEI Assembly, Durham. (abs.) p22.

Macdonald, A. H., Fyfe, W. S., (1985). Rate of serpentinization
in seafloor environments.

Tectonophysics, 116 p123-135.

Macdonald, A. J., Spooner, E. T. C., (1981). Calibration of a
Linkham TH600 programmeable heating-cooling stage
for microthermometric examination of fluid inclusions.

Econ. Geol., v. 76: p1248-1258.

Macdonald, G. A., (1968). Composition and origin of Hawaiian
lavas.

Geol. Soc. Amer. Mem. 116, p477-522.

Malpas, J., Langdon, G., (1984). Petrology of the Upper Pillow
Lava Suite, Troodos, Ophiolite, Cyprus.

In: Gass, I. G., Lippard, S. J., Shelton, A. W., (Eds.)

Ophiolites and oceanic lithosphere.

Blackwell Scientific Publications, Oxford.

Malpas, J., (1979). Two contrasting trondhjemite associations
from transported ophiolites in western Newfoundland.

Initial report. In: F. Barker (Ed.), Trondhjemites, dacites,

and related rocks.

Elsevier, Amsterdam.

Margaritz, M., Taylor, H.P., (1974). Oxygen and hydrogen isotope studies of serpentinization in the Troodos Ophiolite Complex, Cyprus.
Earth Planet. Sci. Lett., 23, p8-14.

McCrae, J.M., (1950). The isotope chemistry of carbonates and a pleo temperature scale.
J. Chem. Phys., v. 18 p849.

Meijer, A., (1980). Primitive arc volcanism and a boninite series: Examples from western Pacific island arcs.
In: D. Hayes, (Ed).; The tectonic and geologic evolution of South - east Asian seas and islands.
American Geophysical Union Geophysical Monograph 23, p269 - 282.

Melson, W.G., Van Andel, T.H., (1966). Metamorphism in the mid-Atlantic Ridge, 22°N latitude.
Marine Geol. 4, p165-186.

Menzies, M., Allen, C., (1974). Plagioclase lherzolite-residual mantle relationships within two eastern Mediterranean ophiolites.

Contrib. Mineral. Petrol., 45, p197-213.

Mitchell, W.S., Aumento, F., (1977). Uranium in oceanic rocks:

DSDP leg 37 .

Can. J. Earth Sci., 14, p794-808.

Miyashiro, A., Shido, F., Ewing, M., (1971). Metamorphism in the
Mid-Atlantic Ridges near 24° and 30°N.

Phil. Trans. Roy. Soc. Lond. A. 268, p589-603.

Moore, E.M., Vine, F.J., (1971). The Troodos Massif, Cyprus
and other ophiolites as oceanic crust: evaluation
and implications.

Phil. Trans. Roy. Soc. London, A268, p443-466.

Morris, J.D., Hart, S.R., (1984). Isotopic and incompatible
element constraints on the genesis of island arc
volcanics from Cold Bay and Amak Island, Aleutians.
Geochim. et Cosmochim. Acta 47. p2015-2030.

Mottl, M.J., Holland, H.D., (1978). Chemical exchange
during hydrothermal alteration of basalt by
seawater I. Experimental results for major and minor
components of seawater.

Geochim. et Cosmochim. Acta. 42. p1103-1115.

Muehlenbachs, K., (1979). The alteration and aging of

the seafloor: oxygen isotope evidence from
DSDP/IPOD legs 51, 52 and 53. In: T. Donnelly et
al., Initial Reports of the Deep Sea Drilling
Project 51-53, part 2, p1159-1167.

U.S. Government Printing Office, Washington D.C.

Muehlenbachs, K., Clayton, R.N., (1972a). Oxygen isotope
studies of fresh and weathered submarine basalts.
Can. J. Earth Sci. 9: p172-184

Muehlenbachs, K., Clayton, R.N., (1972b). Oxygen isotope
geochemistry of submarine greenstones.
Can. J. Earth Sci. 9: p471-478.

Muehlenbachs, K., Clayton, R.N., (1976). Oxygen isotope
composition of the oceanic crust and its bearing
on seawater.
Jour. Geophys. Res. 81: p4365-4369.

Mueller, R.F., Saxena, S.K., (1977). Chemical Petrology.
Springer-Verlag. New York. 394p.

Murton, B.J., Moores, E.M., (1986). Western limassol forest
complex, Cyprus: Part of an upper Cretaceous leaky
transform fault.
Geology, v. 14, p255-258.

- Nitsch, K.H., (1971). Stabilitätsbeziehungen von
prehnit- und pumpellyit-Haltigen Paragenesen.
Contrib. Mineral. Petrol., 30, p240-260.
- Norrish, K., Hutton, J.T., (1969). An accurate X-ray
spectrographic method for the analysis of a wide
range of geological samples.
Geochim. et Cosmochim. Acta 33: p431-451.
- Ohmoto, H. (1972). Systematics of sulphur and carbon
isotopes in hydrothermal ore deposits.
Econ. Geol. 67: p551-578.
- Ohmoto, H., Rye, R.O., (1979). Isotopes of carbon and sulphur.
In: Barnes, H.L., (ed.). Geochemistry of Hydrothermal
ore deposits. 2nd Ed.
Wiley-Interscience, p509-567.
- Pantazis, Th.M., (1967). The geology and mineral resources
of the Pharmakas-Kalavassos area.
Cyprus Geol. Surv. Dept. Mem. No. 9, 190p.
- Pearce, J.A., Cann, J.R., (1971). Ophiolite origin investigated
by discriminant analysis using Ti, Zr and Y.
Earth Planet. Sci. Lett., 12, p339-349.
- Peterman, Z.E., Hedge, C.E., Tourtelot, H.S., (1970). Isotopic

composition of strontium in seawater throughout
Phanerozoic time.

Geochim. et Cosmochim. Acta, 34 p105.

Potter, R. W., Clynne, M. A., Brown, D. L., (1978). Freezing point
depression of aqueous sodium chloride solutions.
Econ. Geol. 73, p284-285.

Rautenschlein, M., Jenner, G. A., Hertogen, J., Hofmann, A. W.,
Kerrick, R., Schminke, H.-U., White, W. M., (1985). Isotopic
and trace element composition of volcanic glasses
from the Akaki Canyon, Cyprus: implications for the
origin of the Troodos ophiolite.
Earth Planet. Sci. Lett., 75, p369-383.

Riley, J. P., Chester, R., (1971). Introduction to Marine
Chemistry. Academic Press. London.

RISE Project Group, (1979). Massive deep-sea
sulphide ore deposits discovered on the
East Pacific Rise. Nature, 227, p523-528.

Robertson, A. H. F., (1977). Tertiary uplift of the
Troodos massif, Cyprus.
Geol. Soc. Amer. Bull., 88, p1763-1772.

Robinson, P. T., Melson, W. G., O'Hearn, T., Schminke, H. U.,

(1983). Volcanic glass composition of the
Troodos ophiolite, Cyprus.

Geology, v. 11, p400-404.

Roedder, E., (1967). Fluid inclusions as samples of
ore fluids. In: H. L. Barnes, (Ed.). Geochemistry
of hydrothermal ore deposits.

Holt, Rinehart and Winston, New York. p515-574.

Roedder, E., (1979). Fluid inclusions as samples of
ore fluids. In: H. L. Barnes, (Ed.). Geochemistry
of hydrothermal ore deposits. 2nd Ed.

Wiley-Interscience, New York. p684-737.

Roedder, E., (1984). Fluid Inclusions: An introduction
to studies of all types of fluid inclusions,
gas, liquid or melt trapped in materials from
Earth and space, and their applications to the
understanding of geologic processes.

Reviews in mineralogy, v. 12. (Ribbe, P. H., Ed.).

Mineral. Soc. Amer., Washington, D. C. 644p.

Rona, P. A., Lowell, R. P., (1980) ., (Eds.), Seafloor
spreading centres. Dowden, Hutchinson and Ross,
Inc. 367p.

Rosenbauer, R. J., Bischoff, J. L., (1983). Uptake and transport of heavy metals by heated seawater. A summary of the experimental results. In: P. A. Rona, K. Bostrom, L. Laubier, Smith, K. L., (Eds.). Plenum Press, New York.

Schiffman, P., Williams, A. E., Evarts, R. C., (1984). Oxygen isotope evidence for submarine hydrothermal alteration of the Del Puerto ophiolite, California. Earth Planet. Sci. Lett., 70, p207-220.

Schminke, H.-U., Rautenschlein, M., Robinson, P. T., Mehegan, J. M., (1983). Troodos extrusive series of Cyprus: A comparison with oceanic crust. Geology, 11, p405-409.

Sclater, J. G., Franceteau, J., (1970). The implications of terrestrial heat flow observations on current tectonic and geothermal models of the crust and upper mantle of the Earth. Geophys. J. Roy. Ast. Soc., 20, p509-542.

Searle, D. L., (1972). Mode of occurrence of the cupriferous pyrite deposits of Cyprus. Trans. Instn. Min. Metall. (sect. B: Appl. earth sci.), 81,

B189-197

Seki, Y., (1972). Lower grade stability limit of
epidote in the light of natural occurrences.

J. Geol. Soc. Japan, 78, p405-413.

Seyfried, W.E., Bischoff, J.L., (1977). Hydrothermal
transport of heavy metals by seawater: The
role of seawater/basalt ratio.

Earth Planet. Sci. Lett., 34, p71-77.

Seyfried, W.E., Mottl, M.J., Bischoff, J.L., (1978).

Seawater/basalt ratio effects on the chemistry
and mineralogy of spilites from the ocean floor.

Nature, 275, p211-213.

Seyfried, W.E., Bischoff, J.L., (1981). Experimental

seawater-basalt interaction at 300°C and
500 bars: Chemical exchange, secondary mineral
formation and implications for the transport
of heavy metals.

Geochim. et Cosmochim. Acta, 45, 135-147

Seyfried, W.E., Mottl, M.J., (1982). Hydrothermal

alteration of basalt by seawater under
seawater-dominated conditions.

Geochim. et Cosmochim. Acta, 46p985-1002.

Shepard, T. J., (1981). Temperature-programmable heating, freezing stage for microthermometric analysis of fluid inclusions:

Econ. Geol., v. 76, p1244-1247.

Sleep, N. H., Wolery, T. J., (1978). Thermal and chemical constraints on venting of hydrothermal fluids at mid-ocean ridges.

J. Geophys. Res., 83, p5913-5922.

Sleep, N. H., (1983). Hydrothermal convection at ridge axes. In: P. A. Rona, K. Bostrom, L. Laubier, K. L. Smith, (Eds.). Hydrothermal Processes at Ridge Axes.

Plenum Press, New York. p71-83

Smewing, J. D., (1975). The metamorphism of the Troodos massif, Cyprus.

Unpubl. Ph.D. thesis, Open University, 267p.

Smith, A. L., (1970). Spinel, perovskite, and coexisting Fe-Ti oxide minerals. Am Mineral., 55, p264-269.

Smith, P. J., (1978).

Hydrothermal water and heat flow.

Nature, 271. p13-14.

Sorby, H.C., (1858). On the microscopic structure
of crystals, indicating the origin of minerals
and rocks.

Quart. Jour. Geol. Soc., London. 14 (1), p453-500.

Spooner, E.T.C., Fyfe, W.S., (1973). Sub-seafloor
metamorphism, heat and mass transfer.

Contrib. Mineral. Petrol. 42, p287-304.

Spooner, E.T.C., Beckinsale, R.D., Fyfe, W.S., (1974).

¹⁸O-enriched ophiolitic metabasic rocks
from E. Liguria, Pindos and Troodos.

Contrib. Mineral. Petrol., 47, p41-62.

Spooner, E.T.C., (1976). The strontium isotopic
composition of seawater-ocean crust
interaction.

Earth Planet. Sci. Lett., 31, p167-174.

Spooner, E.T.C., Bray, C.J., (1977). Hydrothermal
fluids of seawater salinity in ophiolitic
sulphide ore deposits in Cyprus.

Nature, 266, p808-812.

Spooner, E.T.C., (1977). Hydrodynamic model for the
origin of the ophiolitic cupriferous pyrite

ore deposits of Cyprus. In: Volcanic Processes
in Ore Genesis: London. Instn. Min. Metall. and
Geol. Soc. p58-71.

Stakes, D., Vanko, D. A., (1986) Multistage hydrothermal
alteration of gabbroic rocks from the failed-
Mathematician Ridge.
Earth Planet. Sci. Lett., 79, p75-92.

Steinmann, G., (1927) Die ophiolithischen zonen in
dem mediterranen Ketengebirge.
14th Intern. Geol. Congr. Madrid 2, p638-667.

Straus, J. M., Schubert, G., (1977) Thermal convection of
water in a porous medium: effect of temperature
and pressure dependent thermodynamic and
transport properties.

Strens, R. G. J., (1968) Properties of the Al-Fe-Mn
epidotes. Mineralog. Mag., 35, p464-475.

Taylor, H. P., Epstein, S., (1962) Relationships
between $^{18}\text{O}/^{16}\text{O}$ ratios in coexisting
minerals of igneous and metamorphic rocks.
Geol. Surv. Amer. Bull., 73, p481-480, 675-694.

Taylor, H. P., (1967). Oxygen isotope studies of hydrothermal mineral deposits. In: H. L. Barnes, (Ed.) Geochemistry of Hydrothermal Ore Deposits. Holt, Rinehart and Winston, New York. p109-142.

Taylor, H. P., (1968). The oxygen isotope geochemistry of igneous rocks. Contrib. Mineral. Petrol., 19, 1-71.

Taylor, S. R., (1965). Geochemical analysis by spark source mass spectrography. Geochim. et Cosmochim. Acta, 29, p1243-1261.

Thayer, T. P., (1969). Peridotite-gabbro complexes as keys to the petrology of mid-ocean ridges. Geol. Soc. Am. Bull. 80, p1515-1522.

Thompson, A. B., (1971). PCO_2 in low-grade metamorphism: Zeolite, carbonate, clay mineral, prehnite relations in the system $\text{CaO-Al}_2\text{O}_3\text{-SiO}_2\text{-CO}_2\text{-H}_2\text{O}$. Contrib. Mineral. Petrol., 33, p145-161.

Tomasson, J., Kristmannsdottir, H., (1972). High temperature alteration minerals and thermal brines, Reykjanes, Iceland.

Contrib. Min. Petrol., 36, p123-134.

Uyeda, S., (1978). The New View Of The Earth.

W.H. Freeman and Co., San Francisco. 217p.

Vanko, D.A., Batiza, R., (1982). Gabbroic rocks

from the ~~Mathematician~~ failed rift.

Nature, 300, p742-744.

Vanko, D.A., (1986). High-chlorine amphiboles from

oceanic rocks: Product of highly saline fluids?

Am. Mineral., v. 71: p51-59

Verhoogen, J., Turner, F.J., Weiss, L.E., Wahrhaftig, C.,

Fyfe, W.S., (1970). The Earth.

Holt, Rinehart and Winston, New York, 748p.

Vine, F.J., Poster, C.K., Gass, I.G., (1973).

Aeromagnetic survey of the Troodos Massif,

Cyprus. Nature, 244, p34-38.

Williams, D.L., Von Herzen, R.P., (1974). Heat loss

from the Earth: New estimates.

Geology, 2, p327-328.

Williams, H., Turner, F.J., Gilbert, C.M., (1982).

Petrography. An introduction to the study

of rocks in thin sections.

W.H. Freeman and Co., San Francisco. 626p.

Wilson, A.D., (1955). A new method for the determination
of ferrous iron in rocks and minerals.

Bull. Geol. Surv. Gt. Britain 9 : p56-58.

Wilson, R.A.M., (1959). The geology of the Xeros-Troodos
area. Mem. Geol. Surv. Cyprus No. 1, 135p.

Winkler, H.G.F., Nitsch, K.H., (1963). Bildung von Epidot.

Naturwissenschaften, 50, p612-13.

Wolery, T.J., Sleep, N.H., (1976). Hydrothermal circulation
and geochemical flux at mid-ocean ridges.

Jour. Geol., 84, p249-275.

Wu, T.-W., (1984). The geochemistry and petrogenesis
of some granitoids in the Grenville province
of Ontario and their tectonic implications.

Unpubl. Ph.D. thesis, Univ. Western Ontario. 623p.

Yanatieva, O.K., (1946). Solubility polytherms in

the systems $\text{CaCl}_2\text{-MgCl}_2\text{-H}_2\text{O}$ and

$\text{CaCl}_2\text{-NaCl-H}_2\text{O}$. Zh. Prikl. Khim. 19, 709-22